6-1-2017

The Mechanistic Requirements Of Passive H+ Import Through The Na,k-Atpase

Kevin S. Stanley
Illinois State University, ksstanl@ilstu.edu

THE MECHANISTIC REQUIREMENTS OF PASSIVE H^+ IMPORT THROUGH THE NA,K-ATPASE

Kevin S. Stanley

114 Pages

This work focuses on the elucidation of the mechanism of passive proton import through the Na,K-ATPase. This enzyme uses the energy in ATP hydrolysis to exchange three intracellular Na^+ for two extracellular K^+ to maintain ion gradients within the cell, and while in the absence of physiological external Na^+ and K^+, the phosphorylated externally open (E2P) conformation passively imports protons, generating an inward current (I_H). Chapter one reports on the effects of intracellular cations and nucleotides to shift the Na,K-ATPase into the E2P conformation. We identified that a combination of either internal Na^+ and ATP or K^+ and Pi. In chapter two, we investigated the effects of extracellular inhibitors on the ability for H^+ to enter through the E2P conformation. We used two different known extracellular tetrapropylammonium (TPA) and ethylenediamine (EDA) in order to block extracellular access at different expected depths within the Na,K-ATPase. Using a combination of electrophysiological and biochemical techniques, the results showed that TPA inhibits the Na,K-ATPase as well as I_H near the extracellular surface as previously demonstrated. EDA on the other hand, inhibited at or near the shared sites, induced dephosphorylation and accentuate I_H at acidic pH 6.0.

The appendix of this work shows that while perpetually pseudo-phosphorylated by BeF_3^- the Na,K-ATPase, Na^+ and K^+ are still able to interact in the phosphorylated conformation.

KEYWORDS: Na,K-ATPase, Na Pump, Electrophysiology, Tetrapropylammonium, Ethylenediamine, Passive Proton Import

THE MECHANISTIC REQUIREMENTS OF PASSIVE H^+ IMPORT THROUGH THE NA,K-ATPASE

KEVIN S. STANLEY

A Dissertation Submitted in Partial
Fulfillment of the Requirements
for the Degree of

DOCTOR OF PHILOSOPHY

School of Biological Sciences

ILLINOIS STATE UNIVERSITY

2017

THE MECHANISTIC REQUIREMENTS OF PASSIVE H^+ IMPORT THROUGH THE NA,K-ATPASE

KEVIN S. STANLEY

COMMITTEE MEMBERS:

Craig Gatto, Chair

Andres Vidal-Gadea

Jon Friesen

Pablo Artigas

Paul Garris

ACKNOWLEDGMENTS

My time in graduate school was both a great and terrible time of my life, although nobody mentions the bad part in the acknowledgements they tend to make the person more than the great times. During these moments I have always had someone to help get me through it. A big part of my support structure came from my close friends, Ronald and Austin, as well as all of my immediate family who know who they are. I also want to thank my fellow graduate students who could directly relate to what I had been going through. Among them Brian and Amanda are the two people have been the most influential during my time at ISU. Both are great friends who would give the shirt off their back for someone in need and helped me to deal with difficult people and situations by dealing with my complaints and being so open with their friendship and experience. Along with these individuals, faculty member, Pablo Artigas, Andres Vidal-Gadea, Paul Garris, Wolfgang Stein, Rachel Bowden, Ben Sadd, Scott Sakaluk, Ryan Paitz (Ya that's right he's faculty now) and Steve Juliano, have all been a strong influence on my development academically and personally. I have and will always respect them in and out of the lab/classroom as each conversation has helped me in some form or fashion during my time at ISU to prepare for the future or deal with the present.

My biggest acknowledgements are Jeff Helms, Craig Gatto and my parents, who without their support, I wouldn't have completed this doctorate at ISU. First, Jeff Helms who over the course of my degree I have had more conversations than I could even count. From life and death and the journey betwixt them, to the physiology of how my grandfather (rest his soul) survived an aortic aneurism rupture for over an hour and a half ambulance ride. I still hold true to my thought that a cigarette got lodged in that sucker after he

practically ate them for 50 years. Helms will be in my life until the end and I look forward to visiting him in Montana for some fly fishing trips in the foreseeable future. Next is my pain in the ass advisor Craig Gatto, the bane of my existence and one of the best things that has ever happened to me. I can't honestly imagine my life without him at this point in time, we are uncomfortably similar in so many ways (still should probably get one of those DNA kits done). He showed me good, real people can succeed and thrive in academia while still having a life. Each and every opportunity he has provided me with has made me a better person and scientist. Even though he may not know it, I have understood for a long time that he always had my best interest in mind and was constantly pushing me (passively) to be the best I me possible since day 1. Like a thorn in your side that you can't wait to get rid of, then when it's gone… ya kinda miss it. Finally, my mom and dad who have been by my side since forever, supporting me through my entire life and PhD. I talk to them every day, sometimes about the weather in northern Wisconsin, other days about whether a Masters degree would be better for me long term. Either way I know I wouldn't have gotten here without them, nor would I want to be. I don't know where my life will go, but I love knowing that I will be able to talk to both of them whenever I need, and know the love is unconditional regardless of how many times I try to burn down our house. I love and thank each of you for being in my life.

K. S. S.

CONTENTS

CHAPTER I FIGURES

CHAPTER II FIGURES

CHAPTER III FIGURES

CHAPTER I

INTRODUCTION

INTRODUCTION

The Na^+/K^+-ATPase (NKA) is a fundamental membrane bound ion transporter found in nearly all mammalian cells. This transporter's primary function is to maintain Na^+ and K^+ ion homeostasis within the cell, by pumping both ions against their electrochemical gradients. This heterodimeric enzyme is a member of the P-type ATPase super-family, containing a large α-catalytic subunit (4 isozymes) with a conserved aspartic acid residue, which is phosphorylated and dephosphorylated during specific steps of the catalytic sequence (1). Along with the α-subunit, a regulatory β-subunit (3 isozymes) (2) acting as a chaperone for proper NKA folding, assembly, and trafficking from the endoplasmic reticulum to the plasma membrane (3). In addition, there is a less understood auxiliary FXYD-subunit (7 isozymes) which has distinct tissue specific effects (4,5). The NKA harvests the energy released from ATP hydrolysis throughout the cycle to fuel the mechanical work required to transport 3 Na^+ ions out and 2 K^+ ions into the cell (1).

The NKA alternates between two primary conformational changes from internally open (E1) to open externally (E2). The Post-Albers cycle outlines the mechanism for NKA with a basic 4-step kinetic model, beginning with an empty E1 state binding 3 Na^+ ions to an ATP-bound internally open state (Figure 1) (6,7). The intracellular binding order is thought to occur first with 2 Na^+ in the "shared sites" (i.e. sites that reciprocally bind 2 Na^+ or 2 K^+ during the cycle), then 1 Na^+ binds within the "Na-exclusive site" (8). Following 3 Na^+ binding a phosphoenzyme intermediate is formed by high affinity ATP binding (0.1-0.5 μM), where a nucleophilic attack of the γ-phosphate of ATP by the conserved aspartic acid (conserved **D**KTG sequence) forms the phosphorylated NKA intermediate E1P(3Na), concomitantly occluding the 3 Na^+ ions (9). A spontaneous conformational

change then takes place, opening the NKA to the extracellular environment, releasing the 3 Na^+ ions, first from the Na-exclusive site followed by the shared sites and thus forming E2P. Once open extracellularly, the NKA has a high affinity for extracellular K^+ (~0.1 mM) and binds $2K^+$ to the shared sites where they become occluded and facilitate the hydrolysis of the aspartylphosphoanhydride, producing E2(2K) (1). The resulting $2K^+$-occluded dephosphorylated conformation [$E_2(2K^+)$] spontaneously undergoes the conformational change back to the inside completing the cycle and re-forming E1 (1). This E2 to E1 conversion is the rate-limiting step in the cycle, but can be accelerated ~10-fold with low affinity ATP binding (~300-500 μM). While each step of this cycle is fully reversible (indicated by arrows in scheme 1), in physiological conditions each step favors the forward direction mentioned above.

Physiological impact of Na^+,K^+-ATPase

Although relevant in nearly all mammalian cell function, the NKA plays an invaluable role in primary excitable tissues, e.g. neuronal and cardiac. The homeostatic Na^+ and K^+ gradients produced by the NKA are critical for action potential generation by these tissues. In these and other tissues, the Na^+-gradient is particularly important for many other cellular processes such as cell volume, pH, and intracellular Ca^{2+} regulation. For example, the active extrusion of Na^+ by the NKA maintains osmoregulation of a cell as water efflux follows Na^+ export. Similarly, the Na^+ gradient is pertinent to intracellular Ca^{2+} regulation, where the potential energy produced by the Na^+ gradient allows for the extrusion of 1 Ca^{2+} by coupling it to the passive import of 3 Na^+ though the Na^+/Ca^{2+}-exchanger (NCX) (10). Without a proper Na^+ gradient, Ca^{2+} buildup in the cell would

cause a myriad of problems due to unregulated Ca^{2+} signaling, not the least of which is to initiate apoptosis.

Passive proton influx through the Na^+,K^+-ATPase

As evident from the $3Na^+/2K^+$ exchange stoichiometry, the NKA is electrogenic since it exports +1 net charges per cycle. Thus, by definition the pump cycle is also membrane potential sensitive. Although less obvious, it is also important to note that specific steps of the NKA cycle have voltage-dependent properties (11). Extracellular ion binding events by both Na^+ and K^+ change with voltage, specifically hyperpolarizing potentials preferentially shift the NKA towards the E2P and E1P(3Na) conformations (12). Hyperpolarizing potentials also present an unexpected phenomenon of a noncanonical passive import of H^+ ions (I_H) through the NKA (13,14). This I_H current was initially found in an extracellular environment void of Na^+ and K^+, where hyperpolarizing voltages induced this passive current (13). Multiple groups independently determined that this current was carried by H^+ ions, with subsequent work determining H^+ ions traverse the NKA through the Na-exclusive site at hyperpolarizing voltages in E2P (14-19).

Poul Nissen and Hanne Poulsen's labs have shown there are NKA mutations in the α-subunit which have been implicated with I_H, but the etiology of these potential disease causing mutations are not entirely understood (20,21). Although uncommon, these mutations have been identified in α-1 and α-2 NKA with pronounced I_H in α-1 specifically expressed in adrenal zona glomerulosa cells in both physiological Na^+ and K^+ (21). Depending on the implicated mutation, I_H has been proposed to cause either excess H^+ or Na^+ accumulation within the cell (21). A similar mutation in α-2 presents analogous

effects, where I_H is present in physiological [Na^+] in some patients with Familial hemiplegic migraine type 2 (FHM2) (20).

Functional work to understand the implications of extracellular ions on I_H has been performed in both physiological and non-physiological conditions to better understand I_H properties (18). Although I_H under physiological conditions appears negligible, understanding its mechanism will provided important information for understanding its role underlying potential disease causing mutations. The intracellular and extracellular mechanisms of activation for I_H have yet to be characterized fully, which has been the focus of my dissertation work. In defining these mechanisms, we build on our understanding of this I_H phenomenon, with this work being critical in providing a mechanistic framework for future studies in the field and potential disease states with which I_H may play a role.

REFERENCES

1. Kaplan, J. H. 2002. Biochemistry of the Na,K-ATPase. *Annu. Rev. Biochem.* 71:511-535.
2. Blanco, G. 2005. Na/K-ATPase subunit heterogeneity as a mechanism for tissue-specific ion regulation. *Semin. Nephrol.* 25:292-303.
3. Gatto, C., S. M. McLoud, and J. H. Kaplan. 2001. Heterologous expression of Na+-K+-ATPase in insect cells: intracellular distribution of pump subunit. *Am. J. Physiol. Cell. Physiol.* 281:C982-C992.
4. Geering, K. 2005. Function of FXYD proteins, regulators of the Na,K-ATPase. *J. Bioenerg. Biomembr.* 37:387-392.
5. Garty H., and S. J. D. Karlish. 2006. Role of FXYD proteins in ion transport. *Annu. Rev. Physiol.* 68:431-459.
6. Sen, A. K., and R. L. Post. 1964. Stoichiometry and localization of adenosine triphosphate-dependent sodium and potassium transport in the erythrocyte. *J. Biol. Chem.* 239:345–352.
7. Post, R. L., A. K. Sen, and A. S. Rosenthal. 1965. A phosphorylated intermediate in adenosine triphosphate-dependent sodium and potassium transport across kidney membranes. *J. Biol. Chem.* 240:1437–1445.
8. Kanai, R., H. Ogawa, B. Vilsen, F. Cornelius, and C. Toyoshima. 2013. Crystal structure of a Na+-bound Na+,K+-ATPase preceding the E1P state. *Nature.* 502:201-206.
9. Toyoshima, C., M. Nakasako, H. Nomura, and H. Ogawa. 2000. Crystal structure of the calcium pump of sarcoplasmic reticulum at 2.6 A resolution. *Nature.* 405:647-655.

10. Guyton and Hall. Textbook of Medical Physiology.

11. DeWeer, P., D. C. Gadsby, and R. F. Rakowski. 1988. Voltage-dependence of the Na,K pump. *Ann. Rev. Physiol.* 50:225-241.

12. Nakao, M., and D. C. Gadsby. 1986. Voltage dependence of Na translocation by the Na/K pump. *Nature.* 323:628–630.

13. Rakowski, R. F., L. A. Vasilets, J. LaTona, and W. Schwarz. 1991. A negative slope in the current voltage relationship of the Na+/K+ pump in Xenopus oocytes produced by reduction of external [K+]. *J. Membr. Biol.* 121:177–187.

14. Li, C., K. Geering, and J. D. Horisberger. 2006. The third sodium binding site of Na,K-ATPase is functionally linked to acidic pH-activated inward current. *J. Membr. Biol.* 213:1–9.

15. Visilets, A., K. Khater, and R. F. Rakowski. 2004. Effect of extracellular pH on pre-steady state and steady-state current mediated by the Na+/K+ pump. *J. Memb. Biol.* 198:65-76.

16. Rettinger, J. 1996. Characteristics of Na+/K(+)-ATPase mediated proton current in Na(+)- and K(+)-free extracellular solutions. Indications for kinetic similarities between H+/K(+)-ATPase and Na+/K(+)-ATPase. *Biochim Biophys Acta.* 1282:207-215.

17. Wang, X., and J. D. Horisberger. 1995. A conformation of Na(+)-K+ pump is permeable to proton. *Am. J. Physiol.* 268:C590–C595.

18. Mitchell, T. J., C. Zugarramurdi, J. F. Olivera, C. Gatto, and P. Artigas. 2014. Sodium and proton effects on inward proton transport through Na/K pumps. *Biophys. J.* 106:2555-2565.

19. Vedovato, N., and D. C. Gadsby. 2014. Route, mechanism, and implications of proton import during Na+/K+ exchange by native Na^+/K^+-ATPase pumps. *J. Gen. Physiol.* 143:449–464.

20. Poulsen, H., H. Khandelia, J. P. Morth, M. Bublitz, O. G. Mouritsen, J. Egebjerg, and P. Nissen. 2010. Neurological disease mutations compromise a C-terminal ion pathway in the Na+/K+-ATPase. *Nature.* 467:99-102.

21. Azizan, E. A. B., H. Poulsen, P. Tuluc, J. Zhou, M. V. Clausen, A. Lieb, C. Maniero, S. Garg, E. G. Bochukova, W. Zhao, L. H. Shaikh, C. A. A. Brighton, E. D. Teo, A. P. Davenport, T. Dekkers, B. Tops, B. Kusters, J. Ceral, G. S. H. Yeo, S. G. Heogi, I. McFarlane, N. Rosenfeld, F. Marass, J. Hadfield, W. Margas, K. Caggar, M. Solar, J. Deinum, A. C. Dolphin, I. S. Farooqi, J. Striessnig, P. Nissen and M. J. Brown. 2013. Somatic mutations in ATP1A1 and CACNA1D underlie a common subtype of adrenal hypertension. *Nat. Genet.* 45:1055-1060.

FIGURES

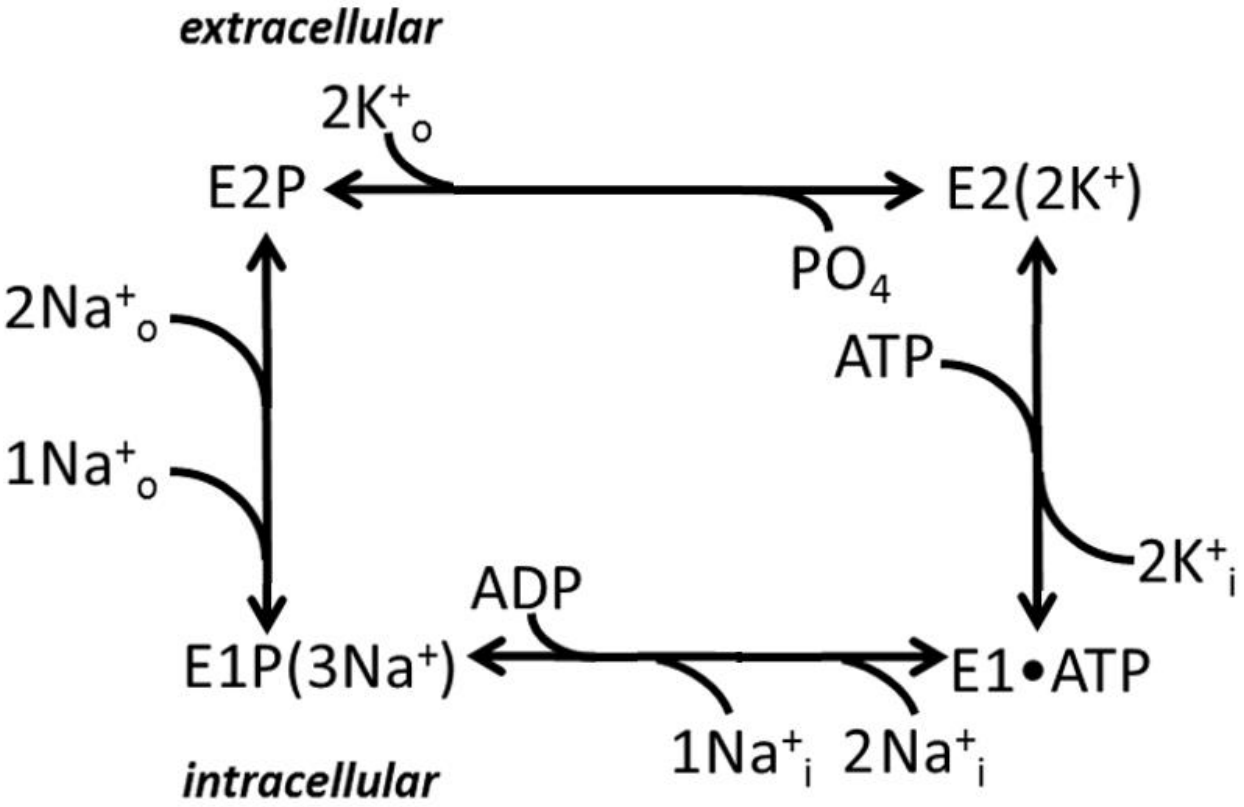

FIGURE 1. *Post-Albers reaction scheme of Na^+,K^+-ATPase reaction cycle.* The basic 4-step sequence for active Na^+ and K^+ transport are shown in the reaction cycle.

CHAPTER II

INTRACELLULAR REQUIREMENTS FOR PASSIVE PROTON TRANSPORT THROUGH THE NA,K-ATPASE

ABSTRACT

The Na^+,K^+-ATPase (NKA or Na/K pump) hydrolyzes one ATP to exchange three intracellular Na^+ (Na^+_i) for two extracellular K^+ (K^+_o) across the plasma membrane by cycling through a set of reversible transitions between phosphorylated and dephosphorylated conformations, alternately opening ion-binding sites externally (E2) or internally (E1). With subsaturating $[Na^+]_o$ and $[K^+]_o$, the phosphorylated E2P conformation passively imports protons generating an inward current (I_H), which may be exacerbated in NKA-subunit mutations associated with human disease. To elucidate the mechanisms of I_H, we studied the effects of intracellular ligands (transported ions, nucleotides, and beryllium fluoride) on I_H and, for comparison, on transient currents measured at normal Na^+_o (Q_{Na}). Utilizing inside-out patches from Xenopus oocytes heterologously expressing NKA, we observed that 1) in the presence of Na^+_i, I_H and Q_{Na} were both activated by ATP, but not ADP; 2) the $[Na^+]_i$ dependence of I_H in saturating ATP showed $K_{0.5,Na}$ = 1.8 ±.0.2 mM and the [ATP] dependence at saturating $[Na^+]_i$ yielded $K_{0.5,ATP}$ = 48 ± 11 μM (in comparison, Na^+_i-dependent Q_{Na} yields $K_{0.5,Na}$ = 0.8 ± 0.2 mM and $K_{0.5,ATP}$ = 0.43 ± 0.03 μM; 3) ATP activated I_H in the presence of K^+_i (~15% of the I_H observed in Na^+_i) only when Mg^{2+}_i was also present; and 4) beryllium fluoride induced maximal I_H even in the absence of nucleotide. These data indicate that I_H occurs when NKA is in an externally open E2P state with nucleotide bound, a conformation that can be reached through forward Na/K pump phosphorylation of E1, with Na^+_i and ATP, or by backward binding of K^+_i to E1, which drives the pump to the occluded E2(2K), where free P_i (at the micromolar levels found in millimolar ATP solutions) promotes external release of occluded K^+ by backdoor

NKA phosphorylation. Maximal I_H through beryllium-fluorinated NKA indicates that this complex mimics ATP-bound E2P states.

INTRODUCTION

Maintaining Na^+ and K^+ in electrochemical disequilibrium between the cytoplasm and extracellular milieu is critical for the physiology of animal cells, as the potential energy stored in these electrochemical gradients is exploited for common cellular processes such as cell volume regulation, pH balance, excitability, and secondary active transport. These gradients are established and maintained solely by the Na^+,K^+-ATPase (NKA, also known as the Na/K pump), a member of the P-type ATPase family of integral membrane proteins, which primarily use the chemical energy in ATP to transport ions across the lipid bilayer against their electrochemical gradients.

In each catalytic cycle, the NKA transports three Na^+ ions out of the cell in exchange for two K^+ ions at the cost of one ATP molecule (1) while transiting through the cycle of fully reversible partial reactions known as the Post-Albers kinetic scheme (Fig. 1), alternating between the phosphorylated and dephosphorylated forms of two major conformations: E1, in which the ion-binding sites open to the inside, and E2, where the ion-binding sites open to the outside (2). The forward cycle (clockwise in Fig. 1) starts when three Na^+_i ions bind to the intracellularly facing sites, promoting phosphorylation of the pump from ATP (with high affinity, $K_{0.5} < 1$ µM) and forming E1P with the concomitant occlusion of three Na^+ ions within the protein. E1P spontaneously relaxes to E2P, leading to external Na^+ release. Subsequent binding of two K^+_o closes external ion access as the 2 K^+ ions are occluded, accelerating hydrolysis of the phosphoenzyme and P_i release. The rate-limiting step in the cycle is K^+ deocclusion and release to the inside by the dephosphorylated pump, a reaction that is significantly accelerated by direct binding of ATP with low affinity ($K_{0.5}$ ~100 µM, without hydrolysis).

In addition to the full reaction cycle, which produces an outward current due to extrusion of one net charge per cycle (3), several other Na/K pump partial reactions produce electrical signals. When voltage pulses are applied in the absence of K^+_o and the presence of Na^+_o with Na^+_i and ATP, the voltage-dependent release and rebinding of Na^+ from the external side produce a transient current, also known as the transient charge movement (Q_{Na}), as the protein transitions between the Na-occluded E1P(3Na^+) and Na^+-free E2P states (4,5). A similar external binding reaction, with lower voltage dependence, is seen in the absence of Na^+_o, with nonsaturating K^+_o and K^+_i and P_i (6,7), although measurement of this reaction requires large membrane surfaces with a very high Na/K pump density.

Another current-producing functional mode occurs in the absence of externally saturating $[Na^+]_o$ and $[K^+]_o$ (i.e., when externally facing sites are not fully occupied). In this instance, the passive permeation of protons by the NKA generates a voltage-dependent inward current (I_H) at negative potentials. Over the last 20 years, many laboratories have characterized I_H, focusing mainly on its extracellular requirements and the effect of mutagenesis (8–16), which led to the current view suggesting that protons are imported when the pump is in E2P. However, studies of the intracellular requirements for this current have been limited (17).

The NKA is composed of a catalytic α-subunit (of which there are four isoforms) and an auxiliary β-subunit (with three isoforms). Aside from I_H through wild-type Na/K pumps, some disease-related mutations of the α1 and α2 subunits also modify its transport characteristics and induce passive currents (sometimes referred to as leak currents) under conditions with high Na^+_o (where wild-type I_H is negligible due to near

saturation of externally facing sites with Na^+ and K^+). All hyperaldosteronism-inducing α1 mutations studied so far (18), as well as one mutation in the α2 subunit linked to familial hemiplegic migraine (13,19), display inward currents at negative voltages (see also (20) for a recent review). These modified leak currents, some of which appear to transport Na^+ instead of H^+, were proposed to be a gain-of-function that mediates the pathophysiological effect of the mutations (18).

Here, we used giant patches excised from Xenopus oocytes heterologously expressing ouabain-resistant pumps to perform a detailed study of the intracellular requirements for I_H in the absence of Na^+_o, and compared them with the requirements for Q_{Na} in the presence of Na^+_o. Although our results reveal that both transport modes require phosphorylated pumps, we observed a large distinction between these two transport modes: in the presence of Na^+_i, maximal I_H requires low-affinity binding of ATP to E2P ($K_{0.5}$ ~100 µM), whereas Q_{Na} only requires phosphorylation by ATP with high affinity ($K_{0.5}$ ~0.5 µM). Finally, we demonstrate that beryllium-fluorinated (i.e., NKA-$BeF3^-$) pumps present I_H even in the absence of nucleotide, suggesting that the conformation promoted by this phosphate analog mimics an externally open E2P state with nucleotide bound to the pump. These results are discussed in the context of the Post-Albers scheme (Fig. 1) and previous studies of partial reactions of the Na/K pump.

MATERIALS AND METHODS

Oocyte preparation and molecular biology

Oocytes were enzymatically isolated by 1–2 h of incubation (depending on the degree of desired defolliculation) in Ca^{2+}-free OR2 solution at pH 7.4 (in mM: 82.5 NaCl, 2 KCl, 1 $MgCl_2$, 5 HEPES) with 0.5 mg/mL collagenase type IA. Enzymatic treatment was followed by four 15-min rinses in Ca^{2+}-free OR2 and two rinses in OR2 with 1.8 mM Ca^{2+}. The ouabain-resistant Xenopus Q120R/N131D (RD)-α1 and the β3 subunit, both in the pSD5 vector, were linearized with BglII and transcribed with an SP6 mMESSAGE mMACHINE (Thermo Fisher Scientific, Waltham, MA). Oocytes were injected with an equimolar mixture of cRNA for RDα1 and β3 cRNA, and then maintained in SOS solution (in mM: 100 NaCl, 2 KCl, 1.8 $CaCl_2$, 1 $MgCl_2$, and 5 HEPES) supplemented with horse serum and antimycotic-antibiotic solution (Gibco Anti-Anti; Thermo Fisher Scientific) at 16°C for 2–6 days until recordings were obtained. The RD double substitution mimics the residues responsible for the naturally ouabain-resistant rat-α1 subunit (21), allowing for selective inhibition of endogenous pumps with 1 µM ouabain and the acquisition of measurements exclusively from exogenous pumps.

Solutions

Extracellular solutions contained 1 µM ouabain and (in mM) 133 methane sulfonic acid, 10 HEPES, 5 $Ba(OH)_2$, 1 $Mg(OH)_2$, 0.5 $Ca(OH)_2$, titrated to pH 6.0 with 125 N-methyl D-glucamine (NMG^+) or to pH 7.6 with NaOH. Cl^- (10 mM) was added to pipette solutions by mixing with 125 mM NMG-Cl or NaCl to maintain electrode reversibility. The cytoplasmic bath solution for patch experiments contained (in mM) 110 glutamic acid, 10 tetraethylammonium-Cl, 10 HEPES, 5 EGTA, 1 $MgCl_2$, pH 7.4, with 110 NMG, KOH, or NaOH. Intermediate Na^+_i and K^+_i concentrations were obtained by mixing Na^+_i or K^+_i with

NMG^+_i. The osmolality of all recording solutions was 250–260 mOsmol/kg. MgATP, $TRIS_2ATP$, Na_2ADP, KADP, or K_2HPO_4 was added from 200 mM stocks (pH 7.4 with NMG^+_i). Adenosine 5'-(β,γ-imido)triphosphate (AMPPNP, tetra Li^+ salt) was directly added to the solutions (brought to pH 7.4 with NMG^+). All nucleotides were obtained from Sigma-Aldrich (St. Louis, MO). Equimolar Mg^{2+} was added from a 200 mM $MgCl_2$ stock to all intracellular solutions to which Li^+, K^+, or Na^+ nucleotide salt was added to maintain ~1 mM free Mg^{2+} (except for the experiment shown in Fig. 8, where Mg^{2+} was omitted from the intracellular solution). Beryllium fluoride was added from a stock solution containing 10 mM $BeSO_4$ and 250 mM NaF (pH 7.4 with NMG^+) to form the NKA-$BeF3^-$ complex.

Electrophysiology

Giant patches were formed and excised 3–6 days after oocyte injection using fire-polished, wide-tipped (~20 µm diameter), thick-walled borosilicate pipettes coated with Sylgard. The extracellular pipette solution was either NMG^+_o at pH 6.0 (to measure I_H) or Na^+_o at pH 7.6 (to measure Q_{Na}) with 1 µM ouabain to inhibit endogenous Na/K pumps. A Dagan 3900A integrating patch-clamp amplifier, Digidata 1322 or 1550A A/D board, and pClamp software (Molecular Devices, Sunnyvale, CA) were used for data acquisition at 20 or 100 kHz (filtered at 5 or 10 kHz).

Determination of P_i in ATP solutions

To determine free P_i, we employed the same ammonium molybdate colorimetric assay used in our previous Na^+,K^+-ATPase assays (22,23). Briefly, we generated a standard curve by diluting a 1 mM Na_2PO_4 solution into duplicate samples of 1, 5, 10, 20, 50, and 100 µM final [Na_2PO_4] in a 0.5 mL total volume of NMG intracellular solution.

Similarly, 0.5 mL of the same intracellular solution containing 4 mM of MgATP was prepared in duplicate. The vials were incubated at room temperature for 60 min and 1 mL of stopping solution (330 mM ascorbic acid, 0.5% ammonium molybdate, 0.5 M HCl) was added and further incubated for 10 min at room temperature. Then 1.5 mL of ACG solution (20 g/L Na-arsenate, 20 g/L Na-citrate, and 2% glacial acetic acid) was added and incubated for 5 min at room temperature, and sample absorbance was determined at 800 nm (VersaMax microplate reader; Molecular Devices). The amount of P_i present in the ATP solutions was determined by the slope of the standard curve.

Data analysis

Nucleotide and Na^+_i apparent affinities ($K_{0.5}$) were obtained by fitting the data to the Hill equation: $I = I_{max}\ ([S]^{nH}/(K_{0.5}{}^{nH} + [S]^{nH}))$ for inward current (Eq. 1) or $Q_{tot} = Q_{max}([S]^{nH}/(K_{0.5}{}^{nH} +[S]^{nH}))$ for transient charge movement. A rectangular hyperbola was used for nucleotides (Eq. 1, nH = 1). Transient charge (Q) movement was obtained by integrating the area under the relaxation curve in the $_{OFF}$ (as in Ref. (24)). Charge versus voltage (Q-V) curves were fitted with a Boltzmann distribution: $Q = Q_{hyp}\text{-}Q_{tot}/(1 + \exp(z_q e((V\text{-}V1/2)/kT)$ (Eq. 2) where Q_{hyp} is the charge moved by hyperpolarizing voltage pulse, Q_{tot} is the total charge moved, $V_{1/2}$ is the center of the distribution, z_q is the apparent valence of an equivalent charge that traverses the whole membrane electric field, and e, k, and T have their usual meanings (cf. Ref. (25)). kT/e = 25.4 mV at room temperature (22°C in our experiments); kT/ez_q is also called the slope factor because it refers to the steepness of the curve. All analyses were performed using pClamp and Origin (OriginLab, Northampton, MA). All intracellular $K_{0.5}$ values were obtained at pH 7.4.

RESULTS

Activation of I_H by Na^+_i

A typical experiment from an inside-out patch exposed to a pH 6 NMG^+ extracellular solution in the pipette demonstrates that MgATP activates I_H when added to a solution containing 20 mM Na^+_i, but not when NMG^+_i is the only intracellular monovalent cation (Fig. 2). The holding current (V_h = -50 mV) recorded using a slow time base exhibits ramp-shaped vertical deflections in the continuous trace corresponding to the application of 50-ms-long step voltage pulses. The currents induced by such pulses at the times indicated by lowercase letters in Fig. 2 A are shown at a faster acquisition rate (20 kHz, filter 5 kHz) in Fig. 2 B. The current-voltage (I-V) curves (Fig. 2 C) plot the average steady-state current of the MgATP-induced signal (current with MgATP minus current without MgATP; i.e., b – a and d - c) during the last 5 ms of the pulses against the applied voltage. Activation of I_H by Na^+_i and MgATP resembles the requirements for activation of transient currents in the presence of external Na^+ (Q_{Na}) when inside-out patches are bathed by Na^+_i and MgATP (24,26).

We measured the Na^+_i concentration dependence of I_H in the presence of 4 mM MgATP (Fig. 3). Stepwise increases in $[Na^+]_i$ on a typical patch held at -80 mV gradually increased the inward holding current, an effect that was reversed by MgATP withdrawal (Fig. 3 A). The normalized I_H-V plots at different $[Na^+]_i$ values (Fig. 3 B) illustrate their similar voltage dependences. The average MgATP-activated current at -140 mV was plotted as a function of $[Na^+]_i$ (Fig. 3 C) and fitted to Eq. 1 (solid line) to obtain the apparent Na^+ affinity (inverse of $K_{0.5}$). The best fit parameters, $K_{0.5}$ = 1.8 ± 0.2 mM and nH = 1.7 ±

0.2, are similar to those previously reported for Na^+_i activation of Q_{Na} (dotted line, $K_{0.5}$ = 0.8 ± 0.1 mM; nH = 2.5 ± 0.6, n = 5 (24)).

Nucleotide dependences of I_H and Q_{Na} in Na^+_i solutions

The apparent affinity for activation of I_H by Na^+_i is ~10-fold higher than the apparent affinity of processes with significant cycling, such as Na^+,K^+-ATPase activity ($K_{0.5}$= 10–20 mM (27,28)), where the fractional occupancy of the E1 state that binds Na^+_i is reduced. Given that Na^+_i and MgATP facilitate I_H, we hypothesized that phosphorylation is required to activate I_H. We tested this directly by determining the effect of adding ADP (Fig. 4, A and B) or nonhydrolysable ATP analogs that are known to interact with the pump (29,30) (i.e., AMPPNP (cf. Fig. 7 below) and AMPPCP (not shown)). As expected, sole application of these nucleotides did not activate I_H, demonstrating that phosphorylation is required for I_H to occur in the presence of Na^+_i.

Phosphorylation by ATP of the E1 conformation in the presence of Na^+_i occurs with high apparent affinity ($K_{0.5ATP}$ < 1 µM) (31). In contrast, there is a low-affinity interaction of ATP with E2 states, which is known to accelerate K^+ deocclusion in the normal cycle ($K_{0.5ATP}$~ 100 µM) (31). To obtain a more complete picture of the states required for each noncanonical current mode, we compared the ATP concentration dependences of Q_{Na} (Fig. 5) and IH (Fig. 6), which have not been reported previously. The superimposed current traces from a patch bathed in 125 mM Na^+_o (Fig. 5 A) were obtained by subtracting the current elicited by pulses from -50 mV to -160 mV and +40 mV in the absence of ATP from current induced by the same pulses with 1 µM ATP (thick line) or 4 mM ATP (thin line). The integrals of the ATP-induced transient currents when the pulses were returned to -50 mV (Q_{OFF}) in the same patch were plotted against the pulse voltage in the Q_{OFF}-V

plot (Fig. 5 B). The normalized Q_{tot}, obtained from the Boltzmann fits of the Q-V curves at different [ATP] values (Fig. 5 C) were plotted as a function of [ATP] (Fig. 5 D). The $K_{0.5ATP}$ = 0.43 ± 0.03 µM shows that Q_{Na} requires only phosphorylation of the pumps, and not low-affinity binding of ATP to E2. Also, ATP binding does not significantly alter the Q-V curve position on the voltage axis, as there is no correlation between [ATP] and the similar $V_{1/2}$ values (one-way ANOVA, p = 0.32; SAS software, SAS Institute, Cary, NC).

A different response was observed from the [ATP] dependence of I_H (Fig. 6). A representative recording obtained at -80 mV from a patch with NMG^+_o (pH 6.0) solution in the pipette illustrates a full-dose response for ATP in 20 mM Na^+_i (Fig. 6 A). The average I_H-V curves from six patches at different [ATP] values (Fig. 6 B) demonstrate that the effect of ATP is not saturating at high micromolar concentrations: the average I_H at -140 mV as a function of [ATP] (Fig. 6 C) was fitted with the Michaelis-Menten equation (Eq. 1, nH = 1, solid line) with $K_{0.5,ATP}$ = 48 ± 11 µM. This value indicates that high-affinity Na/K pump phosphorylation is insufficient for max I_H, in contrast to the observation of Q_{Na} activation in Fig. 5, and suggests that I_H requires simultaneous low-affinity ATP binding to E2. For comparison, the fit for Q_{tot} (dotted line in Fig. 5 D, $K_{0.5,ATP}$ = 0.43 ± 0.03 µM) is also shown in Fig. 6 C.

To demonstrate the simultaneous requirement of phosphorylation and low-affinity binding, we applied 10 µM ATP, a concentration that would saturate high-affinity phosphorylation (of E1), but not low-affinity binding (to E2), in combination with 1 mM AMPPNP (Fig. 7). A representative experiment from a patch held at -50 mV is shown in Fig. 7 A and the average nucleotide-induced I-V curves are shown in Fig. 7 B.

Intracellular ion dependence of I_H

Because Na^+_i must be present to phosphorylate the Na/K pump by ATP, we evaluated whether it is possible to activate I_H in the presence of K^+ as the sole intracellular monovalent cation substrate (Fig. 8). MgATP activated I_H in the presence of Na^+_i as well as in the presence of K^+_i, although the ATP-induced current in K^+_i was smaller (Fig. 8, A and B; $I_{H,K}/I_{H,Na} = 0.13 \pm 0.01$, n = 19), in quantitative disagreement with previous reports (17).

In contrast to the results obtained in the presence of Na^+_i, ADP induced the same currents as ATP in the presence of K^+_i (Fig. 8 B), suggesting that I_H could be activated without phosphorylation. However, I_H activation by nucleotides in the presence of K^+_i could be due to backdoor phosphorylation if there is enough free P_i in ATP- and ADP-containing solutions. ATP failed to activate current in the absence of Mg^{2+}_i (Fig. 8 B, open stars). As Mg^{2+} is essential for phosphorylation, this experiment demonstrates that activation of I_H by MgATP in K^+_i is due to backdoor phosphorylation via the contaminating MgP_i in solution. The free P_i of a 4 mM MgATP solution after 1 h at room temperature was 12 ± 1 µM (measured colorimetrically; see Materials and Methods). To directly demonstrate the effect of P_i, we added 25, 50, and 200 µM P_i to the 20 mM K^+_i + 4 mM MgATP solution (Fig. 9). P_i augmented I_H in a dose-dependent manner, with 200 µM inducing twice as much current as MgATP alone.

Proton current in beryllium-fluoride-inhibited pumps

When bound to the conserved aspartic acid in the P domain of P-type ATPases, beryllium fluoride acts as a phosphate analog forming an NKA-BeF_3^- complex stabilizing an externally-open E2P-like structure (32). Consistent with this, it inhibits Na/K pump

cycling by promoting a state capable of binding ouabain with high affinity (33). Recently, utilizing a slightly different Xenopus-α1 ouabain-resistant mutant (C113Y), Vedovato and Gadsby (14) showed that injection of beryllium fluoride into Xenopus oocytes inhibits NKA function, but does not alter the I_H seen in the absence of Na^+_o and K^+_o. The patch-clamp experiments with NMG^+_o (pH 6) in the pipette (Fig. 10) show that 1) the NKA-BeF_3^- complex transports a slightly larger I_H than 4 mM ATP alone (Fig. 10, A and B), 2) the effects of beryllium fluoride are irreversible (within the experimental duration; Fig. 10 B), and 3) once the E2-BeF_3^- complex is formed, the pump does not require ATP binding to activate I_H (Fig. 10, A and B).

DISCUSSION

The Post-Albers scheme (34,35) has withstood 50 years of studies and still captures the essence of how the Na/K pump works. Since it was first proposed, many articles have described the equilibrium constants and reaction rates of individual partial reactions using open (e.g., (36)) or sided membrane preparations (e.g., (5,6)). Although in this study we focused on gaining a deeper mechanistic understanding of the inward leak that has been studied by several laboratories in the last few years, the results presented here also shed light on the requirements for the Na^+-dependent transient charge movement that reflects the E2P-E1P transition, on the backdoor phosphorylation of the pump, and on the inhibition of the Na/K pump by beryllium fluoride. Below, we discuss our results in the context of previous studies, beginning with the conditions that facilitate I_H through the Na/K pump.

Conditions needed for I_H when Na^+_i is present

We observed that 4 mM ATP induced a large I_H (Figs. 2, 4, and 8), consistent with all previous whole-cell studies in which I_H was studied with Na^+_i and ATP, including those conducted in oocytes (8–16) and ventricular myocytes (15). If Na^+_i was present without nucleotide, or in the presence of AMPPNP (Fig. 7), ADP (Fig. 8), and AMPPCP (not shown), all of the pumps were trapped in the E1 state with three Na^+ ions bound (Fig. 1) and I_H was absent. The lack of activation by nonhydrolyzable nucleotides demonstrates the requirement for phosphorylation. The high apparent affinity for Na^+_i activation of IH ($K_{0.5}$ = 1.8 mM; Fig. 3) is consistent with this interpretation.

Although phosphorylation is necessary in the presence of Na^+_i, it is not sufficient to produce maximal I_H. The low affinity seen in the ATP concentration dependence for I_H

activation (Fig. 6) indicates that in addition to phosphorylation, maximal I_H also requires nucleotide binding to E2P, a conformation with low affinity for ATP (30,31). The nearly identical currents observed with 4 mM ATP or with 10 mM ATP + 1 mM AMPPNP (Fig. 7) further demonstrate that robust downhill proton import only occurs from E2P when ATP is bound. Thus, binding of ATP to the ion-empty E2P state (reached after release of Na^+ by the phosphorylated pump) is required to promote a conformational change, which activates I_H. This ATP-induced conformational change, which must not involve a full return to E1 (as it would shut down I_H), probably causes the high temperature dependence previously described for I_H (12). (It is hard to conclude definitely whether the small (10% of maximal) I_H observed in the three experiments with 1 mM ATP (Fig. 6) represents the I_H supported by phosphorylated pumps without ATP bound.)

Activation of I_H without Na^+_i with K^+_i; backdoor phosphorylation

Rettinger (17) utilized patches excised from oocytes (expressing Torpedo α1/β1 and rat α1/mouse β1 Na^+,K^+-ATPase) to partially study the intracellular conditions in which I_H is observed. The author reported that K^+_i and Na^+_i induced nearly identical I_H values in the presence of MgATP. In contrast, we observed a significantly smaller I_H in K^+i compared with Na^+_i. Given our results demonstrating the requirement of pump phosphorylation with Na^+_i (Fig. 2), it was unexpected to observe I_H in K^+_i, because ATP cannot phosphorylate pumps in the absence of Na^+_i. Even more surprising, though, was the finding that ADP, which can mimic ATP binding at the low-affinity site (30) without ever producing phosphoenzyme (31), also activated I_H.

Therefore, we thought that spontaneous ATP or ADP hydrolysis was supplying enough inorganic phosphate for backdoor phosphorylation of E2(K2)-occluded pumps,

thus promoting E2P in a fraction of the pumps. Although we were careful to take out frozen aliquots just before applying them to the patch, it is possible that nucleotide hydrolysis occurred during shipment or after storage (in neutral solution at -20°C). We did determine the level of free P_i with one preparation of fresh MgATP at ~12 µM, but total P_i could vary from batch to batch and with time in the freezer. Because I_H was not activated by ATP without Mg^{2+}, we conclude that formation of the phosphoenzyme is required for I_H. This conclusion is based on the fact that Mg^{2+} is required for backdoor phosphorylation, but not for intracellular K^+ binding or for acceleration of K^+ deocclusion (30).

The $K_{0.5}$ for P_i varies with the experimental conditions, being reduced by K^+ and ATP (37,38) or occluded Rb^+ (39), and in our conditions it is expected to be above 250 µM, consistent with the doubling of I_H by addition of 200 µM P_i (Fig. 9). The lack of I_H when only NMG^+_i is present must mean that in the presence of NMG^+ alone, the pump remains in an E1 state, impairing backdoor phosphorylation. Therefore, in the presence of K^+_i, the pumps bind K^+_i and transition to E2(K2), from where a fraction of them are phosphorylated by MgP_i, releasing K^+ externally. This induces I_H as the pumps remain in E2P with ATP bound.

Q_{Na} and I_H requirements: similarities and distinctions

The dependence of Q_{Na} on MgATP confirms our previous report (24) that this mode of function absolutely requires ATP-dependent phosphorylation in the presence of Na^+_i. It appears that ATP binding does not significantly affect the position of the Q-V curve on the voltage axis, as the $V_{1/2}$ values of the Q-V curves were not significantly different between ATP concentrations, with the possible exception of 0.2 µM (Fig. 5 C); the apparent shift in the curve at 0.2 µM is probably due to the small signal size. The lack of

an obvious effect of ATP on $V_{1/2}$ (the differences at 0.2 μM ATP were not significant in the ANOVA) contrasts the effects of ADP described by Peluffo (40), probably reflecting that only ADP accelerates dephosphorylation of E1P (2).

Conformation mimicked by beryllium-fluorinated pumps

A novel, to our knowledge, observation is that beryllium fluoride activates I_H maximally, even after ATP has been removed (Fig. 10). This indicates that the E2-BeF_3^--inhibited Na^+,K^+ ATPase mimics an E2P state (or states, as this is not a simple open channel) with ATP bound. Although this is not clear in the SERCA crystal structures in complex with BeF_3^-, which were solved in the presence or absence of nucleotides (41,42), a recent structure of bovine α1β1γ-BeF_3^- showed a 10° difference in the position of the N-domain compared with the pig α1β1γ-BeF_3^- structure complexed with ouabain (43). Because a similar tilt in the N-domain was observed in pig α1β1γ-E2BeF_3^- in complex with bufalin, the authors favored the idea that movement of the N-domain is not induced by the phosphate analog inhibitor, but by the crystal-packing conditions. Our results obtained with a functioning Na/K pump show that BeF_3^- may indeed induce movement of the N-domain to mimic the ATP-bound E2P, which certainly may be enhanced by some experimental or crystallographic conditions.

CONCLUSIONS

Our results demonstrate that the wild-type inward proton current mediated by the Na/K pump occurs whenever a significant number of pumps are open extracellularly in the presence of high intracellular ATP and externally nonsaturating concentrations of Na^+ and K^+. This externally open, phosphorylated state can be achieved by Na/K pump phosphorylation 1) in the presence of intracellular Na^+ and ATP, moving the pump in the forward direction toward E2P, or 2) in the presence of intracellular K^+ and P_i, moving the pump in the reverse direction. Extrapolating from the data of Post and Sen (35) and Heyse et al. (36), it appears that as little as 15 µM P_i can induce some E2P formation, which could explain the I_H we observed in the presence of K^+_i and Mg^{2+}_i (Fig. 8 B) (we estimate that 10–20 µM P_i was present in these experiments due to contamination from the commercial batches of ATP used). It will be interesting to evaluate whether similar mechanisms are involved in NKA mutations associated with familial hemiplegic migraine or hyperaldosteronism, where these pumps may exhibit I_H under physiological conditions.

ACKNOWLEDGMENTS

We thank Dr. Luis Reuss for critically reading the manuscript, and Adam Bernal for oocyte preparation. This work was supported by grants from the National Science Foundation (MCB-1515434 to P.A. and R15-GM061583 to C.G.).

REFERENCES

1. Sen, A. K., and R. L. Post. 1964. Stoichiometry and localization of adenosine triphosphate-dependent sodium and potassium transport in the erythrocyte. *J. Biol. Chem.* 239:345–352.
2. Post, R. L., A. K. Sen, and A. S. Rosenthal. 1965. A phosphorylated intermediate in adenosine triphosphate-dependent sodium and potassium transport across kidney membranes. *J. Biol. Chem.* 240:1437–1445.
3. Rakowski, R. F., D. C. Gadsby, and P. De Weer. 1989. Stoichiometry and voltage dependence of the sodium pump in voltage-clamped, internally dialyzed squid giant axon. *J. Gen. Physiol.* 93:903–941.
4. Nakao, M., and D. C. Gadsby. 1986. Voltage dependence of Na translocation by the Na/K pump. *Nature.* 323:628–630.
5. Holmgren, M., J. Wagg, ..., D. C. Gadsby. 2000. Three distinct and sequential steps in the release of sodium ions by the Na+/K+-ATPase. *Nature.* 403:898–901.
6. Castillo, J. P., H. Rui, ..., M. Holmgren. 2015. Mechanism of potassium ion uptake by the Na(+)/K(+)-ATPase. *Nat. Commun.* 6:7622.
7. Peluffo, R. D., and J. R. Berlin. 1997. Electrogenic K+ transport by the Na(+)-K+ pump in rat cardiac ventricular myocytes. *J. Physiol.* 501:33–40.
8. Rakowski, R. F., L. A. Vasilets, ...,W. Schwarz. 1991. A negative slope in the current voltage relationship of the Na+/K+ pump in Xenopus oocytes produced by reduction of external [K+]. *J. Membr. Biol.* 121:177–187.

9. Efthymiadis, A., J. Rettinger, and W. Schwarz. 1993. Inward-directed current generated by the Na^+,K^+ pump in Na(+)- and K(+)-free medium. *Cell Biol. Int.* 17:1107–1116.

10. Li, C., K. Geering, and J. D. Horisberger. 2006. The third sodium binding site of Na,K-ATPase is functionally linked to acidic pH-activated inward current. *J. Membr. Biol.* 213:1–9.

11. Wang, X., and J. D. Horisberger. 1995. A conformation of Na(+)-K+ pump is permeable to proton. *Am. J. Physiol.* 268:C590–C595.

12. Meier, S., N. N. Tavraz, ..., T. Friedrich. 2010. Hyperpolarization activated inward leakage currents caused by deletion or mutation of carboxy-terminal tyrosines of the Na+/K+-ATPase alpha subunit. *J. Gen. Physiol.* 135:115–134.

13. Poulsen, H., H. Khandelia, ..., P. Nissen. 2010. Neurological disease mutations compromise a C-terminal ion pathway in the Na+/K+-ATPase. *Nature.* 467:99–102.

14. Vedovato, N., and D. C. Gadsby. 2014. Route, mechanism, and implications of proton import during Na+/K+ exchange by native Na^+/K^+-ATPase pumps. *J. Gen. Physiol.* 143:449–464.

15. Mitchell, T. J., C. Zugarramurdi, ..., P. Artigas. 2014. Sodium and proton effects on inward proton transport through Na/K pumps. *Biophys. J.* 106:2555–2565.

16. Ratheal, I. M., G. K. Virgin, ..., P. Artigas. 2010. Selectivity of externally facing ion-binding sites in the Na/K pump to alkali metals and organic cations. *Proc. Natl. Acad. Sci. USA.* 107:18718–18723.

17. Rettinger, J. 1996. Characteristics of Na+/K(+)-ATPase mediated proton current in Na+- and K+-free extracellular solutions. Indications for kinetic similarities between H+/K(+)-ATPase and Na+/K(+)-ATPase. *Biochim. Biophys. Acta.* 1282:207–215.

18. Azizan, E. A., H. Poulsen, ..., M. J. Brown. 2013. Somatic mutations in ATP1A1 and CACNA1D underlie a common subtype of adrenal hypertension. *Nat. Genet.* 45:1055–1060.

19. Tavraz, N. N., T. Friedrich, ..., M. Dichgans. 2008. Diverse functional consequences of mutations in the Na+/K+-ATPase alpha2-subunit causing familial hemiplegic migraine type 2. *J. Biol. Chem.* 283:31097–31106.

20. Friedrich, T., N. N. Tavraz, and C. Junghans. 2016. ATP1A2 mutations in migraine: seeing through the facets of an ion pump onto the neurobiology of disease. *Front. Physiol.* 7:239.

21. Price, E. M., and J. B. Lingrel. 1988. Structure-function relationships in the Na,K-ATPase alpha subunit: site-directed mutagenesis of glutamine-111 to arginine and asparagine-122 to aspartic acid generates a ouabain-resistant enzyme. *Biochemistry.* 27:8400–8408.

22. Gatto, C., S. Lutsenko, and J. H. Kaplan. 1997. Chemical modification with dihydro-4,4'-diisothiocyanostilbene-2,2'-disulfonate reveals the distance between K480 and K501 in the ATP-binding domain of the Na,K-ATPase. *Arch. Biochem. Biophys.* 340:90–100.

23. Johnson, N. A., F. Liu, ..., C. Gatto. 2009. A tomato ER-type Ca2+-ATPase, LCA1, has a low thapsigargin-sensitivity and can transport manganese. *Arch. Biochem. Biophys.* 481:157–168.

24. Yaragatupalli, S., J. F. Olivera, ..., P. Artigas. 2009. Altered Na+ transport after an intracellular alpha-subunit deletion reveals strict external sequential release of Na+ from the Na/K pump. *Proc. Natl. Acad. Sci. USA.* 106:15507–15512.

25. Patti, M., C. Fenollar-Ferrer, ..., I. C. Forster. 2016. Cation interactions and membrane potential induce conformational changes in NaPi-IIb. *Biophys. J.* 111:973–988.

26. Hilgemann, D. W. 1994. Channel-like function of the Na,K pump probed at microsecond resolution in giant membrane patches. *Science.* 263:1429–1432.

27. Blanco, G. 2005. The NA/K-ATPase and its isozymes: what we have learned using the baculovirus expression system. *Front. Biosci.* 10:2397–2411.

28. Vilsen, B. 1993. A Glu329–>Gln variant of the alpha-subunit of the rat kidney Na+,K+-ATPase can sustain active transport of Na+ and K+ and Na+,K+-activated ATP hydrolysis with normal turnover number. *FEBS Lett.* 333:44–50.

29. Artigas, P., and D. C. Gadsby. 2004. Large diameter of palytoxin-induced

30. Na/K pump channels and modulation of palytoxin interaction by Na/K pump ligands. *J. Gen. Physiol.* 123:357–376.

31. Forbush, B., 3rd 1987. Rapid release of 42K and 86Rb from an occluded state of the Na,K-pump in the presence of ATP or ADP. *J. Biol. Chem.* 262:11104–11115.

32. Post, R. L., C. Hegyvary, and S. Kume. 1972. Activation by adenosine triphosphate in the phosphorylation kinetics of sodium and potassium ion transport adenosine triphosphatase. *J. Biol. Chem.* 247:6530–6540.

33. Olesen, C., M. Picard, ..., P. Nissen. 2007. The structural basis of calcium transport by the calcium pump. *Nature.* 450:1036–1042.

34. Cornelius, F., Y. A. Mahmmoud, and C. Toyoshima. 2011. Metal fluoride complexes of Na,K-ATPase: characterization of fluoride-stabilized phosphoenzyme analogues and their interaction with cardiotonic steroids. *J. Biol. Chem.* 286:29882–29892.

35. Albers, R.W. 1967. Biochemical aspects of active transport. *Annu. Rev. Biochem*. 36:727–756.

36. Post, R. L., and A. K. Sen. 1965. An enzymatic mechanism of active sodium and potassium transport. *J. Histochem. Cytochem.* 13:105–112.

37. Heyse, S., I. Wuddel, ..., W. St€urmer. 1994. Partial reactions of the Na,K-ATPase: determination of rate constants. *J. Gen. Physiol.* 104:197–240.

38. Askari, A., and W. H. Huang. 1984. Reaction of (Na+ + K+)-dependent adenosine triphosphatase with inorganic phosphate. Regulation by Na+, K+, and nucleotides. *J. Biol. Chem.* 259:4169–4176.

39. Huang,W. H., and A. Askari. 1984. Regulation of (Na++K+)-ATPase by inorganic phosphate: pH dependence and physiological implications. *Biochem. Biophys. Res. Commun.* 123:438–443.

40. Forbush, B., 3rd 1987. Rapid release of 42K or 86Rb from two distinct transport sites on the Na,K-pump in the presence of Pi or vanadate. *J. Biol. Chem.* 262:11116–11127.

41. Peluffo, R. D. 2004. Effect of ADP on Na+-Na+ exchange reaction kinetics of Na,K-ATPase. *Biophys. J.* 87:883–898.

42. Toyoshima, C., S. Yonekura, ..., S. Iwasawa. 2011. Trinitrophenyl derivatives bind differently from parent adenine nucleotides to Ca2+-ATPase in the absence of Ca2+. *Proc. Natl. Acad. Sci. USA.* 108:1833–1838.

43. Clausen, J. D., M. Bublitz, ..., P. Nissen. 2016. Crystal structure of the vanadate-inhibited Ca2+-ATPase. *Structure.* 24:617–623.

44. Gregersen, J. L., D. Mattle, ..., L. Reinhard. 2016. Isolation, crystallization and crystal structure determination of bovine kidney Na+,K+-ATPase. Acta Crystallogr. *F Struct. Biol. Commun.* 72:282–287.

FIGURES

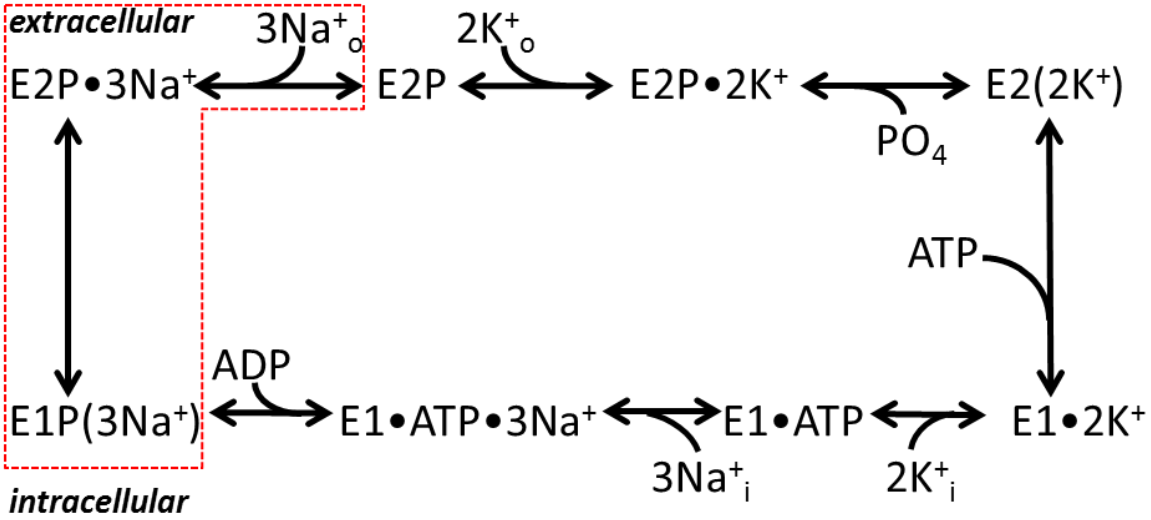

FIGURE 1. *Post-Albers reaction scheme of NKA function.* The dotted box shows the transitions responsible for voltage-dependent transient charge movement.

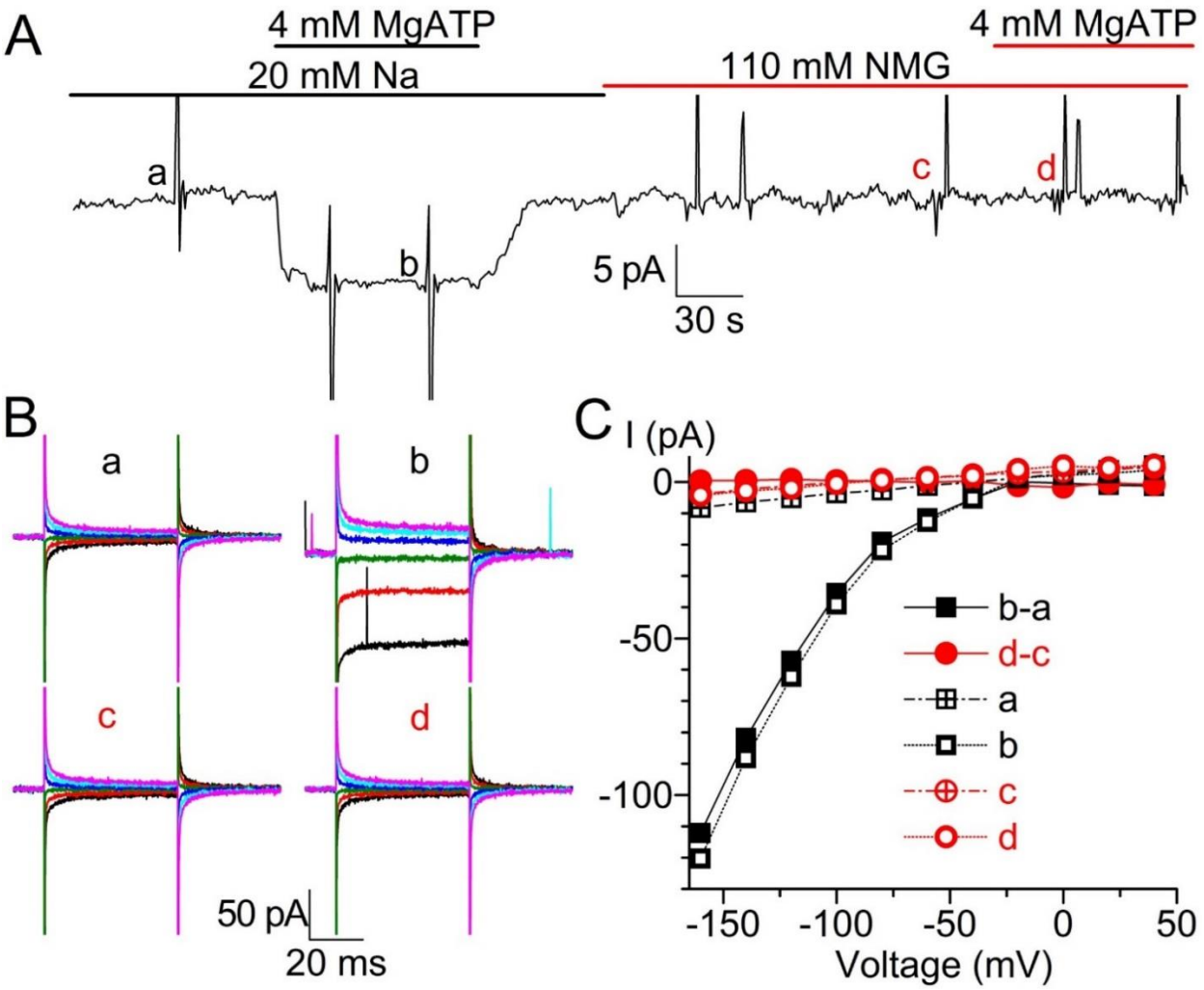

FIGURE 2. *I_H activation by Na^+_i and ATP.* (A) Continuous current recording from a patch held at -50 mV, 4 days after cRNA injection. (B) Fast temporal resolution of the family of current traces obtained at the times indicated by small caps (a–d) in (A) by pulses to -160 mV, -120 mV, -80 mV, -40 mV, 0 mV, and +40 mV. (C) I-V plot of the average current during the last 5 ms of each pulse, as a function of the applied voltage in a–d and the MgATP-activated current (a-b and c-d).

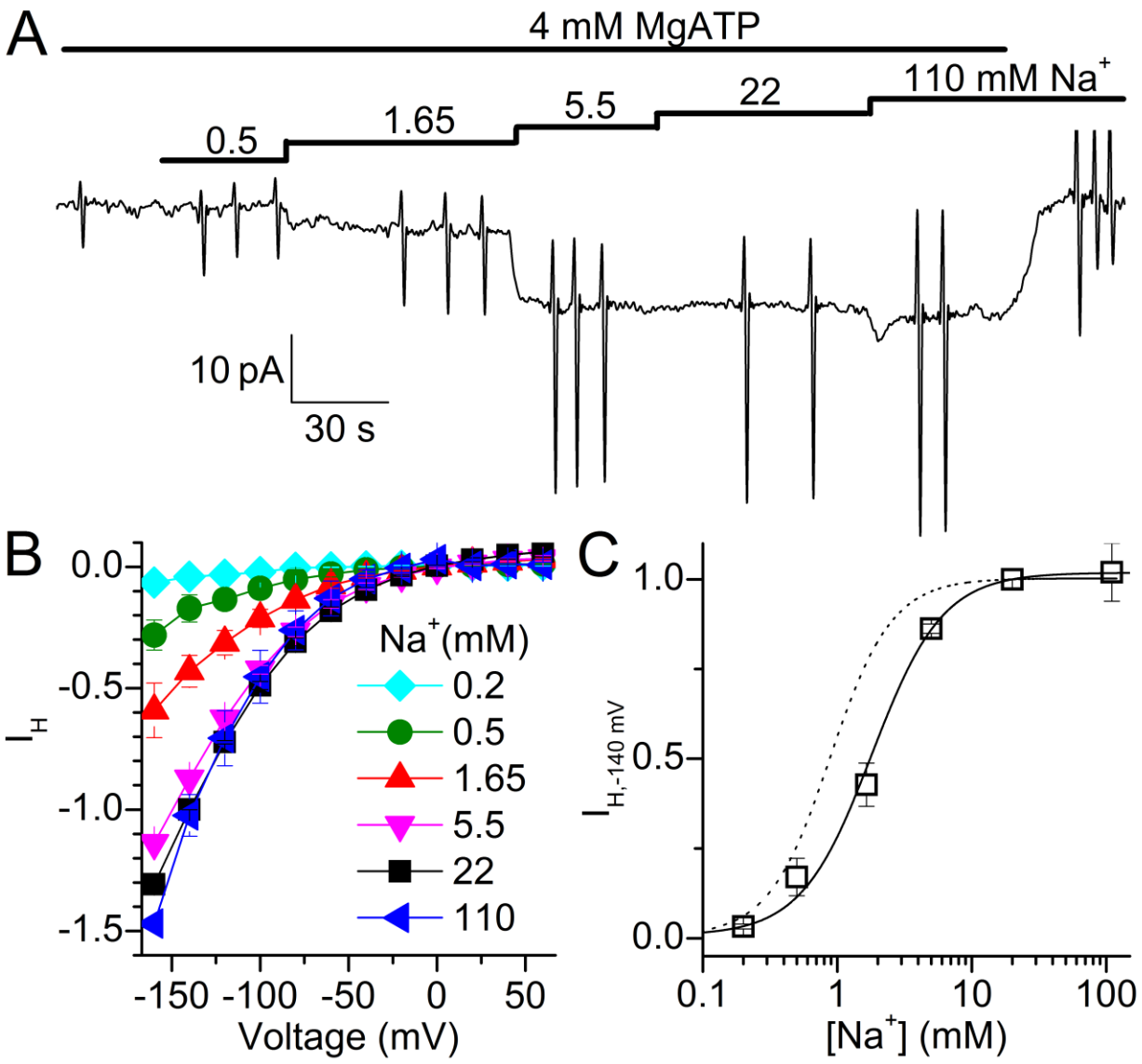

FIGURE 3. *Na^+_i dependence of I_H.* (A) Recording from a patch at V_h = -80 mV in the presence of different [Na^+_i]. (B) MgATP-activated I-V curves at the indicated [Na^+_i], normalized to I_H at -140 mV, 20 mM Na^+_i. (C) I_H at -140 mV as a function of [Na^+_i]. The solid line represents a fit to the Hill function (Eq. 1), with parameters in the text. The dotted line represents a fit of the [Na^+_i]-dependence of charge movement to Eq. 1 (from Ref. (24)). Data in (B) and (C) are means = SEM from four patches.

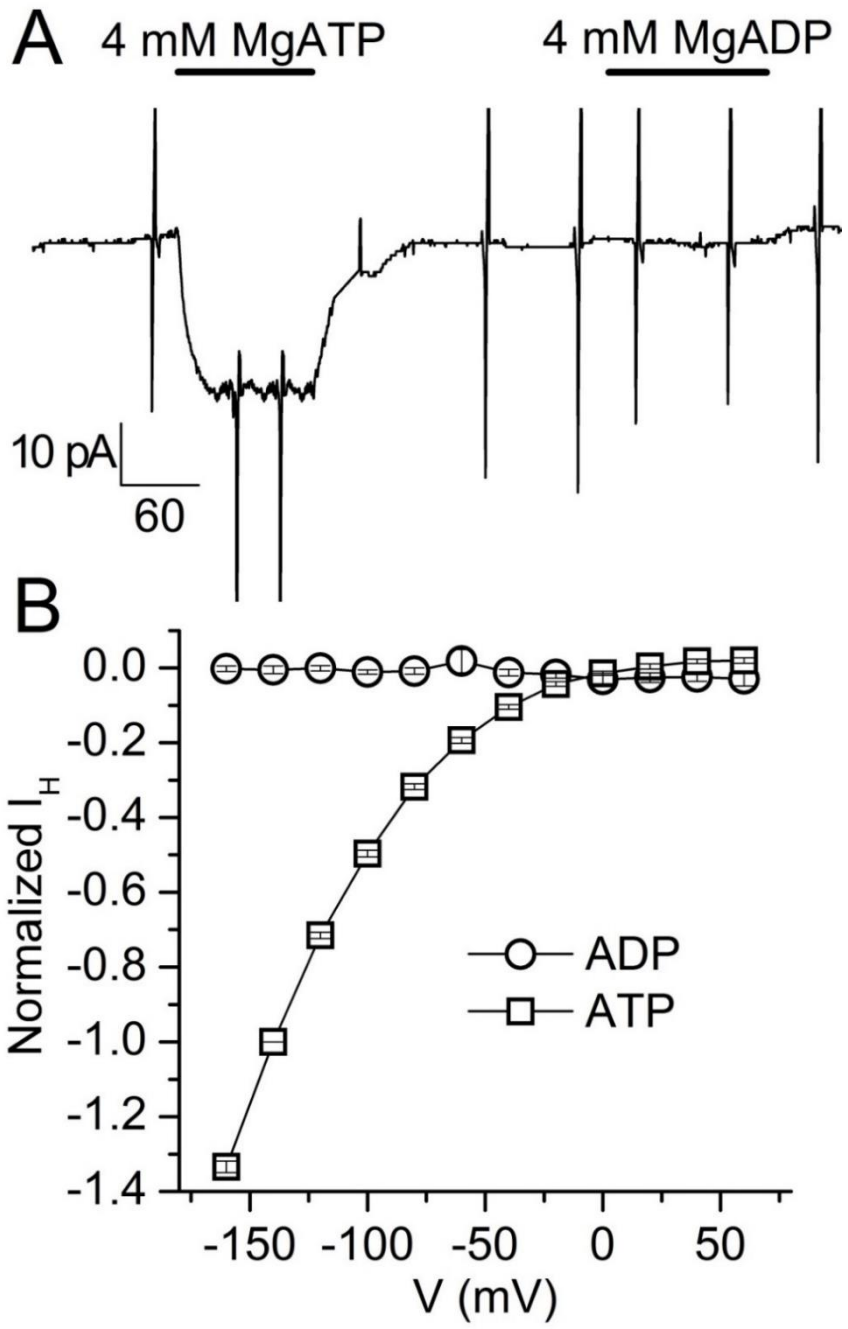

FIGURE 4. *Nucleotide effects on I_H with 20 mM Na^+_i.* (A) Recording from a patch at V_h = -50 mV on which MgATP and MgADP (4 mM) were applied. (B) Nucleotide-induced I_H-V curve normalized to the I_H at -140 mV with MgATP. Data are means 5 SEM from six patches.

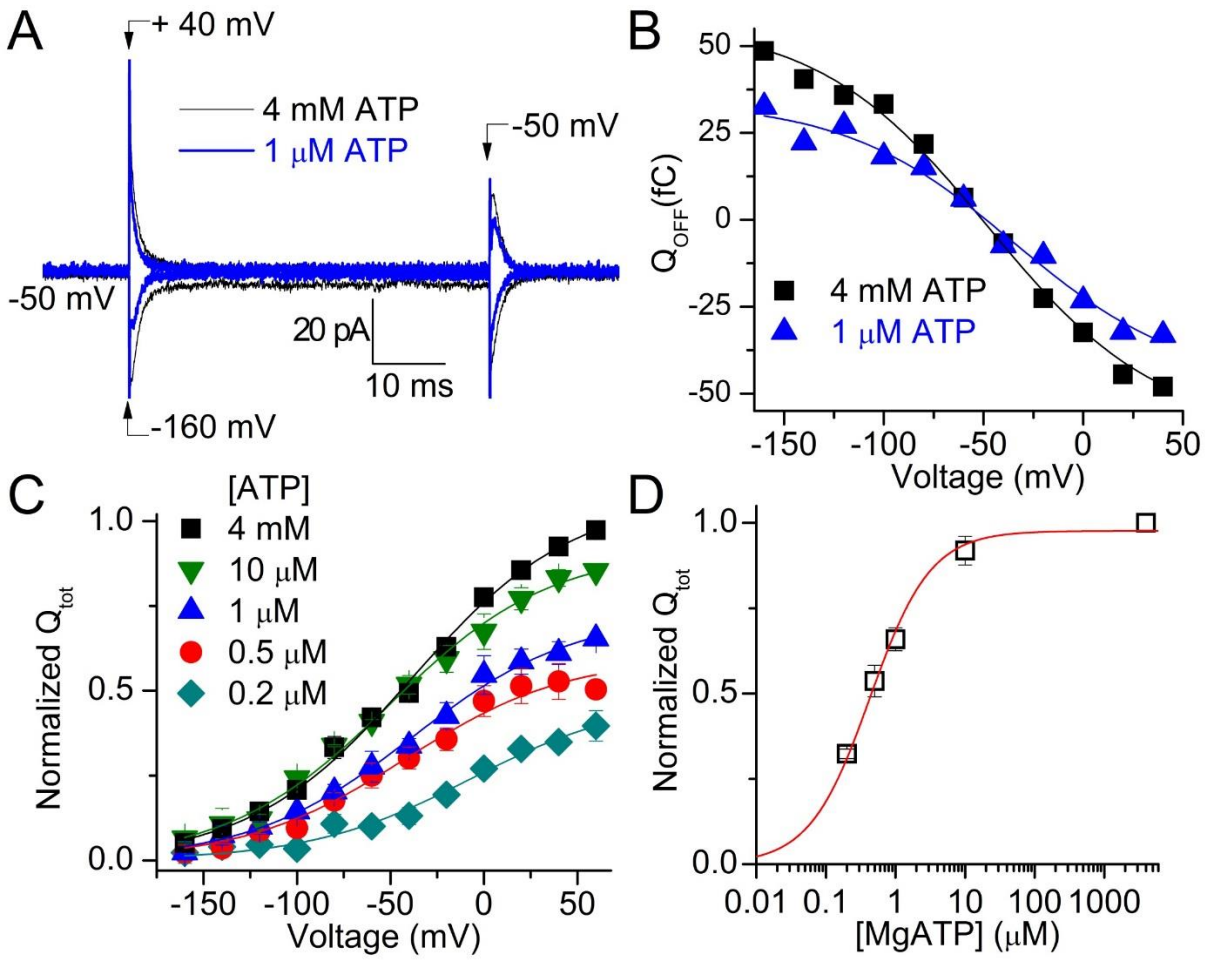

FIGURE 5. *MgATP activation of Q_{Na} in 20 mM Na^+_i, with 125 mM Na^+_o (pH 7.6).* (A) MgATP-induced current (current in ATP minus current without ATP) elicited by voltage pulses from V_h = -50 mV to -160 mV or +40 mV. (B) Q_{OFF}-V curve for the patch in (A). Continuous lines represent global fits using the Boltzmann function (Eq. 2) with a shared slope factor kT/ez_q = 43 mV, Q_{tot} = 81.3 fC, $V_{1/2}$= -35 mV at 1 μM MgATP, and Q_{tot} = 120 fC, $V_{1/2}$ = -41 mV at 4 mM MgATP. (C) Average Q_{OFF}-V curves from five patches in which different [MgATP] were applied, normalized to Q_{tot} at 4 mM MgATP. Lines represent fits of Eq. 2 to the average data; the best fit $V_{1/2}$ values were -7.2 ± 9.0, -42 ± 4.7, -38 ± 5.2, -50 ± 5.2, and -38 ± 4.5 mV for 0.2 μM, 0.5 μM, 1 μM, 10 μM, and 4 mM ATP, respectively.

No clear change in slope factor with [ATP] was observed in individual experiments; therefore, the slope factor was shared in the global fit; kT/ez_q = 43 ± 3 mV. (D) Q_{tot} as a functionn of [MgATP]. Continuous lines represent fits using Eq. 1 (nH = 1) to the whole data set from five patches with $K_{0.5,ATP}$ = 0.43 ± 0.03 µM.

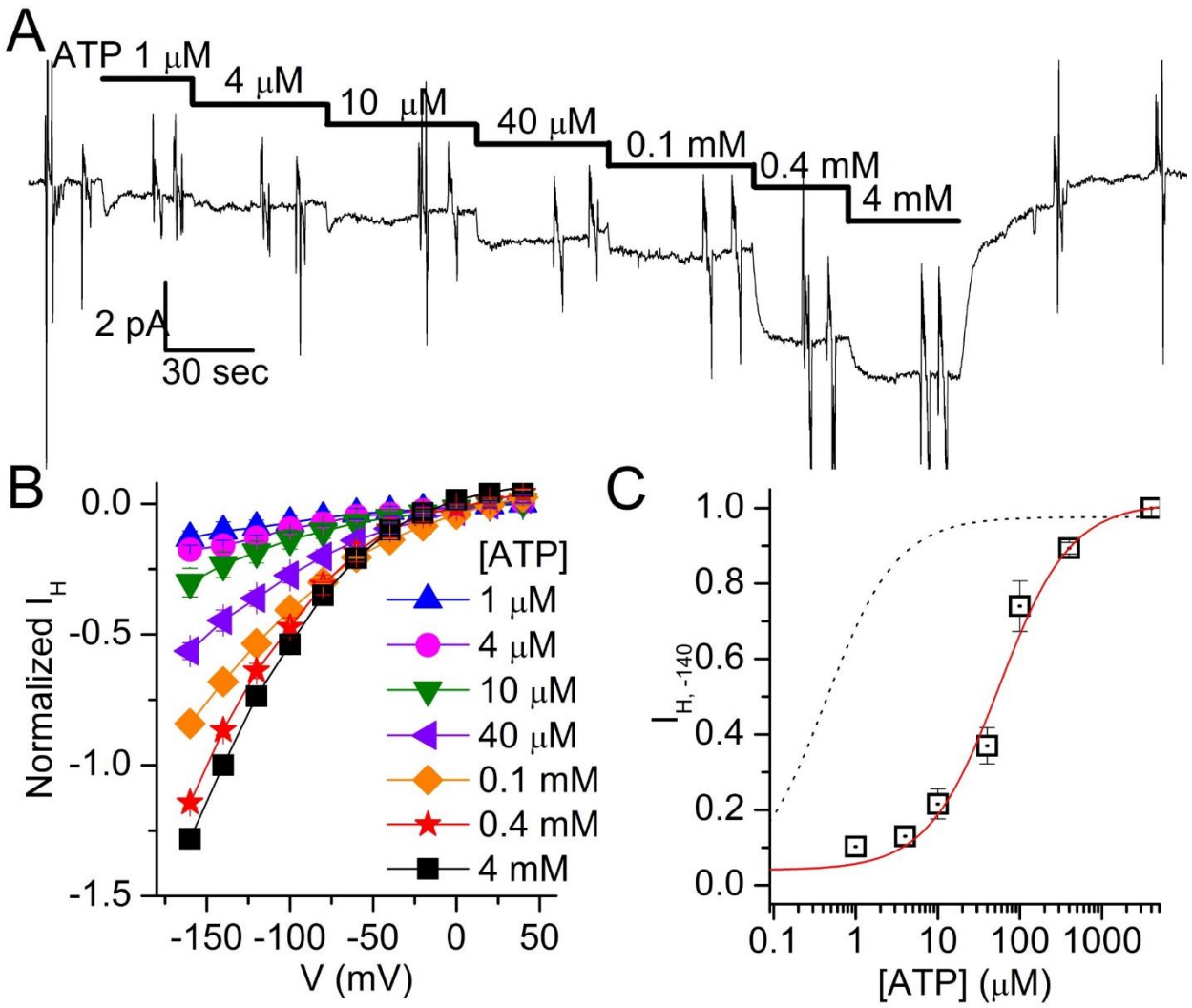

FIGURE 6. *ATP activation of I_H.* (A) Continuous current recording from a patch at V_h = -80 mV, with NMG^+_o (pH 6) in the pipette, to which increasing [ATP] were added in the presence of 20 mM $Na+_i$. (B) Average I_H-V from six patches at different [ATP], normalized to I_H at -140 mV with 4 mM ATP. (C) [ATP] dependence of I_H activation in Na^+_i at -140 mV. The solid line is the fit obtained using a rectangular hyperbola (Eq. 1, nH = 1) with $K_{0.5ATP}$ = 55.8 μM. The dotted line is the fit from Fig. 5 D.

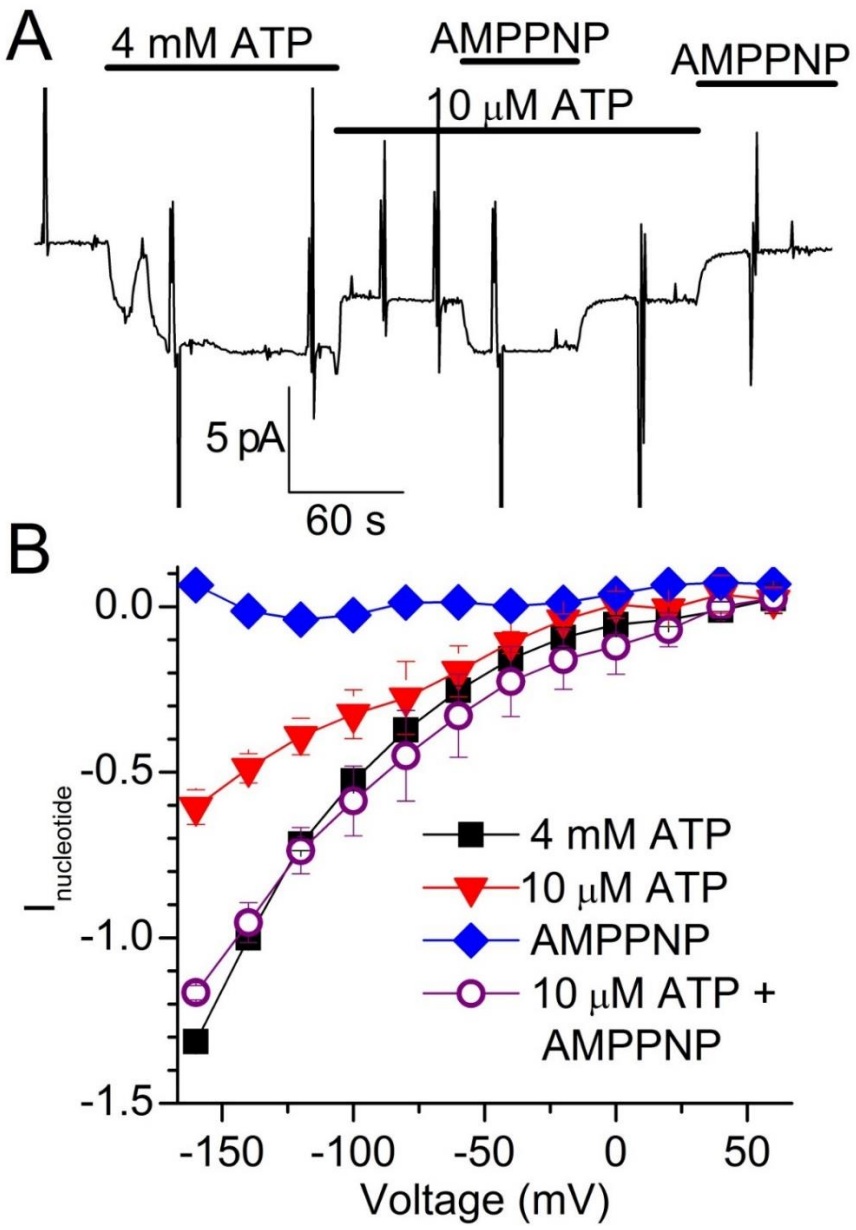

FIGURE 7. *I_H in 20 mM Na^+_i requires phosphorylation and ATP binding.* (A) Recording from a patch at -50 mV on which ATP (10 mM and 4 mM) and AMPPNP (1 mM) were applied as indicated. (B) Average current induced by 4 mM ATP, 10 μM ATP, 1 mM AMPPNP, and 10 μM ATP + 1 mM AMPPNP; data from three patches, normalized to I_H at -140 mV in 4 mM MgATP.

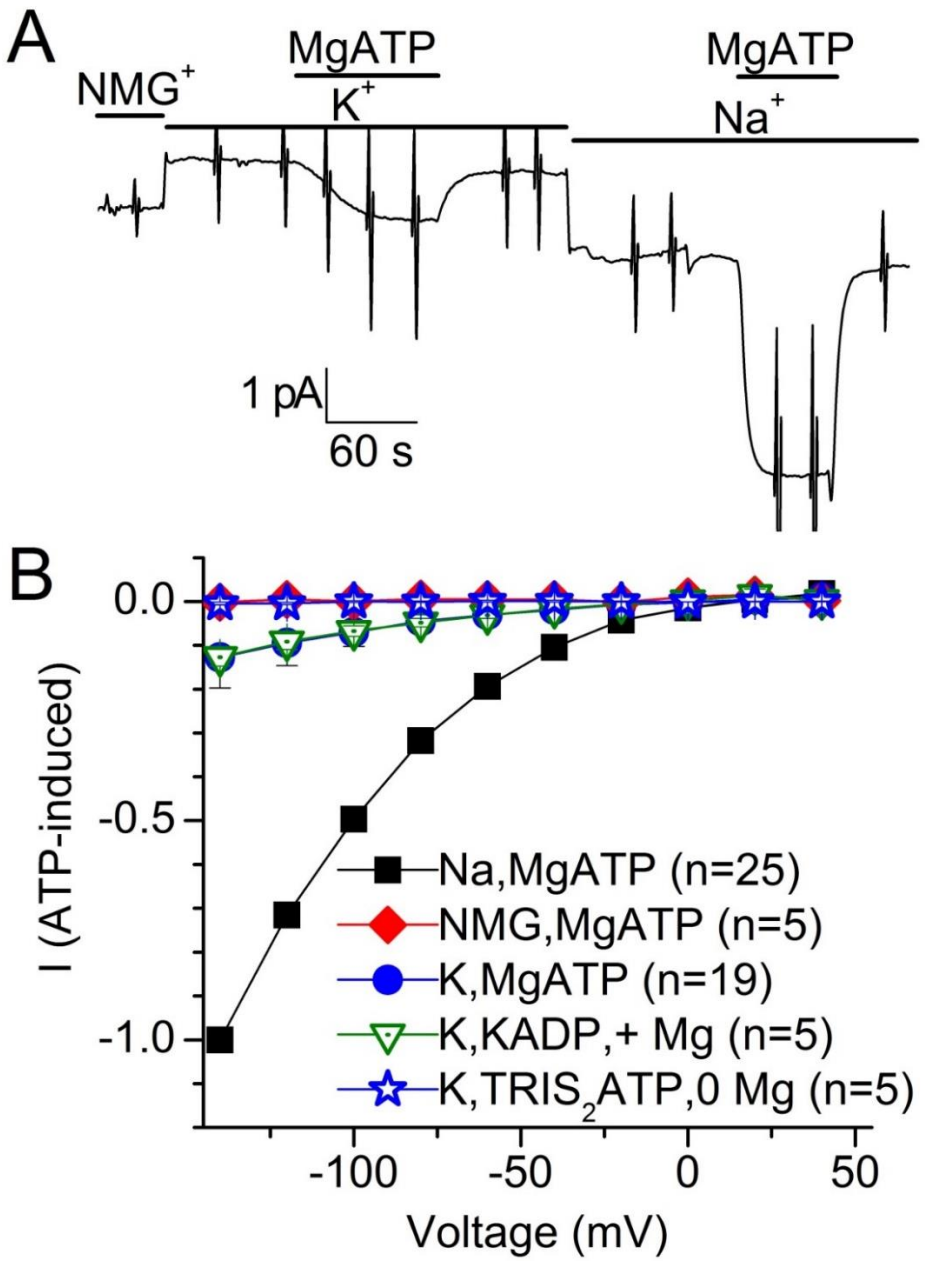

FIGURE 8. *I_H with K^+_i.* (A) Recording from a patch at V_h = -50 mV, with NMG^+_o (pH 6) in the pipette, to which 4 mM ATP was added in the presence of Na^+_i or K^+_i. (B) I_H-V induced by nucleotides (MgATP, K-ADP, or $TRIS_2$-ATP as indicated) in the presence of 110 mM NMG^+_i,20 or 110 mM K^+_i, or 20 or 110 mM Na^+_i, normalized to I_H at -140 mV with 4 mM ATP and Na^+_i. The number of experiments is indicated in parentheses.

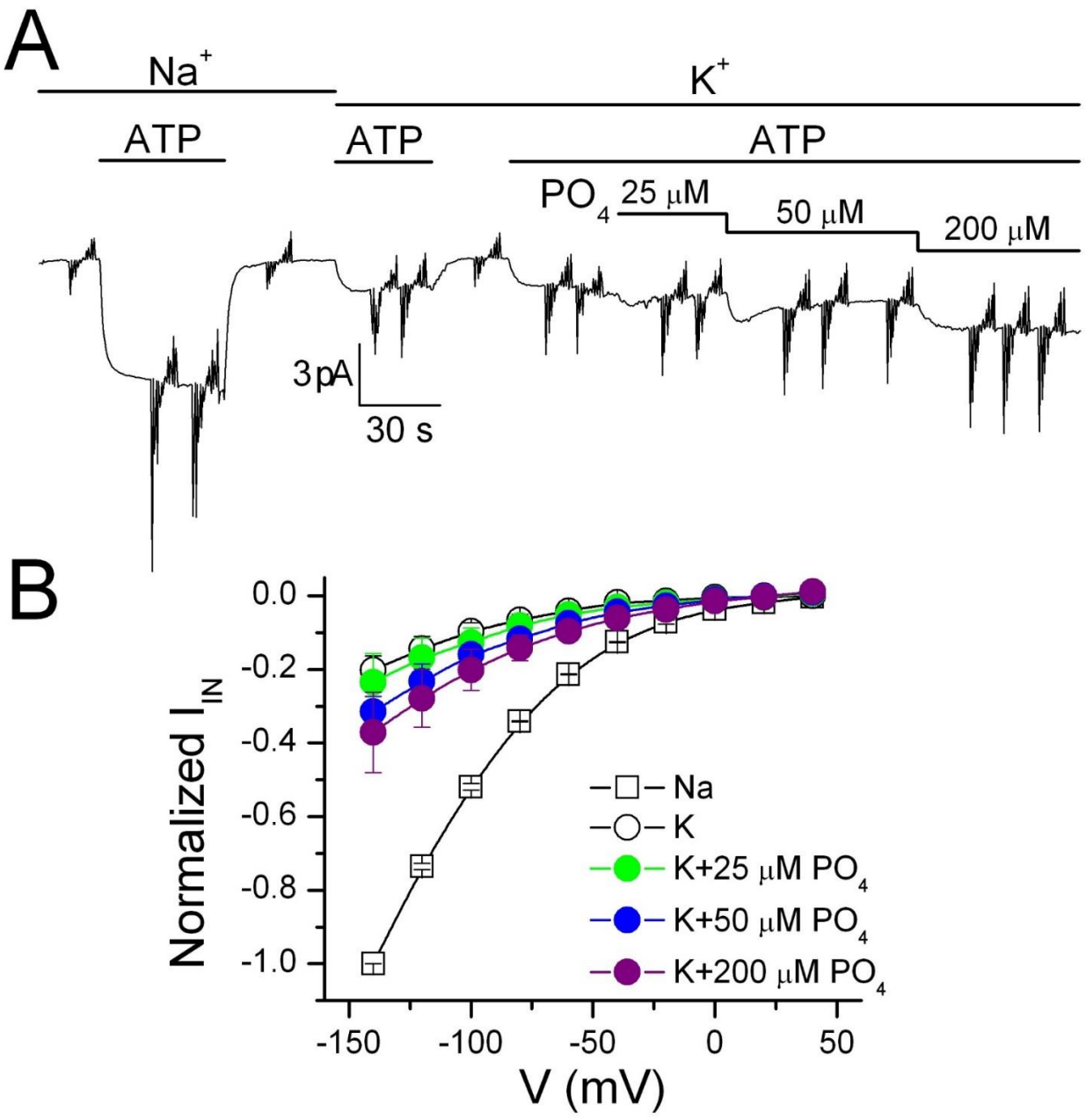

FIGURE 9. *Currents activated by P_i in the presence of MgATP.* (A) Patch recording at -50 mV with NMG^+_o pH 6 in the pipette. I_H was activated by the indicated [P_i] in solution with 20 mM K^+_i and 4 mM ATP. (B) I-V plot showing P_i+ATP-activated I_H normalized to I_H activated by 20 mM Na^+_i+ATP at -140 mV (n = 2).

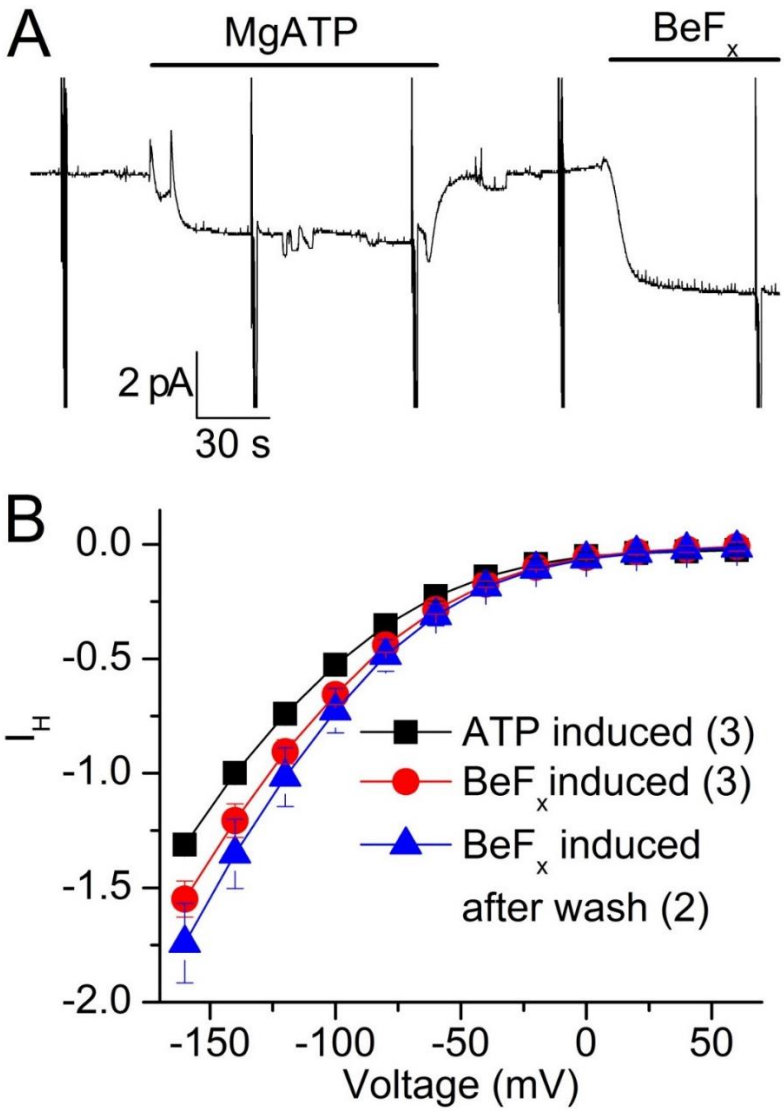

FIGURE 10. *Beryllium fluoride activation of I_H.* (A) Recording from a patch at V_h= -80 mV with NMG^+_o (pH 6) in the pipette, showing activation of inward current by MgATP (4 mM) and by beryllium fluoride (0.5 mM) in the presence of 20 mM Na^+_i. (B) Voltage dependence of the average beryllium-fluoride- or ATP-induced current (n = 3). The beryllium-fluoride-induced I-V curve was obtained after beryllium fluoride withdrawal (n = 3).

CHAPTER III

EXTRACELLULAR ACCESS AND SHARED SITE BINDING MODULATES INWARD PROTON TRANSPORT THROUGH THE NA,K-ATPASE

ABSTRACT

The effects of two distinct organic amines were tested for their inhibitory properties on the Na,K-ATPase (NKA or Na pump) under voltage-clamped conditions. These amines, tetrapropylammonium (TPA) and ethylenediamine (EDA), were shown to inhibit the NKA in two discrete manners. EDA, a divalent organic cation with two titratable amine groups, competitively inhibited extracellular K^+ (K^+_o) in a voltage-dependent manner. TPA, a large quaternary organic cation, competitively inhibited K^+_o in a voltage-independent manner with a similar potency. For Na^+-dependent transient charge movement (Q_{Na}), TPA inhibited in by reducing apparent Na^+_o affinity, while EDA inhibited the total amount of charge moved and appeared to increase the apparent Na^+_o affinity. In the absence of both Na^+_o and K^+_o, passive inward proton current (I_H) was demonstrated to be inhibited by TPA in a concentration dependent manner. EDA however, had no effect on I_H at pH 7.6 and accentuated at pH 6.0. The effects with EDA all independently binding may be at or near the shared sites (possibly occluded), we therefore tested the biochemical effects of EDA on phosphorylation and in tryptic digestion kidney NKA. Following a 50 minute trypsin digestion, EDA stabilized a ’19-kDa’ C-terminal fragment known to contain occluded K+, which TPA was unable to stabilize. EDA was also able to dephosphorylate the NKA similar to that of K^+, while EDA and Na^+ stabilized the phosphorylated NKA. These results are the best to date that EDA becomes occluded within the shared sites.

INTRODUCTION

The maintenance of ionic gradients across the cell membrane is pivotal for cell function and survival. The Na,K-ATPase (Na pump or NKA), a member of the P-Type ATPase family of transporters, is responsible for maintaining Na^+ and K^+ gradients in most animal cells. The Na^+ gradient established and maintained by the Na pump is also involved in pH balance, cell volume regulation, and secondary active transport. The NKA exports 3 Na^+ ions and imports 2 K^+ ions via a series of fully reversible conformational changes (1,2), where two ion binding sites (shared sites) reciprocally bind 2 Na^+ or 2 K^+, while the third ion binding site solely binds Na^+ (Na-exclusive site) (3,4). This enzyme alternates between two predominant conformations, internally open (E1) and externally open (E2). Briefly, the Na pump cycle follows the Albers-Post scheme (1,2) being phosphorylated by ATP upon internal binding of 3 Na^+ ions (E1P), inducing a conformational change to outward facing (E2P) where the 3 Na^+ ions are released (Fig. 1). Next, 2 K^+ ions bind externally to the shared sites facilitating dephosphorylation as the K^+ ions become occluded within the enzyme. The rate limiting step in the cycle is the conformational change back to E1 with the deocclusion of K^+ to the cytoplasm, which is accelerated by low affinity ATP binding (5).

The Na pump is electrogenic in nature, extruding +1 net charge per cycle (6), which can be measured electrophysiologically as outward pump current (I_P), under normal ionic conditions (i.e. external K^+ and internal Na^+). Similarly, individual steps within the cycle can be monitored through their distinct electrical signals. For example, transient charge movement (Q_{Na}) in the presence of external Na^+, and absence of external K^+, characterizes the binding, occlusion, and release of Na^+ within the protein during

transitions from E2P to E1P($3Na^+$) (7-9). Similar binding, occlusion and release of extracellular K^+ has been documented in the presence of high intracellular and extracellular K^+, devoid of both internal and external Na^+, (10,11).

In our recent work, we identified the intracellular requirements for I_H (16), demonstrating the Na pump must be in the E2P conformation for the proton influx to occur, in agreement with other investigators (4,14,15,17-20). Each of the groups studying Na pump mediated I_H have concluded independently that the Na-exclusive site is the probable location of extracellular proton access (4,14-20). Poulsen et al. (21) and Azizan et al. (22) have suggested pathophysiological implications of this inward current is present in hyperaldosteronism-inducing mutations (22), as well as one mutation identified in familial hemiplegic migraine (21). According to the high-resolution crystal structures of the Na pump, these mutations in either the Na-exclusive site or shared sites, altering ion affinity, I_H and membrane potential (21-23).

Our understanding of ion binding and selectivity within the Na pump, as well as how the extracellular facing shared sites relate to I_H through the Na^+ exclusive site, remain unclear. Two amines, tetrapropylammonium (TPA) and ethylenediamine (EDA) have been used extensively in biochemical binding competition studies of NKA (24-30). TPA competes with extracellular K^+ and is incapable of binding intracellularly (24, 27-29), while EDA has been shown to competitively inhibit both K^+-activated ATPase activity and Na^+-activated phosphorylation (27-30). The use of these two amines in combination will enhance our understanding of Na^+ and K^+ ion binding and selectivity, as well as allow us to identify extracellular shared site binding effects on I_H, without the complications associated with Na^+ and K^+ binding (e.g. forward and reverse cycling).

In this study, we used Two-Electrode Voltage Clamp (TEVC) on *Xenopus laevis* oocytes heterologously expressing ouabain-resistant Na pumps, along with biochemistry on purified Ovine kidney Na pump, to study the extracellular mechanism of I_H. We found that both TPA and EDA compete with K^+ to inhibit I_P, but only EDA inhibition is voltage-dependent. Surprisingly, the two compounds had opposite effects on I_H; TPA blocked I_H at both pH 7.6 and pH 6.0, whereas EDA had no effect at pH 7.6 and accentuated I_H at pH 6.0. With respect to Q_{Na}, TPA reduced extracellular Na^+ affinity, while EDA inhibited Q_{Na} by reducing the total charge moved and appearing to increase Na^+ affinity, similar to K^+. Previous reports suggest that EDA might be occluded like K^+ ions (26, 27), thus we tested this possibility biochemically, finding EDA, like K^+, accelerated dephosphorylation of EP, in contrast to TPA which stabilized EP. Tryptic digestion experiments also revealed that EDA binding puts NKA in a unique conformation that retards protease efficiency. The ion binding effects on the rate of trypsinolysis of NKA proceed with Na > TPA > K > EDA. EDA stabilized the K^+-protectable '19-kDa' C-terminal fragment from tryptic digestion, while TPA (like Na^+) did not stabilize this fragment. In addition, EDA stabilized several larger fragments from tryptic digestion suggesting that the enzyme conformational mobility might be more restricted with EDA bound than with K^+ bound. These data are the strongest to date suggesting that EDA can be occluded within the NKA shared sites.

The separate inhibitory qualities of TPA and EDA reveal that the extracellular vestibule and the shared sites proper have different modulatory actions on I_H. TPA binding within the vestibule opening, which narrows towards the shared sites, inhibits I_H presumably by preventing direct access to the Na-exclusive site. EDA on the other hand appears to bind directly within the shared sites which is permissive to I_H through the Na-

exclusive site and even stimulatory at pH 6.0. Our current work provides evidence that 1) H^+ ions utilize the common access pathway of the extracellular vestibule to enter the Na-exclusive site for I_H, 2) and shared site binding modifies I_H, 3) TPA and EDA inhibition occur in separate regions of the extracellular vestibule, and 4) EDA is potentially occluded within the shared sites.

MATERIALS AND METHODS

Oocyte preparation and molecular biology

As described by Ratheal et al. (31) oocytes were enzymatically isolated by 1-2 hr incubation (depending on degree of desired defolliculation) in Ca^{2+}-free OR2 solution at pH 7.4 (in mM: 82.5 NaCl, 2 KCl, 1 $MgCl_2$, 5 HEPES) with 0.5 mg/mL collagenase Type IA. Enzymatic treatment was followed by four 15-min rinses in Ca^{2+}-free OR2 and two rinses in OR2 with 1.8 mM Ca^{2+}. The ouabain-resistant *Xenopus* Q120R/N131D (RD)-α1 and the β3 subunit, both in the pSD5 vector, were linearized with *Bgl*II and transcribed with SP6 mMessage machine (Ambion). Oocytes were injected with an equimolar mixture of cRNA for RD-α1 and β3 cRNA and then maintained in SOS solution (in mM: 100 NaCl, 2 KCl, 1.8 $CaCl_2$, 1 $MgCl_2$, and 5 HEPES), supplemented with horse serum and antimycotic-antibiotic solution (Anti-Anti, Gibco), at 16°C for 2-6 days until recording. The RD double substitution mimics the residues responsible for the naturally-ouabain-resistant rat-α1 subunit (32), allowing for selective inhibition of endogenous pumps with 10 μM ouabain and enabling measurements exclusively from exogenous pumps.

Solutions

Oocytes were Na-loaded by 1-h incubation in a solution containing (in mM) 150 HEPES, 20 tetraethylammonium-Cl, and 0.2 EGTA (pH 7.2 with NaOH) until experimentation. Extracellular hydroxide solutions contained in mM: 133 methane sulfonic acid (MS), 5 $Ba(OH)_2$, 1 $Mg(OH)_2$, 0.5 $Ca(OH)_2$, titrated with 125 NMG^+, 125 NaOH or 120 EDA. Extracellular chloride solutions contained in mM: 5 BaCl2, 1 MgCl2, 0.5 CaCl2, and 125 NaCl, 120 TPA-Cl or 133 HCl titrated with 125 NMG^+. Solutions were buffered with 10 HEPES at pH 7.6 and 10 MES at pH 6.0. Intermediate TPA-Cl and EDA

concentrations were achieved by mixing with external NMG-Cl or NMG^+ respectively. External K^+ was added from a 3 M K-MS stock. Osmolarity of all recording solutions was 250-260 mosmol/kg.

Electrophysiology

An OC-725C amplifier (Warner Instruments, Hamden, CT), a Digidata 1550 A/D board, a Minidigi 1A, and pClamp 10 software (Molecular Devices) were used for Two-Electrode Voltage-Clamp recordings. Signals were filtered at 2 kHz and digitized at 10 kHz. Resistance of both microelectrodes (filled with 3M KCl) was 0.5–1 MΩ.

Data analysis

All apparent affinities ($K_{0.5}$) were obtained by fitting the data to the Michaelis Menten equation (Eq. 1): $I = I_{max}\ ([S]^{n_H}/(K_{0.5}^{n_H} + [S]^{n_H}))$ (Eq. 1). All half maximal inhibitor affinities (IC_{50}) were obtained by fitting the date to a modified Michaelis Menten (Hill1) equation (Eq. 2): $I = I_{min} + (I_{max} – I_{min})\ ([S]^{n_H}/(K_{0.5}^{n_H} + [S]^{n_H}))$ (Eq. 2). Transient charge (Q_{Na}) movement was obtained by integrating the area under the relaxation curve in the ON (as in ref. 24). Charge vs. voltage (Q-V) curves were fit with a Boltzmann distribution (Eq. 3): $Q = Q_{hyp} - Q_{tot}/(1 + e^{(V-V_{1/2})/k})$ (Eq. 3), where Q_{hyp} is the charge moved by hyperpolarizing voltage pulse, Q_{tot} is the total charge moved, $V_{1/2}$ is the center of the distribution and k is the slope factor. Differences between treatment conditions in EP measurements (Fig. 9) were analyzed using a One-Way ANOVA, with a significance at P = 0.01.

Na,K-ATPase purification from sheep kidney

Na,K-ATPase (NKA) was purified from sheep kidney as described by Costa et al. (33). Briefly, the outer medulla was dissected from sheep kidneys and homogenized in a blender with 250 mM sucrose in Buffer C: 25 mM imidazole, and 1 mM EDTA (pH 7.2).

The homogenate was centrifuged at 4°C for 20 min at 9,000 rpm. The supernatant was again centrifuged at 4°C for 45 min at 16,000 rpm, and the pellet (microsomes) resuspended in Buffer C, and protein concentration determined by Bradford Assay. The microsomes were then diluted to 10 mg/mL, incubated for 10 min at room temperature in ATP-treatment solution: 6 mM Na_2ATP, 12 mM Tris, 1 mM Na_2EDTA, 1 mM $NaHCO_3$, 25 mM imidazole, and 1 mM EDTA (pH 7.2), followed by 10 min incubation at room temperature in ATP-treatment solution with 0.3% sodium dodecyl sulfate (SDS). Treated microsomes were then layered on top of a three-step sucrose gradient (in Buffer C) 15%, 25%, 45% and centrifuged in a swinging bucket rotor (Beckman SW-28) at 4°C for 2.5 hours at 25,000 rpm. Collected membrane fractions at the 25-45% interface were brought up to 50 mL of Buffer C, centrifuged at 4°C for 1 hour at 70,000 rpm and pellets resuspended in Buffer C containing 250 mM sucrose. Protein concentration was determined with a Bradford Assay.

Proteolytic cleavage, gel electrophoresis and immunoblot

Proteolytic cleavage was performed as described by Mares et al. (34), using 150 µg of purified NKA membranes pre-incubated with 30 mM histidine, and 1 mM EDTA (pH 7.0) for 30 min at 24°C along with either (in mM) 20 KCl, 120 EDA, 60 TPA, or 120 NaCl. Following this incubation, 20 µg of trypsin (Sigma) was added and mixtures incubated at 37°C between 15 min and 1 hour. Proteolysis was terminated with SDS sample buffer (150 mM Tris, 2.4 M Urea, 3% SDS, and 0.01% Bromophenol Blue, pH 7.2). Treated NKA membranes were ran on 15% SDS-polyacrylamide gel electrophoresis (PAGE) at constant 4°C in 250 mM Tris, 2 M Glycine, and 1% SDS, with 10 µg of each treatment and ran at constant voltage. After electrophoresis, the gel was transferred to a

Nitrocellulose membrane in a solution containing 10 mM CAPS (pH 11.0), 10% methanol, at 180 nA for 2 hours. Membrane was blocked with Soy Milk (35), probed and incubated with anti-KETYY antibody (gift from Jim Kyte, University of California, San Diego) overnight. The primary antibody was washed three times with phosphate-buffered saline + 0.1% Tween-20, incubated for 1 h with HRP-conjugated goat anti-mouse antibody and washed three times with phosphate-buffered saline + 0.1% Tween-20. Bands were detected via supersignal substrate kit (Pierce, Rockford, IL) according to the manufacturer's protocol.

Phosphorylation by [^{32}P]ATP

The amount of EP was determined similarly to methods reported previously (24). These experiments dealt with whether inhibitors would prevent or facilitate dephosphorylation of E2P. In these experiments, EP was first formed by incubating ~25 µg of purified enzyme in 10 mM NaCl (or 10 mM KCl as a control), 145 mM choline chloride, 35 mM Tris, 3.5 mM MgCl2, pH 7.5 and 10 µM [^{32}P]ATP on ice for 1 min. Next, indicated [choline chloride], 10 mM EDTA and 25 mM KCl, 120 mM EDA or 60 mM TPA were added and incubated for an additional 30 seconds on ice. As a control, purified enzyme was incubated in EP forming solution with 2 mM ouabain, without [^{32}P]ATP for 2 minutes prior to incubation in the [^{32}P]ATP solution indicated above on ice for 1 min followed by 30 second incubation in 120 mM choline chloride and 10 mM EDTA on ice. Each reaction was quenched by adding 5% trichloroacetic acid, 3 mM Tris-Pi and 1.5 mM Tris-ATP, filtered through a 0.45 µm filter and washed three times in the same solution. Each condition was assayed via liquid scintillation spectroscopy in triplicate. All analyses were performed using pClamp and Origin (OriginLab Corp., Northampton, MA).

RESULTS

Organic amine inhibition of K^+-activated current

TEVC was performed on oocytes expressing ouabain-resistant RDα1-β3 NKA to determine whether TPA and EDA inhibit K^+_o-induced pump current (I_P) under our conditions. Both TPA (Fig. 2A) and EDA (Fig. 2B) inhibited K^+_o-induced I_P across voltages from -180 mV to +40 mV (Fig. 2). The IC_{50} values for TPA and EDA on I_P inhibition in the presence of 3mM K^+ were calculated (via Eq. 2) and plotted as a function of voltage (Fig. 2C). TPA inhibited I_P in a voltage-independent manner, whereas EDA inhibited in a voltage-dependent manner (Fig. 2C). TPA inhibited I_P in a dose-dependent manner with a maximum inhibition of 68.2 ± 4.8% at -180 mV and 78.6 ± 7.7% at +40 mV (Fig. 2A). EDA was a more effective inhibitor of I_p at 82.5 ± 2.9% at -180 mV and 87.3 ± 2.0% at +40 mV (Fig. 2B). The K^+_o-dependence of I_P was determined in the absence (black circles) and presence of either 10 mM TPA (red squares) or 10 mM EDA (blue triangles) (Fig. 3). The average currents at 0 mV were fitted to Eq. 1 to determine the $K_{0.5}$ for K^+ in each condition, revealing that apparent affinity for K^+ was increased by both inhibitors ($K_{0.5,K^+}$ was 0.24 ± 0.03 mM, 1.77 ± 0.36 mM, and 1.92 ± 0.25 mM in NMG, TPA, and EDA, respectively), yet V_{max} was not reduced (Fig. 3A). Thus, both inhibitors show competition with extracellular K^+, consistent with previous biochemical studies (24-30). Plotting $K_{0.5}$ for K^+ as a function of voltage in the absence and presence of the organic amines, revealed a slight voltage-dependence for the $K_{0.5,K^+}$ in NMG, which was greatly accentuated in the presence of TPA, and nullified in the presence of EDA (Fig. 3C).

Inhibition of I_H by TPA

Figure 4A shows a continuous recording from an RDα1-β3 NKA expressing oocyte; extracellular K^+ application produced outward current confirming pump plasma membrane expression (Fig. 4A, upward deflection). Application of extracellular NMG solution at pH 6.0 induced a passive H^+ influx (I_H), consistent with previous reports (13,15,18). TPA application reduced this I_H in a concentration dependent manner (Fig. 4) at both pH 6.0 and 7.6 (Fig. 4B and 3C, respectively). At hyperpolarizing voltages (-180 to -80 mV) maximal TPA inhibition of I_H at pH 7.6 and 6.0 was 66.5% ± 0.5 and 54.4% ± 0.1, respectively (Fig. 4D). The IC_{50} values for TPA inhibition of I_H at pH 7.6 (5.93 ± 0.82 mM) and 6.0 (5.98 ± 0.77) were obtained by fitting the data to equation 2; the values were similar to the TPA IC_{50} for I_P inhibition (Fig. 2C) as well as ATPase inhibition of the NKA (24). At pH 7.6, there was nearly a two-fold increase in TPA affinity between -180 mV and -80 mV (Fig. 4E, filled squares), with no voltage-dependent change in TPA affinity at pH 6.0 (Fig. 4E, open squares).

Multifaceted effects of EDA on I_H

Since both TPA and EDA competitively inhibit extracellular K^+ binding (Fig. 3A and 24-27,30), we hypothesized EDA, like TPA, would inhibit I_H. However in contrast to TPA, EDA enhanced I_H in a dose-dependent manner at pH 6.0 (Fig. 5A), augmenting I_H by 35% at -80 mV and 115% at -180 mV (Fig. 5B). Paradoxically, EDA did not alter I_H at pH 7.6 (Fig. 5C). The data for EDA activation of I_H at pH 6.0 were fitted to Eq. 1 to determine the apparent affinity ($K_{0.5}$), which remained relatively constant across voltages (4.36 ± 1.17 mM and 5.35 ± 1.86 mM at -180 and -80 mV, respectively) (Data not shown). However,

ethylamine (1 titratable nitrogen group) was shown to only inhibit I_H at both pH 7.6 and 6.0 (Supplemental Fig. 2).

With 2 distinct pKa values of 10.71 and 7.56 at 0°C (36), EDA is dually protonated at pH 6.0, while at pH 7.6 there are a portion of molecules either singly or dually protonated. The lack of effect at pH 7.6 may be due to both singly and dually protonated EDA counteracting eachother for activation and inhibition. This lead us to study the effect of EDA on I_H at pH 8.6, in an attempt to elucidate the effects of EDA while singly-protonated. At pH 8.6 however, I_H cannot be measured as the NKA produces outward current in the absence of K^+ (presumably H^+ efflux) when oocytes are intracellularly loaded with Na^+ at pH 7.4 (31). However at pH 8.6, a measureable passive inward current at negative voltages has been shown and appears to be carried by, guanidinium (I_{Gua}) through the Na-exclusive site (31,37). In these conditions, we show the I_{Gua} at pH 8.6 is inhibited by EDA (Fig. 5D).

Organic amine inhibition of Na^+-induced transient charge movement (Q_{Na})

TPA and EDA exhibited different properties in transient charge movement (extracellular binding and release of Na^+) (Q_{Na}) (7-9). Figure 6 illustrates ouabain-sensitive Q_{Na} in the absence (5A) and presence of 20 mM TPA (5B). TPA had two pronounced effects: first, it reduced total transient charge moved at positive voltage with an increase in the total charge moved at negative voltages, and second, it reduced the rate of NKA relaxation at negative voltages. The effect of TPA on Q_{ON}, regarding both charge distribution (Q_{Tot}) as a function of voltage (Q-V) and relaxation rates, are shown in figures 5C and 5D, respectively. A -25mV shift of the center of the charge distribution curve (i.e. the $V_{1/2}$) is approximately a 2-fold reduction in Na^+_o apparent affinity (9,38).

Thus, TPA reduced external Na^+ affinity by approximately 2-fold, 4-fold and 8-fold at 5 mM, 10 mM and 20 mM TPA, respectively (Fig. 6C). TPA also reduced NKA relaxation rates at negative voltages in a dose-dependent manner (Fig. 6D).

Experiments were repeated individually with EDA (Fig. 7A) and K^+ (Fig. 7B), both of which had effects opposite to those observed with TPA. EDA reduced the total number of charges moved in a dose-dependent manner and shifted the $V_{1/2}$ towards more positive voltages (Fig. 7A), consistent with an apparent increased affinity for extracellular Na^+. There was a total reduction of ~2/3 in total charge with 15 mM EDA (saturating osmolarity), which may be indicative of the combinatorial binding of $1EDA^{++}$ with $1Na^+$, inducing charge movement. To get at this question we reduced external [Na^+] from 125 mM to 60 mM (-25 mV shift, with no total charge reduction), allowing us to use a higher [EDA] without altering osmolarity (Data not shown). The ability of 15 mM EDA to reduce Q_{Na} at 60 mM [Na^+_o] was 65.8 ± 3.2%, while 60 mM EDA inhibited 84.0 ± 1.7% (Data not shown).

Like EDA, the presence of K^+_o reduced the total charges moved in a concentration-dependent manner (Fig. 7A). Addition of K^+ also shifted the $V_{1/2}$ to the right suggesting an apparent increase in extracellular Na^+ affinity by 1.5-fold and 3-fold in 1.0 mM and 3.0 mM K^+, respectively (Fig. 7B). One difference between EDA and K^+ in Q_{Na} (outside of cycling) is that while K^+ did not affect relaxation rates (Fig. 7D), EDA slowed at voltages above -20 mV, -60 mV, and at all voltages in 1 mM, 5 mM and 15 mM, respectively (Fig. 7C). These results, when compared to K^+, are indicative of EDA potentially becoming occluded within the shared sites.

C-terminal stabilization of the NKA α-subunit by EDA

K^+ occlusion has been shown to stabilize a C-terminal fragment of the NKA α-subunit against trypsin digestion (34,39,40). We digested purified renal Ovine NKA with trypsin in the presence of either 20 mM KCl, 120 mM EDA or 60 mM TPA (Fig. 8) (see materials and methods). TPA and KCl both stabilized a ~40 kDa and ~19 kDa C-terminal fragment at 10 minutes, however while KCl was able to maintain these stabilized fragments at 25 and 50 minutes, TPA was not (Fig. 8). EDA stabilized the same '19 kDa' fragment at each time interval, but protected the α-subunit from tryptic digestion better than any other ligand (Fig. 8). These data are consistent with EDA becoming occluded within the shared sites similar K^+ ions (39,40).

Dephosphorylation of NKA by EDA

The likelihood that EDA might be occluded prompted us to test whether it was able to facilitate dephosphorylation of EP in the forward direction analogous to K^+ (Fig. 9). In the pump cycle (Scheme 1), the conformational change induced by the occlusion of K^+ ions from the outside concomitantly facilitates the hydrolysis of the EP conformation (5). Figure 9A shows the residual level of EP following treatment with various ligands. Compared to no ligands (i.e. ChCl), TPA stabilized EP to the greatest extent as previously demonstrated (24). Excess Na^+ also stabilized EP but was not nearly as effective as TPA. (Fig. 9A). Figure 9B shows that EDA accelerated dephosphorylation to the same extent as K^+, as expected if EDA becomes occluded within the shared sites.

DISCUSSION

Crystallographic studies of the NKA ion binding sites, has provided a valuable framework for understanding the mechanism of ion binding and coordination (3,4,41-46). Although ion coordination and selectivity has only recently been explored, our group has been directly involved with identifying both non-canonical ion/metal transport and amino acid residues that play a role in ion interaction within the NKA (15,16,31,37,47,48). Our most recent report demonstrated the intracellular mechanistic of I_H requires externally open E2P conformational state as the access pathway through the NKA (16), in agreement with prior reports (14,15,17-23,37,49,50). We have also attempted to elucidate a mechanism of action extracellularly (15), however this question is much harder to get at, due to the transport properties of monovalent cations. Other extracellular studies have identified specific residues within the Na-exclusive site to be the pathway which H^+ ions traverse through the NKA (17,18), however extracellular access and involvement of the shared sites has yet to be elucidated. The shared sites have been proposed to be a site of inhibition of I_H by 2 H^+, 2 K^+ or 2 Na^+ ions through either binding or inducing a conformational change while at hyperphysiological [H^+] (e.g. pH 5.0) (15). However, these effects are difficult to reconcile due to the variability within the NKA in such acidic conditions (15).

Along with I_H, canonical Na^+ and K^+ binding have also been studied using biochemical tools, primarily inhibitors. The most common NKA inhibitors (i.e. trypsin, chymotrypsin, quaternary amines, vanadate) have been used in order to better understand properties of ion binding and enzymatic function (24-31,39,40,51-53,57,59). We initially set out to study the effects of shared site occupancy on I_H using TPA, a well-

documented extracellular competitive inhibitor of K^+ (24-26,30) in combination with mixed type extra/intracellular inhibitor EDA (27-30). However, in studying these two inhibitors they both presented unique inhibitory effects on IP, QNa and IH. These effects lead us to attempt to elucidate, biochemically, how these compound's properties differ in their ability to inhibit the NKA. Our current work provides evidence that 1) H^+ ions utilize the common access pathway of the extracellular vestibule to enter the Na-exclusive site for I_H, 2) and shared site binding modifies I_H, 3) TPA inhibition at the surface of the extracellular vestibule is distinct from that of EDA and benzyltriethylamine (BTEA), and 4) EDA is potentially occluded in a non-conformationally selective manner (Fig. 10).

Inhibitory effects of K^+ binding by TPA and EDA

While TPA and EDA both compete with extracellular K^+ binding (24-30), we demonstrate that they do so in different ways. TPA has similar inhibitory properties to tetraethylammonium (TEA), inhibiting K^+-activated pump current in a voltage-independent manner (52,53), while EDA inhibited I_P in a voltage-dependent manner. Similar to the $K_{0.5}$ for K^+ (11,12,49,54-56), EDA presented a 2-fold increase in apparent affinity from hyperpolarizing to depolarizing potentials. The increased $K_{0.5}$ for K^+ and IC_{50} for EDA produced by more positive voltages is due to binding within the membrane's electric-field (11,12,31,37,49,50,52-55), thus the binding of both is voltage-sensitive. Extracellular access of cations to the shared sites occurs through a tapered pore (53,57), making it impossible for a large organic amine like TPA to enter deep within the binding well near the shared sites. Thus, its binding is voltage-insensitive.

The different voltage dependencies of TPA, EDA, and K^+ binding alter the way these organic amines reduce $K_{0.5}$ for K^+. For example, TPA has a stronger effect on K^+

affinity at positive voltages than negative. At negative voltages where K^+ binding is enhanced, TPA has a minimal inhibitory effect on K^+ $K_{0.5}$; however, as voltage becomes more positive and the affinity for K^+ decreases, TPA competition is amplified because the TPA IC_{50} does not change with voltage. Both the IC_{50} and increased $K_{0.5}$ for K^+ at 0 mV are similar to previous reports with purified kidney NKA (24). In contrast, EDA competitively increased the $K_{0.5}$ for K^+ to ~2 mM across the entire experimental voltage range, i.e., as both EDA and K^+ binding are voltage-sensitive, their binding affinities are equally affected across voltages and thus the competitive binding between them remains constant between -180 mV to +40 mV. These two effects demonstrate that while both amines directly compete for the E2P empty enzyme conformation (i.e. extracellular shared site access), TPA competes by 'plugging' the vestibule while EDA competes for binding at or near the shared sites directly, which is consistent with previous suggestions (24,26,27).

Shared site binding modulates I_H

Using the extracellular inhibitors TPA and EDA we elucidated whether disrupting access to the shared sites versus direct competition at the shared sites had different effects on I_H. TPA inhibited I_H at both pH 7.6 and pH 6.0, by reducing extracellular ion access. The IC_{50} values for TPA at both pH 7.6 and pH 6.0 at -180 mV were similar. However at more positive voltage TPA apparent affinity at pH 7.6 increased, which may be due to reduced $[H^+]$ or H^+ apparent affinity as voltage increases (13-15). In contrast, at pH 6.0 the IC_{50} for TPA remains unchanged, indicating the reduced $[H^+]$ is likely the cause for the change in TPA affinity at pH 7.6. These results demonstrate I_H is in part mediated by H^+ ions ability to access the NKA extracellularly, regardless of $[H^+]$.

Vedavato and Gadsby (18) demonstrated with cysteine mutations and phosphate analogs that while unable to cycle, K^+ does not appear to effect I_H. However, complete binding and inhibition by BeF_3^- did not occur, so the effects of K^+ are difficult to reconcile (18). Our results with EDA show a mild accentuation of I_H by EDA at pH 7.6 (at -180 mV), while substantial activation of I_H by EDA occurs at pH 6.0. Taking these two effects into account, we studied the impact of EDA under basic conditions (pH 8.6). However, as mentioned in the results, at pH 8.6 outward current is present in the absence of K^+ (presumed to be H^+ efflux as there is a 10-fold in-to-out H^+ gradient under these conditions) (31). Instead we applied guanidinium extracellularly at pH 8.6, which has been shown to enter the Na^+ exclusive site (31) and appears to carry a similar inward current at negative voltages (Fig. 5D), which EDA only inhibited.

One possible contributor to the dichotomous effects observed with EDA might be due to the two distinct pKa values of its amine groups, i.e. 10.71 and 7.56 at 0°C (36). Thus, at pH 8.6 EDA is singly protonated, pH 7.6 both singly and dually protonated EDA molecules exist, and at pH 6.0 EDA would be dually protonated. At pH 8.6 EDA may not reach the shared sites. Being only singly protonated EDA simply blocked the I_{Gua}, in a manner similar to singly charged TPA. At pH 7.6, a mixed effect of both activation and inhibition by EDA^{+1} and EDA^{+2} molecules, respectively, leading to an apparent null effect on I_H. While at pH 6.0, EDA is dually protonated and may act by binding directly to the shared sites, activating I_H, similar to the dis-inhibition effect proposed for Na^+ (15).

Prior reports speculated that in acidic pH, the mild activation of I_H by non-saturating [Na^+] was representative of shared site mixed occupancy of Na^+ and H^+ (14,15,20). Our group proposed in acidic conditions, that H^+ ions bind at the shared sites

inhibiting I_H and that non-saturating [Na^+] dis-inhibits this effect by binding a portion of the shared sites (15). We postulate that when both shared sites are occupied by EDA^{+2}, complete activation of I_H occurs. This observation supports previous claims that H^+ binding to the shared sites act as an inhibitory domain in acidic conditions, which can be alleviated by EDA^{+2} (or Na^+) binding (15). In an attempt to test the hypothesis that the effects of EDA are due to mixed protonation, we studied ethylamine with a single titratable group with a pKa 10.87 (58). Unlike EDA, the singly charged ethylamine only inhibited I_H at both pH 7.6 and 6.0, analogous to the effects observed with TPA, supporting our hypothesis that dual protonation may be critical for EDA directly binding to the shared sites.

Inhibition of Q_{Na} by TPA and EDA

Holmgren and Rakowski (38) demonstrated in Q_{Na} that a -25 mV shift in the $V_{1/2}$ correlates to ~2-fold reduction in extracellular Na^+ affinity, which has been supported by other groups (7-9,35,37,49,50). In Q_{Na}, TPA produced a negative shift in the $V_{1/2}$, therefore inhibiting, similar to its effects on the $K_{0.5}$ for K^+. This decrease in affinity is typical of a competitive inhibitor acting on the extracellular surface. The shifted Q_{Na} curves in the presence of TPA, presents a similar distribution and reduced relaxation rates as C-terminal truncated NKA (37,38,49,50), which was proposed to modify shared sites binding rather than the Na-exclusive site by Yaragatupalli et al. (37).

EDA on the other hand showed nearly identical results to K^+, reducing Q_{Tot} and shifting the $V_{1/2}$ towards more positive voltages. We are the first to report an inhibitor with ability to reduce Q_{Tot} and appear to increase extracellular Na^+ affinity. The reduced Q_{Tot} by EDA could be due to it acting as a dead end inhibitor, stabilizing a proportion of NKA

in a conformation incapable of binding Na^+ or by replacing Na^+ ions within the binding sites. It is probable that EDA acts both ways, becoming occluded within the shared sites as proposed by Forbush (26) and Stekhoven et al. (27), in either E2P(EDA^{+2}:1Na^+) or E2(EDA). If EDA were only capable of acting on like K^+ on the shared sites, there would be no change in relaxation rates and complete inhibition of I_H, due to the E2P conformation being required.

Occlusion of EDA within the shared sites

We used trypsin digestion and dephosphorylation to determine if EDA can act on the shared sites in multiple conformations. Stekhoven and colleagues detected minimal EDA binding to NKA at 100 µM (27). Previous work on the shared sites demonstrated trypsin digested NKA occluded radiolabeled Rb^+ (K^+ analog) within the C-terminal portion of the NKA (39,40). Separate studies then used similar methods to determine BTEA is incapable of stabilizing this C-terminal NKA long term (34). TPA acted similar to BTEA in its competitive inhibition of K^+ and to initially stabilize the C-terminal portion of NKA during trypsin digestion (34,39,40,52,58). EDA however, stabilized the C-terminal fragment potentially occluding within the shared sites (34,39,40). Although K^+ and EDA both stabilize the same C-terminal fragment demonstrated in occlusion, EDA also stabilizes multiple larger fragments indicating it likely holds the enzyme in a more concrete conformation.

EDA stabilized the 19 kDa C-terminal fragment and reduced Q_{Tot} indicating that EDA may become occluded within the shared sites (26,27). We then determined that EDA accelerates dephosphorylation of the NKA (5), which only occurs with shared site occlusion pushing the NKA to E2(EDA). Forbush's (26) original hypothesis proved

accurate as EDA appears to occlude within the shared sites in a similar manner to K^+, while TPA stabilized EP as previously demonstrated (24). Na^+ appears to act as an intermediary between TPA and EDA, indicating that these amines bind in a separate manner. Together, these results (Figs. 4,5,6) are the best evidence to date that EDA may become occluded within the shared sites, similar to 2 K^+. Along with this, the activation of I_H at pH 6.0 and slowing down relaxation rates while reducing Q_{Tot} may be indicative of EDA acting on the shared sites in both E2P and E2 conformations.

CONCLUSIONS

We have demonstrated that TPA inhibits extracellular ion access near the external access pore opening within the extracellular vestibule, while EDA is likely inhibiting by binding or occluding at the shared sites. Our results are the best evidence to date that EDA may occlude within the shared sites, likely in both E2P(EDA^{+2}:1Na) and E2(EDA^{+2}) (Fig. 10). At pH 7.6 and 6.0 I_H is reduced when extracellular access in inhibited by TPA. While the effects of EDA on I_H appear to be dependent upon protonation, blocking while singly protonated and activating while dually protonated. Future studies using EDA could prove invaluable in understanding extracellular ion selectivity. Along with this, both TPA and EDA may provide a unique look into how the shared sites and extracellular access affect I_H in NKA mutations associated with familial hemiplegic migraine and hyperaldosteronism (21-23,60-63).

ACKNOWLEDGMENTS

We thank Sukanyalakshmi Chebrolu, Adam Bernal and Victoria Heath for oocyte preparation. This work was supported by grants from the National Science Foundation (MCB-1515434 to P.A.) and National Institute of Health (R15-GM061583 to C.G.).

REFERENCES

1. Sen, A. K., and R. L. Post. (1964) Stoichiometry and Localization of Adenosine Triphosphate-Dependent Sodium and Potassium Transport in the Erythrocyte. *J. Biol. Chem.* 239:345-352
2. Post, R. L., A. K. Sen, and A. S. Rosenthal. (1965) A Phosphorylated Intermediate in Adenosine Triphosphate-Dependent Sodium and Potassium Transport across Kidney Membranes. *J. Biol. Chem.* 240:1437-1445
3. Kanai, R., H. Ogawa, B, Vilsen, F.Cornelius, and C. Toyoshima. 2013 Crystal structure of a Na+-bound Na+,K+-ATPase preceding the E1P state. *Nature.* 502:201-206.
4. Nyblom, M., H. Poulsen, P. Gourdon, L. Reinhard, M. Andersson, E. Lindahl, N. Fedosova, and P. Nissen. 2013. Ctrystal structure of Na+,K+-ATPase in the Na+-bound state. *Science.* 342:123-127.
5. Kaplan, J.H. 2002. Biochemistry of Na,K-ATPase. *Annu. Rev. Biochem.* 71:511-535.
6. Rakowski, R. F., D. C. Gadsby, and P. De Weer. 1989. Stoichiometry and voltage dependence of the sodium pump in voltage-clamped, internally dialyzed squid giant axon. *J. Gen. Physiol.* 93:903-941.
7. Nakao, M., and D. C. Gadsby. 1986. Voltage dependence of Na translocation by the Na/K pump. *Nature.* 323:628-630.
8. Hilgemann, D.W. 1994. Channel-like function of the Na,K pump probed at microseconds resolution in giant membrane patches. *Science.* 263:1429-1432.

9. Holmgren, M., J. Wagg, F. Bezanilla, R. F. Rakowski, P. De Weer, and D. C. Gadsby. 2000. Three distinct and sequential steps in the release of sodium ions by the Na+/K+-ATPase. *Nature.* 403:898-901.

10. Castillo, J. P., H. Rui, D. Basilio, A. Das, B. Roux, R. Latorre, F. Bezanilla, and M. Holmgren. 2015. Mechanism of potassium ion uptake by the Na(+)/K(+)-ATPase. *Nat. Commun.* 6:7622.

11. Peluffo, R. D., and J. R. Berlin. 1997. Electrogenic K+ transport by the Na(+)-K+ pump in rat cardiac ventricular myocytes. *J. Physiol.* 501(Pt 1) :33-40.

12. Rakowski, R. F., L. A. Vasilets, J. LaTona, and W. Schwarz. 1991. A negative slope in the current-voltage relationship of the Na+/K+ pump in Xenopus oocytes produced by reduction of external [K+]. *J. Membr. Biol.* 121:177-187.

13. Efthymiadis, A., J. Rettinger, and W. Schwarz. 1993. Inward-directed current generated by the Na+,K+ pump in Na(+)- and K(+)-free medium. *Cell biology international* 17:1107-1116.

14. Wang, X., and J. D. Horisberger. 1995. A conformation of Na(+)-K+ pump is permeable to proton. *Am. J. Physiol.* 268:C590-595.

15. Mitchell, T. J., C. Zugarramurdi, J. F. Olivera, C. Gatto, and P. Artigas. 2014. Sodium and proton effects on inward proton transport through Na/K pumps. *Biophys. J.* 106:2555-2565.

16. Stanley, K. S., D. J. Meyer, C. Gatto, and P. Artigas. 2016. Intracellular requirementes for passive proton transport through the Na+,K+-ATPase. *Biophys. J.* 111:2430-2439.

17. Li, C., K. Geering, and J. D. Horisberger. 2006. The third sodium binding site of Na,K-ATPase is functionally linked to acidic pH-activated inward current. *J. Membr. Biol.* 213:1-9.

18. Vedovato, N., and D. C. Gadsby. 2014. Route, mechanism, and implications of proton import during Na+/K+ exchange by native Na+/K+-ATPase pumps. *J. Gen. Physiol.* 143:449-464.

19. Rettinger, J. 1996. Characteristics of Na+/K(+)-ATPase mediated proton current in Na(+)- and K(+)-free extracellular solutions. Indications for kinetic similarities between H+/K(+)-ATPase and Na+/K(+)-ATPase. *Biochim Biophys Acta.* 1282:207-215.

20. Vasilyev, A., K. Khater, and R. F. Rakowski. 2004. Effect of extracellular pH on presteady-state and steady-state current mediated by the Na+/K+ pump. *J. Memb. Biol.* 198:65-76.

21. Poulsen, H., H. Khandelia, J. P. Morth, M. Bublitz, O. G. Mouritsen, J. Egebjerg and P. Nissen. 2010. Neurological disease mutations compromise a C-terminal ion pathway in the Na+/K+-ATPase. *Nature.* 467:99-102.

22. Azizan, E. A. B., H. Poulsen, P. Tuluc, J. Zhou, M. V. Clausen, A. Lieb, C. Maniero, S. Garg, E. G. Bochukova, W. Zhao, L. H. Shaikh, C. A. A. Brighton, E. D. Teo, A. P. Davenport, T. Dekkers, B. Tops, B. Kusters, J. Ceral, G. S. H. Yeo, S. G. Heogi, I. McFarlane, N. Rosenfeld, F. Marass, J. Hadfield, W. Margas, K. Caggar, M. Solar, J. Deinum, A. C. Dolphin, I. S. Farooqi, J. Striessnig, P. Nissen, and M. J. Brown. 2013. Somatic mutations in ATP1A1 and CACNA1D underlie a common subtype of adrenal hypertension. *Nat. Genet.* 45:1055-1060.

23. Spiller, S., and T. Friedrich. 2014. Functional analysis of human Na+/K+-ATPase familial or sporadic hemiplegic migraine mutations expressed in Xenopus oocytes. *World. J. Biol. Chem.* 5:240-253.

24. Gatto, C., J. B. Helms, M. C. Prasse, K. L. Arnett, and M. A. Milanick. 2005. Kinetic characterization of tetrapropylammonium inhibition reveals how ATP and Pi alter access to the Na+-K+-ATPase transport site. *Am. J. Physiol. Cell. Physiol.* 289:C302-C311.

25. Kropp, D. L., and J. R. Sachs. 1977. Kinetics of the inhibition of the Na-K pump by tetrapropylammonium chloride. *Am. J. Physiol.* 264:471-487.

26. Forbush III, B. 1988. The interaction of amines with the occluded state of the Na,K-Pump. *J. Biol. Chem.* 263:7979-7988.

27. Stekhoven, F. M. A. H. S., Y. S. Zou, H. G. P. Swarts, J. Leunissen, and J. J. H. H. M. De Pont. 1989. Ethylenediamine as active site probe for Na+/K+-ATPase. *Biochim. Biophys. Acta.* 982:103-114.

28. Harry, T. W. M., V. D. Hijden, F.M.A.H.S. Stekohven and J. J. H. H. M. De Pont. 1989. Sidedness of the effect of amines on the steady-state phosphorylation level of reconstituted Na+/K+-ATPase. *Biochim. Biophys. Acta.* 987:75-82.

29. Stekhoven, F. M. A. H. S., H. G. P. Swarts, G. K. Lam, Y. S. Zou, and J. J. H. H. M. De Pont. 1988. Phosphorylation of (Na+ + K+)-ATPase; stimulation and inhibition by substituted and unsubstituted amines. *Biochim. Biophys. Acta.* 937:161-176.

30. Gatto, C., J. B. Helms, M. C. Prasse, S. Y. Huang, X. Zou, K. L. Arnett, and M. A. Milanick. 2006. Similarities and differences between organic cations inhibition of the Na,K-ATPase and PMCA. *Biochemistry* 45:13331-13345.

31. Ratheal, I. M., G. K. Virgin, H. Yu, B. Roux, C. Gatto, and P. Artigas. 2010. Selectivity of externally facing ion-binding sites in the Na/K pump to alkali metals and organic cations. *Proc. Natl. Acad. Sci*. 107:18718-18723.

32. Price, E. M., D. A. Rice, and J. B. Lingrel. 1989. Site-directed mutagenesis of a conserved, extracellular aspartic acid residue affects the ouabain selectivity of sheep Na,K-ATPase. *J. Biol. Chem.* 264:21902-21906.

33. Costa, C. J., C. Gatto, and J. H. Kaplan. 2003. Interactions between Na,K-ATPase α-subunit ATP-binding domains. *J. Biol. Chem.* 278:9176-9184.

34. Mares, L. J., A. Garcia, H. H. Rasmussen, F. Cornelius, Y. A. Mahmmoud, J. R. Berlin, B. Lev, T. W. Allen, and R. J. Clarke. 2014. Identification of electric-field-dependent steps in the Na+,K+-pump cycle. *Biophys. J.* 107:1352-1363.

35. Galva, C., C. Gatto, and M. Milanick. 2012. Soymilk: an effective and inexpensive blocking agent for immunoblotting. *Anal. Biochem.* 426:22-23.

36. Weast, R. C. (ed.). 1986-1987. Handbook of Chemistry and Physics. 67th ed. CRC Press, Inc. D-159.

37. Yaragatupalli, S., J. F. Olivera, C. Gatto, and P. Artigas. 2009. Altered Na+ transport after an intracellular α-subunit deletion reveals strict external sequential release of Na+ from the Na/K pump. *Proc. Natl. Acad. Sci.* 106:15507-15512.

38. Holmgren, M., and R. F. Rakowski. 2006. Charge translocation by the Na+/K+ pump under Na+/Na+ exchange conditions: Intracellular Na+ dependence. *Biophys. J.* 90:1607-1616.

39. Karlish, S. J. D., R. Goldschleger, and W. D. Stein. 1990. A 19-kDa C-terminal tryptic fragment of the α chain of Na/K-ATPase is essential for occlusion and transport of cations. *Proc. Natl. Acad. Sci.* 87:4566-4570.

40. Lutsenko, S., and J. H. Kaplan. 1994. Molecular events in close proximity to the membrane associated with the binding of ligands to the Na,K-ATPase. *J. Biol. Chem.* 269:4555-4564.

41. Ogawa, H., T. Shinoda, F. Cornelius, and C. Toyoshima. 2009. Crystal structure of the sodium-potassium pump (Na+,K+-ATPase) with bound potassium and ouabain. *Proc. Natl. Acad. Sci.* 106:13742-13747.

42. Shinoda, T., H. Ogawa, F. Cornelius, and C. Toyoshima. 2009. Crystal structure of the sodium-potassium pump at 2.4 A resolution. *Nature.* 459:446-450.

43. Ogawa, H., F. Cornelius, A. Hirata, and C. Toyoshima. 2015. Sequential substitution of K+ bound to Na+,K+-ATPase visualized by X-ray crystallography. *Nat. Commun.* 6:8004.

44. Morth, J. P., B. P. Pedersen, M. S. Toustrup-Jensen, T. L. Sorensen, J. Petersen, J. P. Andersen, B. Vilsen, and P. Nissen. 2007. Crystal structure of the sodium-potassium pump. *Nature.* 450:1043-1049.

45. Nyblom, M., H. Poulsen, P. Gourdon, L. Reinhard, M. Andersson, E. Lindahl, N. Fedosova, and P. Nissen. 2013. Crystal structure of Na+,K(+)-ATPase in the Na(+)-bound state. *Science.* 342:123-127.

46. Laursen, M., L. Yatime., P. Nissen, and N. U. Fedosova. 2013. Ctrystal structure of the high-affinity Na+K+-ATPase-ouabain complex with Mg2+ bound in the cation binding site. *Proc. Natl. Acad. Sci.* 110:10958-10963.

47. Yu H., I. M. Ratheal, P. Artigas, and B. Roux. 2011. Protonation of key acidic residues is critical for the K+-selectivity of the Na,K pump. *Nat. Struct. Mol. Biol.* 18:1159-1163.

48. Rui. H., P. Artigas, and B. Roux. 2016. The selectivity of the Na(+)/K(+)-pump is controlled by binding site protonation and self-correcting occlusion. *Elife.* 5:e16616.

49. Vedovato, N., and D. C. Gadsby. 2010. The two C-terminal tyrosines stabilize occluded Na/K pump conformations containing Na or K ions. *J. Gen. Physiol.* 136:63-82.

50. Meier, S., N. N. Tavraz, K. L. Durr, and T. Friedrich. 2010. Hyperpolarization-activated inward leakage currents caused by deletion or mutation of carboxy-terminal tyrosines of the Na+/K+-ATPase α-subunit. *J. Gen. Physiol.* 135:115-134.

51. Forbush III, B. 1987. Rapid release of 42K or 86Rb from two distinct transport sites on the Na,K-pump in the presence of Pi or Vanadate. *J. Biol. Chem.* 262:11116-11127.

52. Eckstein-Ludwig, U., J. Rettinger, L. A. Vasilets, and W. Schwarz. 1998. Voltage-dependent inhibition of the Na+,K+ pump by tetraethylammonium. *Biochim. Biophys. Acta.* 1372:289-300.

53. Peluffo, R. D., Y. Hara, and J. R. Berlin. 2004. Quaternary organic amines inhibit Na,K pump current in a voltage-dependent manner: Direct evidence of an extracellular access channel in the Na,K-ATPase. *J. Gen. Physiol.* 123:249-263.

54. Sagar, A., and R. F. Rakowski. 1994. Access channel model for the voltage dependence of the forward-running Na+/K+ pump. *J. Gen. Physiol.* 103:869-893.

55. Jaisser, F., P. Jaunin, K. Geering, B. C. Rossier, and J. D. Horisberger. 1994. Modulation fo the Na,K-pump function by beta subunit isoforms. *J. Gen. Physiol.* 103:605-623.

56. Sturmer, W., R. Buhler, H. J. Apell, and P. Lauger. 1991. Charge translocation by the Na,K-pump: II. Ion binding and release at the extracellular face. *J. Membr. Biol.* 121:163-176.

57. Gradinaru, R. V. and H. J. Apell. 2015. Probing the extracellular access channel of the Na,K-ATPase. *Biochemistry.* 54:2508-2519.

58. Perrin, D. D. 1965. Dissociation constants fo organic bases in aqueous solution. IUPAC Chem Data Ser.

59. Peluffo, R. D., R. M. Gonzalez-Lebrero, S. B. Kaufman, S. Kortagere, B. Orban, R. C. Rossi, and J. R. Berlin. 2009. Quaternary benzyltriethylammonium ion binding to the Na,K-ATPase: A tool to investigate extracellular K+ binding reactions. *Biochemistry*. 48:8105-8119.

60. Beuschlein, F., S. Boulkroun, A. Osswald, T. Wieland, H. N. Nielsen, U. D. Lichtenauer, D. Penton, V. R. Schack, L. Amar, E. Fischer, A. Walther, P. Tauber, T. Schwarzmayr, S. Diener, E. Graf, B. Allolio, B. Samson-Couterie, A. Benecke, M. Quinkler, F. Fallo, P. F. Plouin, F. Mantero, T. Meitinger, P.

Mulatero, X. Jeunemaitre, R. Warth, B. Vilsen, M. C. Zennaro, T. M. Strom, and M. Reincke. 2013. Somatic mutations in ATP1A1 and ATP2B3 lead to aldosterone-producing adenomas and secondary hypertension. *Nat. Genet.* 45:440-445.

61. Williams TA, S. Monticone, V. R. Schack, J. Stindl, J. Burrello, F. Buffolo, L. Annaratone, I. Castellano, F. Beuschlein, M. Reincke, B. Lucatello, V. Ronconi, F. Fallo, G. Bernini, M. Maccario, G. Giacchetti, F. Veglio, R. Warth, B. Vilsen and P. Mulatero. 2014. Somatic ATP1A1, ATP2B3, and KCNJ5 mutations in aldosterone-producing adenomas. *Hypertension.* 63:188-195.

62. Friedrich, T., N. N. Tavraz, and C. Junghans. 2016. ATP1A2 mutations in migraine: Seeing through the facets of an ion pump onto the neurobiology of disease. *Front. Physiol.* 7:239.

63. Kinoshita, P. F., J. A. Leite, A. M. Orellana, A. R. Vasconcelos, L. E. Quintas, E. M. Kawamoto, and C. Scavone. 2016. The influence of Na(+), K(+)-ATPase on glutamate signaling in neurodegenerative diseases and senescence. *Front. Physiol.* 7:195.

FIGURES

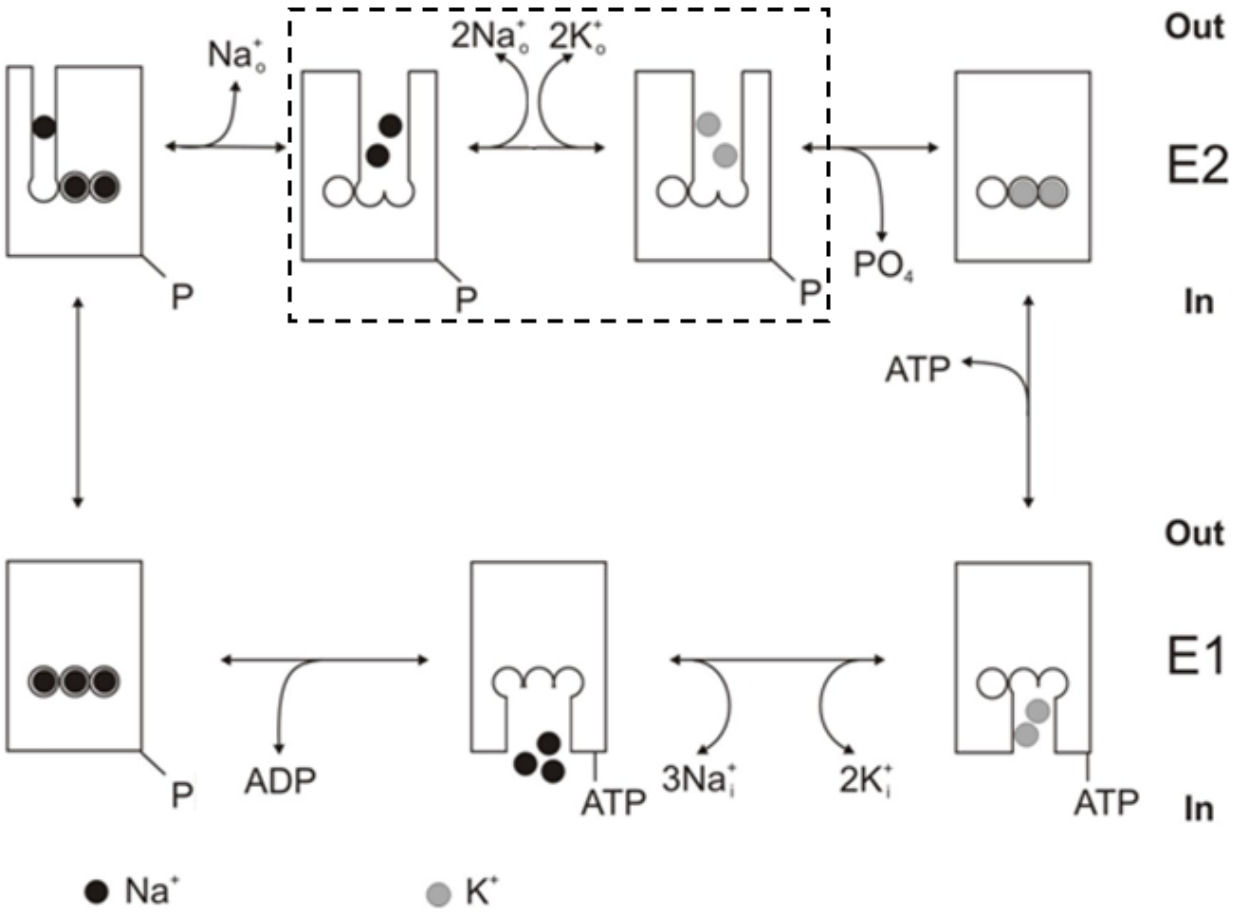

FIGURE 1. *Albers-Post kinetic scheme of the Na,K-ATPase*. Reaction scheme of the Na,K-ATPase shown superimposed with a cartoon representation of transitions involving binding and release of ions. Na^+ ions (black), K^+ ions (gray). The box encloses states which extracellular inhibitors access the Na,K-ATPase.

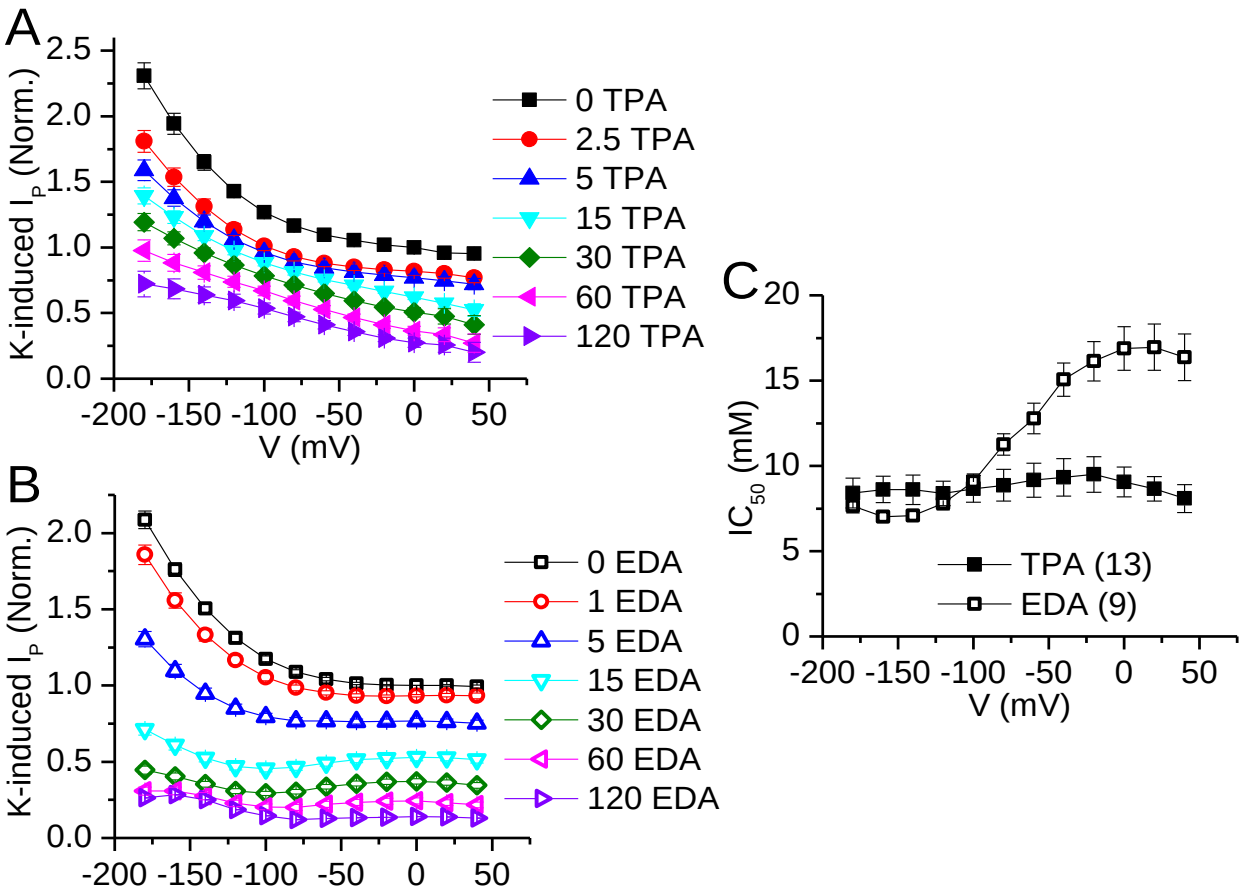

FIGURE 2. *Concentration dependence of TPA and EDA inhibition on K^+-induced I_P.* A) Ouabain-sensitive K^+-induced I-V curves at indicated [TPA] normalized to current induced by 3 mM K^+ in 0 TPA (NMG-Cl) at 0 mV, pH 7.6, identifying a decrease in I_P within increasing [TPA]. B) Ouabain-sensitive K^+-induced I-V curves at indicated [EDA] normalized to current induced by 3 K^+ in 0 TPA (NMG) at 0 mV, identifying a decrease in I_P within increasing [EDA]. C) Plotted IC_{50} of TPA and EDA to inhibit I_P as a function of voltage. IC_{50} for TPA (8.41 ± 0.87 mM at -180 mV and 8.09 ± 0.82 mM at +40 mV) and EDA (8.16 ± 0.46 at -180 mV rising to 15.74 ± 1.86 mM at +40 mV) as a function of

voltage. All values represent average and SEM for both TPA and EDA indicated in parenthesis in C, normalized to 3 mM K^+ in NMG at 0 mV.

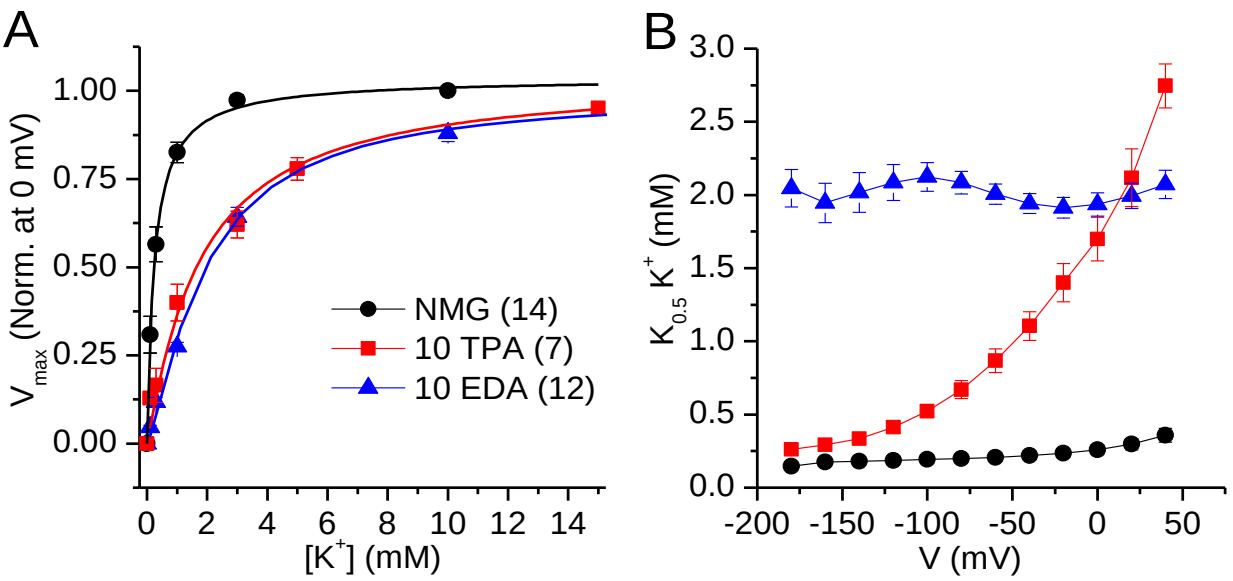

FIGURE 3. *Concentration dependence of K^+ in the presence of extracellular inhibitors*. A) Ouabain-sensitive V_{max} of I_P at 0 mV as a function of increasing [K^+] in the NMG (black), 10 mM TPA (red) and 10 mM EDA (blue). TPA and EDA both increased $K_{0.5}$ for K^+ from 0.24 ± 0.03 mM in NMG to 1.77 ± 0.36 mM in TPA and 1.92 ± 0.25 mM in EDA. B) $K_{0.5}$ for K^+ as a function of voltage in NMG (black), 10 mM TPA (red) and 10 EDA (blue). In NMG $K_{0.5}$ for K^+ (0.15 ± 0.02 mM,0.23 ± 0.03 mM and 0.36 ± 0.05 mM at -180, -40 and +40 mV, respectively) in 10 mM TPA (0.26 ± 0.03 mM, 1.10 ± 0.10 mM and 2.75 ± 0.15 mM at -180, -40 and +40 mV, respectively) and in 10 mM EDA (2.05 ± 0.13 mM, 1.94 ± 0.07 mM and 2.07 ± 0.10 mM at -180, -40 and +40 mV, respectivley). All values in A and B are normalized averages to the indicated number of oocytes in parenthesis with A.

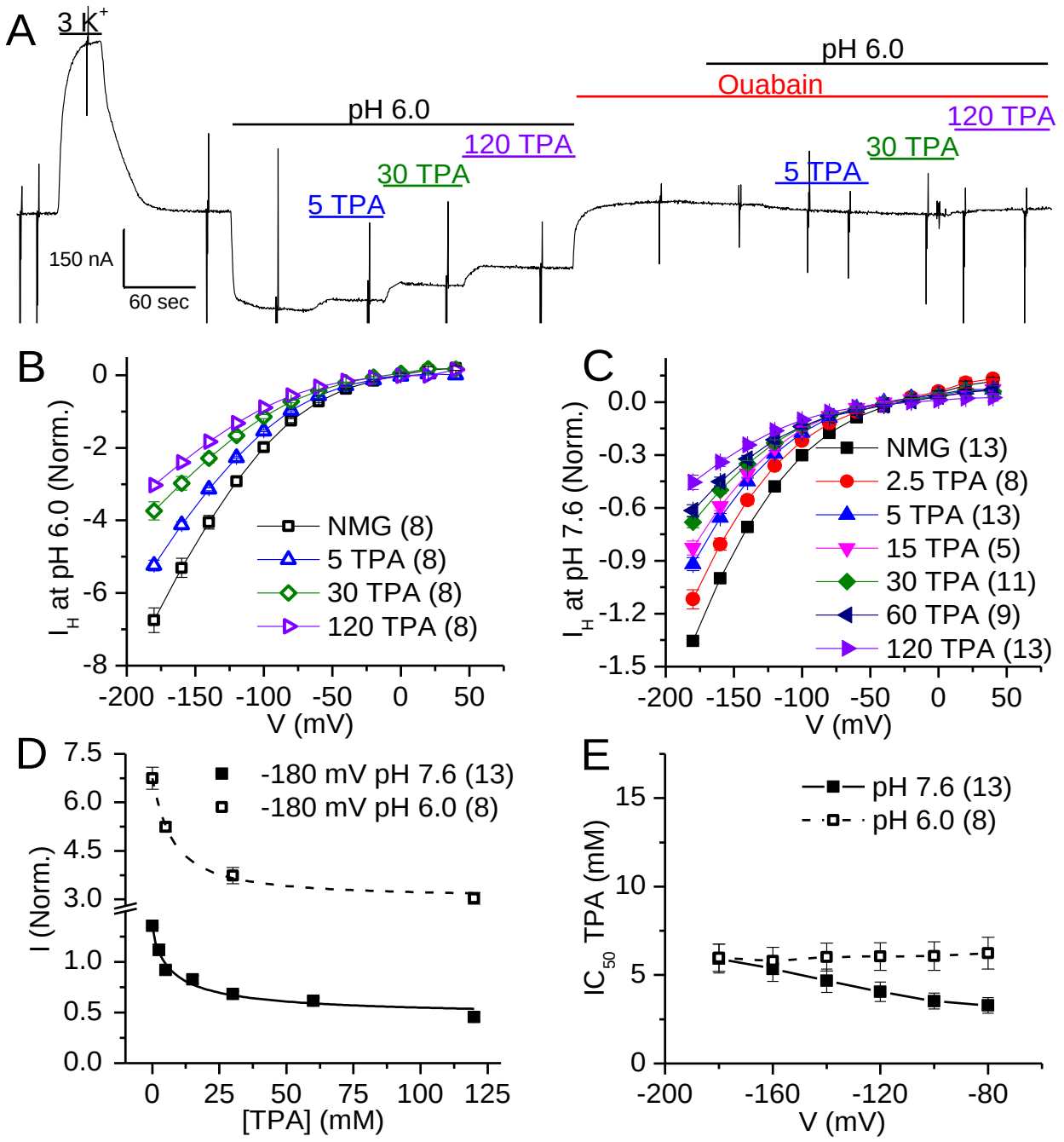

FIGURE 4. *TPA inhibition of I_H*. A) Continuous current recording from a voltage-clamped oocyte held at −50 mV, 4 days after cRNA injection. B) Ouabain-sensitive current-voltage (IV) plot of I_H in the presence of increasing [TPA] at pH 6.0, normalized to the inverse current at -160 mV in NMG-Cl at pH 7.6. C) Ouabain-sensitive IV plot of I_H in the presence

of increasing [TPA] at pH 7.6, normalized to the inverse current at -160 mV in NMG-Cl at pH 7.6. D) Normalized averages of I_H as a function of [TPA] at -180 mV at pH 7.6 (filled squares) and pH 6.0 (open squares), with solid and dotted lines representing a fit to equation 2 at pH 7.6 and 6.0, respectively. E) TPA IC_{50} of I_H as a function of voltage represented by filled squares at pH 7.6 (5.93 ± 0.82 mM at -180 mV and 3.29 ± 0.44 mM at -80 mV) and open squares at pH 6.0 (5.98 ± 0.77 mM at -180 mV and 6.23 ± 0.90 mM at -80 mV). All values represent the normalized averages and SEM of the indicated number of experiments in parenthesis in A, B, C, and D.

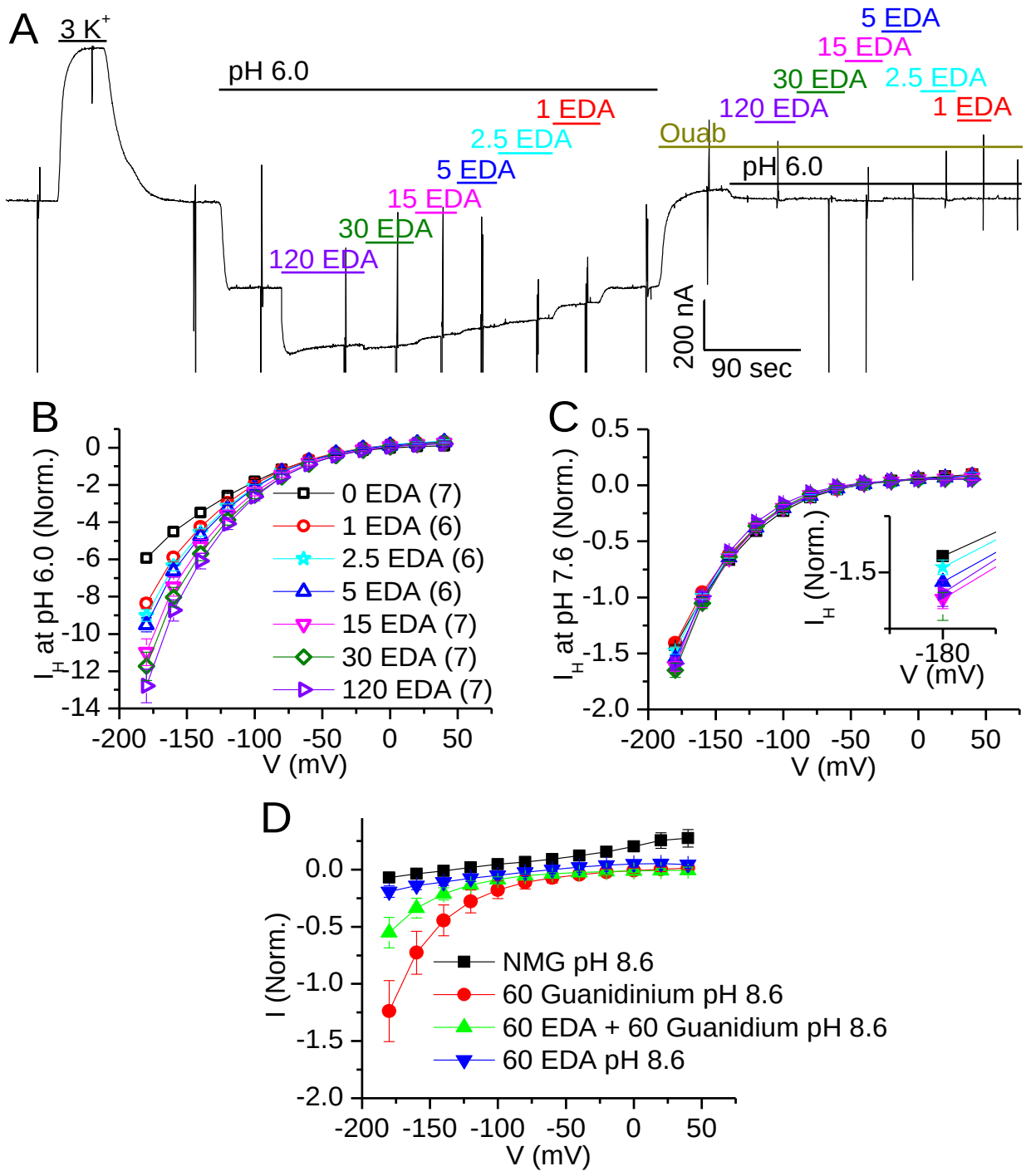

FIGURE 5. *Effects of EDA on I_H at various [H⁺].* A) Continuous recording from a voltage-clamped oocyte held at −50 mV, demonstrating increased I_H at pH 6.0 with increasing [EDA]. B) Ouabain-sensitive IV plot of I_H at increasing [EDA] at pH 6.0, normalized to the

inverse current at -160 mV in NMG at pH 7.6. C) Ouabain-sensitive IV plot of I_H at increasing [EDA] at pH 7.6, normalized to the inverse current at -160 mV in NMG at pH 7.6. *Inset*, zoomed in view of 4C at -180 mV. D) Ouabain-sensitive IV plot of inward current induced by guanidinium (I_{Gua}) at pH 8.6, in the presence (green) and absence (red) of 60 mM EDA, normalized to the inverse current at -160 mV in NMG at pH 7.6. All values represent the normalized average and SEM from between 5 and 7 oocytes.

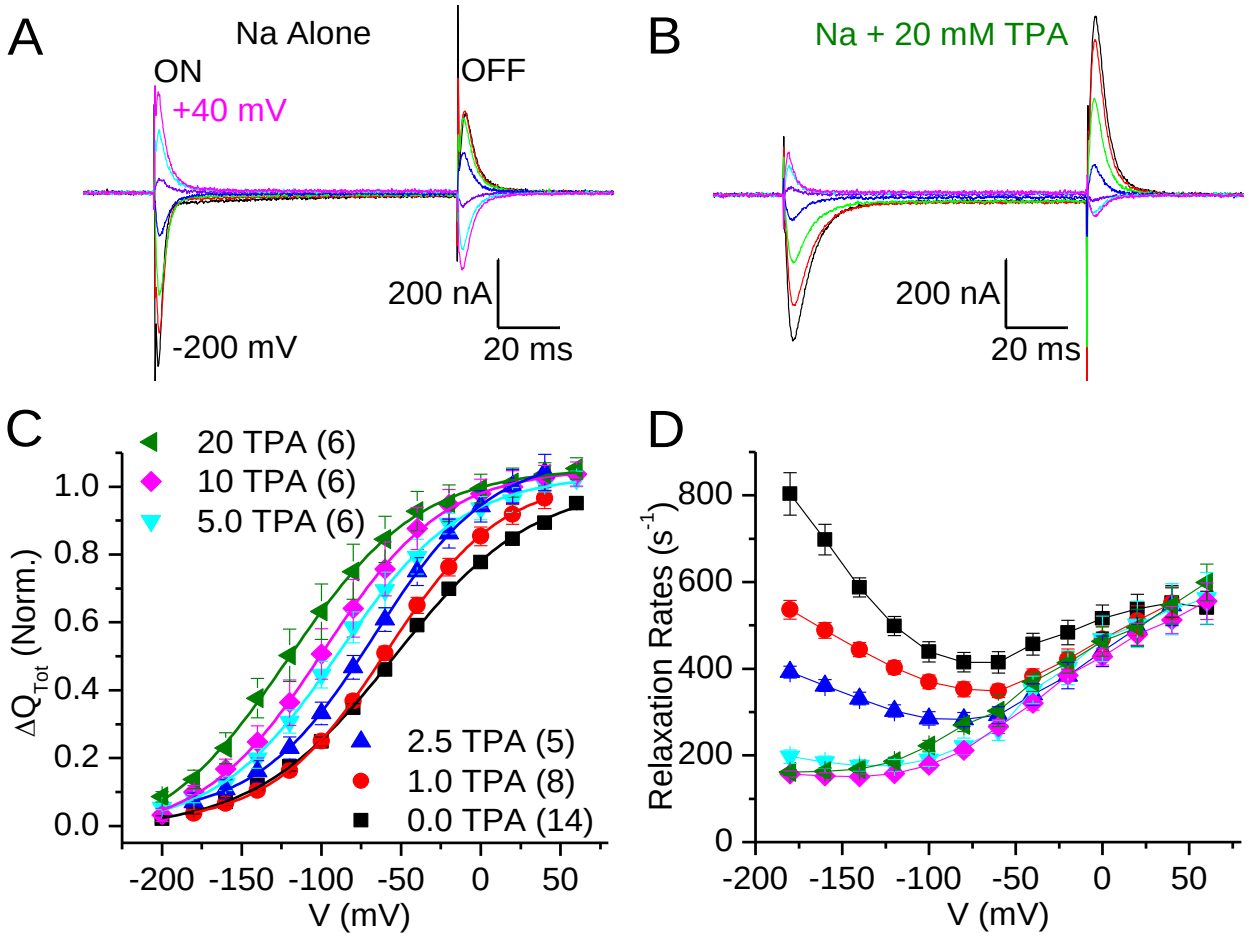

FIGURE 6. *Na-dependent transient charge movement (Q_{Na}) inhibition by TPA.* A and B) Ouabain-sensitive currents measured in the presence of 125 mM Na^+ external without (A) and with (B) 20 mM TPA. Currents elicited by 100–ms pulses from V_h = -50 mV to voltages ranging from -200 to +40 mV in 40-mV increments. C) Normalized Q_{Tot} from integrated currents as a function of voltage (QV) at the indicated concentrations of TPA. Solid lines are a fit of the symbols by equation (Boltzmann). $V_{1/2}$ and kB for each condition were: 0 TPA (black), -54.4 ± 1.6 mV and 43.4 ± 1.8; 1.0 TPA (red), -59.0 ± 0.5 mV and 40.1 ± 0.9; 2.5 TPA (blue), -66.7 ± 0.5 mV and 41.7 ± 1.0; 5.0 TPA (cyan), -88.8 ± 1.4 mV and 38.6 ± 1.4; 10 TPA (magenta), -98.7 ± 1.4 mV and 38.0 ± 1.4; 20 TPA (green), -120.9

± 2.1 mV and 41.3 ± 1.7. D) Averages of single exponential fits to the exponential decay of transient currents stimulated by the ON voltage steps (Relaxation rates) of the slow time components of charge movement. Data points in C are normalized averages and SEM to Q_{Tot} at 0 mM TPA, number of oocytes indicated in parentheses; Data points in D are averages values of the indicated number of oocytes in parenthesis in C.

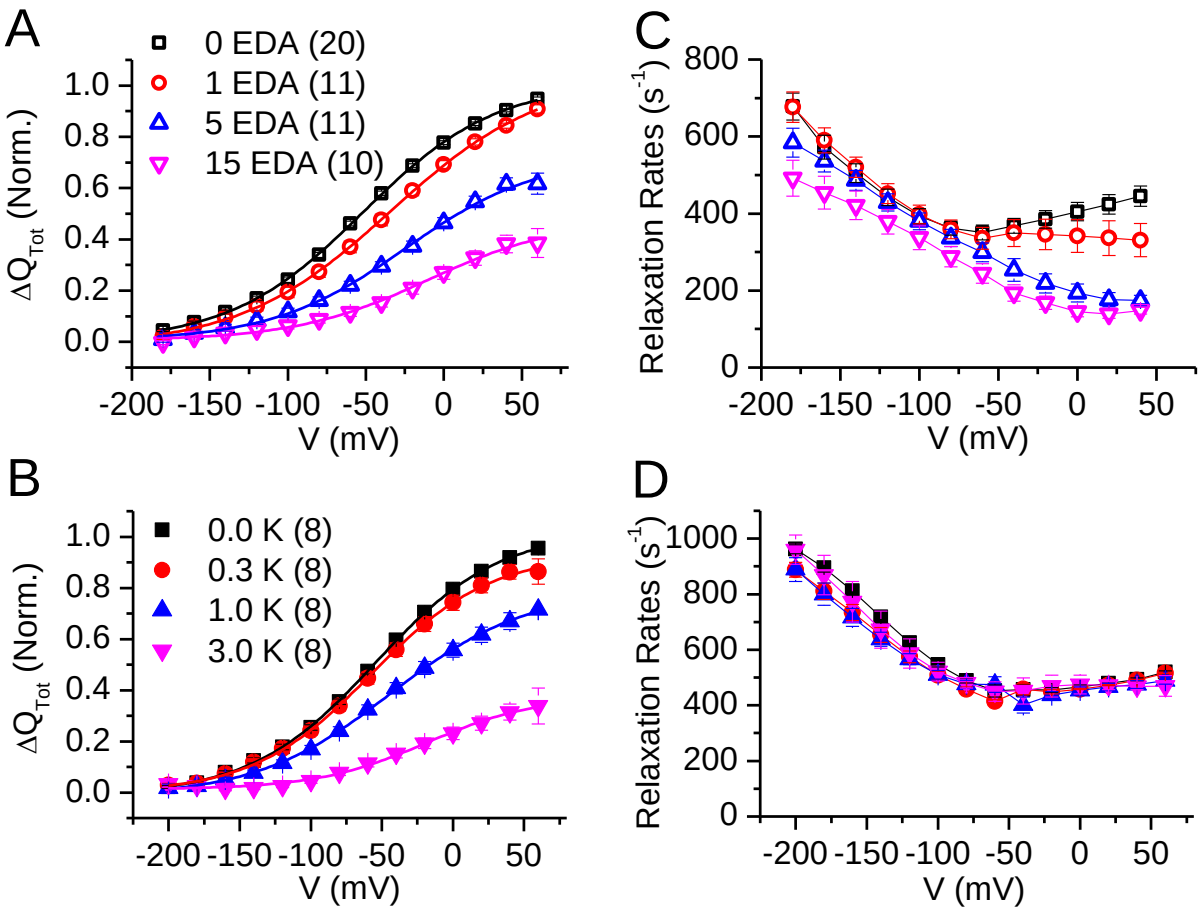

FIGURE 7. *Q_{Na} inhibition by EDA and K^+.* A-B) Ouabain-sensitive normalized QV curves in 125 mM Na^+ external in the presence of increasing concentrations of A) EDA and B) K^+. Solid lines in A are a fit of the symbols by equation (Boltzmann). $V_{1/2}$ and kB for each condition are: 0 EDA (black open), -51.8 ± 1.6 mV and 42.6 ± 1.9 mV; 1.0 EDA (red open), -34.2 ± 2.4 mV and 48.4 ± 2.6 mV; 5 EDA (blue open), -24.5 ± 3.2 mV and 43.1 ± 3.0 mV; 15 EDA (magenta open), -10.5 ± 6.1 mV and 42.6 ± 4.7 mV. Solid lines in B are a fit of the symbols by equation (Boltzmann). $V_{1/2}$ and kB for each condition are: 0 K (black), -54.7 ± 1.2 mV and 43.5 ± 1.3 mV; 0.3 K (red), -57.2 ± 1.2 mV and 41.6 ± 1.3 mV; 1.0 K (blue), -43.8 ± 1.9 mV and 47.5 ± 2.1 mV; 3.0 K (magenta), -18.2 ± 4.2 mV and 38.8 ±

3.4 mV. C-D) Averaged relaxation rates of Q_{Na} as a function of voltage in the presence of increasing concentrations of C) EDA and D) K^+. Values in A and B are normalized averages and SEM to Q_{Tot} at 0 mM EDA (A) and 0 mM K+ (B), respectively; Values in C and D are averages of the indicated number of oocytes in parenthesis with A (paired with C) and B (paired with C).

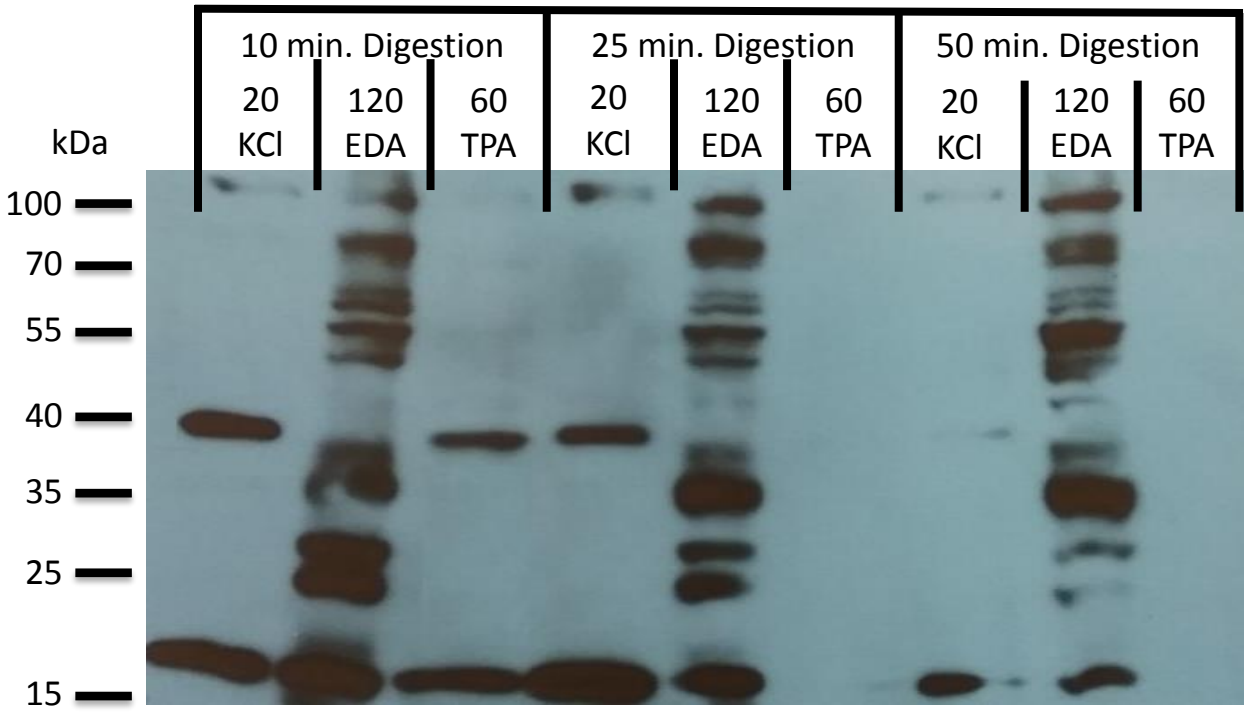

FIGURE 8. *Stabilization of C-terminal trypsin digested NKA α-subunit fragment.* Purified ovine NKA equilibrated in 25 mM histidine, 1 mM EDTA (pH 7.0) with either 20 mM KCl (Lane 1,4,7), 120 mM EDA (Lane 2,5,8), or 60 mM TPA (Lane 3,6,9), was treated with trypsin (1:7.5 with respect to NKA) at 37°C for 10 minutes (Lanes 1-3), 25 minutes (Lanes 4-7), or 50 minutes (Lanes 7-9). Reaction was stopped with SDS loading buffer and each sample was run on a 15% SDS-PAGE gel. NKA α-subunit was probed for using an anti-KETYY antibody, specific for the C-terminus of the NKA α-subunit. Each condition presented different banding patterns at different time intervals (with the exception of 20 KCl and 60 TPA at 10 minute). KCl stabilized three (’19 kDa’, ’40 kDa’ and ‘110 kDa’) at 10, 25 and 50 minutes, while TPA only stabilized these fragments after 10 minutes of digestion. EDA like KCl was able to stabilize a ‘19 kDa’ fragment, along with a number of larger fragments, indicating it maintains the NKA in a more concrete conformation.

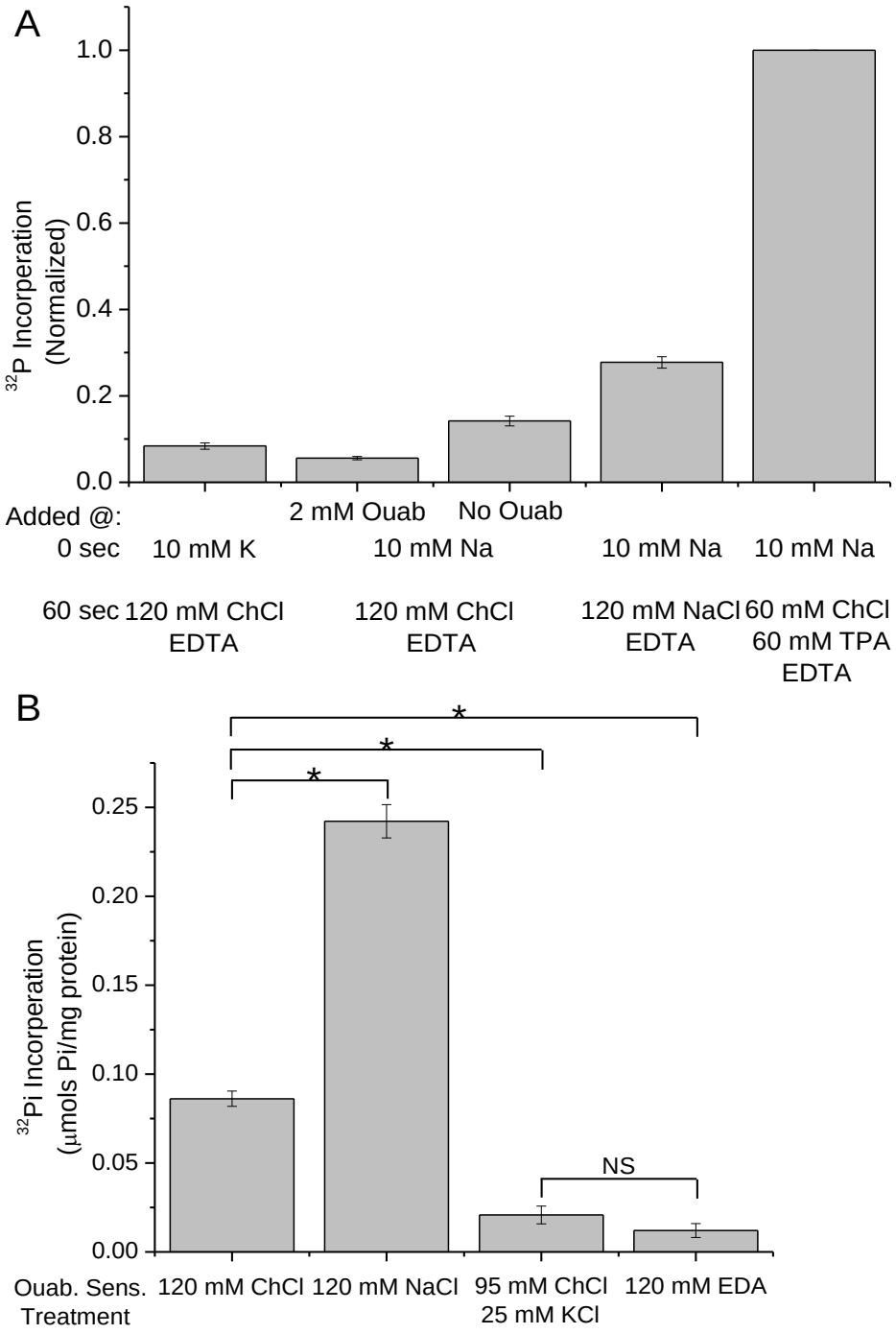

FIGURE 9. *Effect of EDA on phosphoenzyme (EP) dephosphorylation of the Na,K-ATPase.* Purified ovine kidney NKA was phosphorylated for 1 minute in the presence of 10 µM MgATP^{32} on ice, followed by application of 10 mM EDTA (Mg^{2+} chelator, preventing

further EP formation) and the indicated ion conditions for 30 seconds on ice. Enzyme was precipitated with 5% TCA, trapped on a 0.45-µm filter and radioactive ^{32}P was determined. A) After EP formation, spontaneous dephosphorylation was measured in the presence of the indicated ions with 10 mM EDTA. Pre-treated enzyme with 2 mM ouabain and 10 mM KCl were used as controls, as neither is capable of induce EP formation of the NKA. Dephosphorylation prevention occurred in the following potency order, ChCl > NaCl > TPACl, consistent with previous reports (24). B) Ouabain-sensitive dephosphorylation was accelerated in both 25 mM KCl and 120 mM EDA, compared to control (choline chloride). These data are consistent with EDA (like K^+) becoming occluded within the shared sites to induce dephosphorylation. Data shown in A are averages and SEM (n = 4) in triplicate of normalized EP levels in the presence of TPA. *****P < 0.01, EP levels differed significantly from 120 mM ChCl; NS, no significant difference between 25 KCl (95 ChCl) and 120 EDA (P = 0.18).

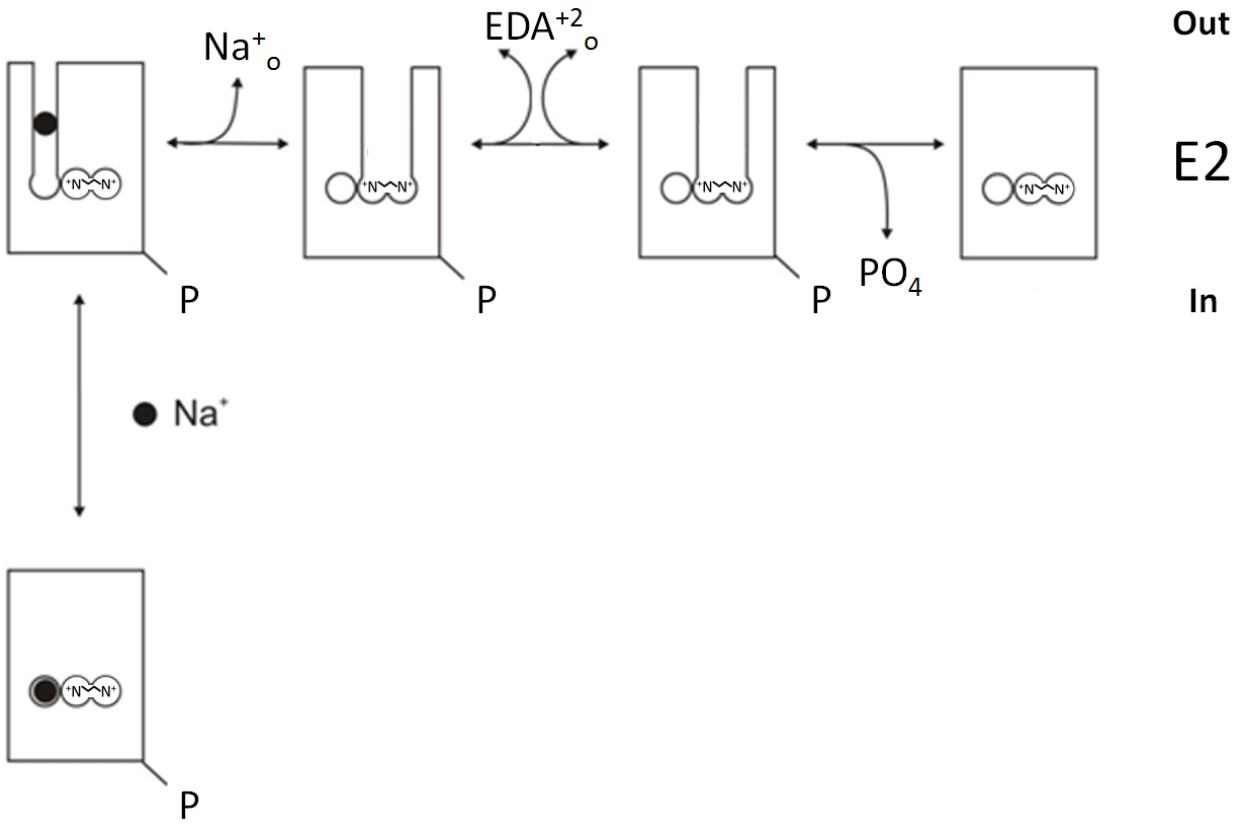

FIGURE 10. *Modified Albers-Post kinetic scheme of the Na,K-ATPase.* Reaction scheme of the Na,K-ATPase shown superimposed with a cartoon representation of transitions involving binding and release of ions. Na^+ ions (black) within the Na-exclusive site and EDA^{+2} within the shared sites.

CHAPTER IV

CONCLUSION

CONCLUSION

The present study initially attempted to identify two main questions regarding the Na,K-ATPase (NKA); 1) What are the intracellular requirements to allow for passive H^+ influx (I_H) through the NKA? And 2) Is extracellular access or extracellular ion binding the cause for extracellular inhibition of I_H? The foundation for this work was based on three primary studies on mechanisms and potential relevance of I_H. A study by Mitchell et al. (1) who identified how the shared sites may act as an inhibitory or activating domain for I_H through the NKA depending on [H^+]. Around the same time Vedovato and Gadsby (2) identified key acidic residues within the Na-exclusive site of the NKA involved in I_H. Furthermore, prior work by Rettinger (3) identified some intracellular cation requirements as well as ATP for I_H. Over the course of these studies, it became clear understanding the extracellular mechanisms of I_H was a part of the bigger understanding of extracellular ion access and binding.

Although Rettinger's work (3) provided strong evidence for intracellular mechanisms of I_H, there were still gaps in our knowledge of the subject. Due to these works I hypothesized that I_H would be activated under conditions which initiate the conformational transition from E1 (internally open) to E2 (externally open). However, this transition requires a phosphorylation dependent reaction in order to open externally. I assessed this question using a three-pronged approach, forward cycling, reverse cycling, and a phosphate analog.

Extracellularly the inhibition of I_H had been isolated to the blockage of passive current in the presence of transportable cations. This method of study is complicated in their effects however, as the "blocking" cations produce their own current through the

NKA. The interpretation of their data was that the shared sites of the NKA may have inhibitory properties on the Na-exclusive site for allowing I_H at physiological pH (1). Along with this a dis-inhibition effect occurred in acidic conditions (pH 5.0), where excess H^+ ions are thought to inhibit at the shared sites, while in a non-saturating [Na^+] I_H activation arises as Na^+ binds to the shared sites, dis-inhibiting H^+ binding (1). One downfall to this is the unknown effect of whether the inhibition by Na^+ is occurring via blockage of H^+ access or competition of Na^+ at the shared sites. I hypothesized that both access and shared site binding may be playing a role in the blockage of IH, so I used two different competitive extracellular inhibitors to answer this question.

In studying the effects of I_H using extracellular blockers, I discovered that the two different inhibitors tetrapropylammonium (TPA) and ethylenediamine (EDA) could be used in combination to better understand extracellular ion access and binding as well (4-10). Since TPA has well known competitive inhibitor of extracellular K^+, we could study its effects knowing it binds somewhere near the large extracellular access vestibule of the NKA. With the effects of TPA acting as a pseudo-control for inhibition, I would be able to identify where and how EDA inhibits extracellularly.

Intracellular activation of I_H

The current known effects of extracellular nucleotides and cations on I_H activation have all been based on a single study by Rettinger (3). However, since this had been the only study in the field on the subject, further information work was necessary to better understand the mechanism. Several different modes of activation for I_H, forward cycling with a combination of internal MgATP and Na^+ induced the conformational change from E1 to E2P, where I_H is known to occur. Backdoor phosphorylation of the NKA in the

presence of excess intracellular K^+ and Mg^{2+} and Pi conformationally shifted from E1 to E2P. Finally, a phosphate analog BeF_3^-, shown to bind in a manner similar to MgPi and pseudo-phosphorylate the NKA to activate I_H in the E2-BeF_3^- conformation (11).

Extracellular effects of organic amine inhibition

Organic amines have been shown to inhibit the NKA for more than 30 years (5) to understand cation binding as well as inhibition properties of the NKA. Two such amines TPA and EDA have been used with some regularity in comparative studies for size effects on inhibition (6,9). While both amines have been shown to be extracellular inhibitors, they are thought to inhibit in different fashions, which I tested using electrophysiology. I first identified the inhibition of both EDA and TPA were competitive for extracellular access and NKA forward cycling, as previously demonstrated (4,7). I identified that EDA presents voltage-dependent inhibition, while TPA was voltage-independent inhibition, which was previous unknown due to studies using purified NKA from kidney (4). Since both compounds are competitive extracellular inhibitors, I was able to measure their effects on the conformational transitions from E2P to E1P($3Na^+$) back to E2P in Na-dependent transient charge movement (Q_{Na}) (12-14). Just as both compounds were able to inhibit cycling in different manners, they both inhibited Q_{Na} in separate ways. TPA inhibited Q_{Na} by shifting the $V_{1/2}$ (midpoint of the voltage distribution) more negatively in a concentration-dependent manner, which has been indicated as a measure of reduced extracellular Na^+ affinity (15). Along with this, TPA also reduced the slow component of the relaxation rate in Q_{Na} (Q_{Slow}) at negative voltages. These results with TPA identify its ability to reduce extracellular Na+ access in the transition from E2P to E1P($3Na^+$). EDA conversely, inhibits Q_{Na} by reducing the total number of charges moved, shifting the $V_{1/2}$

towards more positive voltages, and reducing the Q_{Slow} at positive voltages. The combination of effects in Q_{Na} demonstrate that EDA may become occluded within the shared sites either in the E2(EDA) or E1P($1Na^+$:EDA).

I tested the hypothesis of occlusion within the shared sites using two distinct methods of dephosphorylation which is known to occur during shared site binding in the forward direction, and stabilization of a 19 kDa C-terminal fragment during tryptic digestion. Dephosphorylation measurements showed similar effects of both EDA and K^+, while TPA stabilized the phosphoenzyme (as previously demonstrated (4)). While tryptic digestion experiments showed the stabilization of the aforementioned '19 kDa' C-terminal fragment in the presence of EDA, but not TPA. These results in combination with Q_{Na} identify the best evidence to date that EDA may be occluded within the shared sites, as previously hypothesized (6,7).

Finally, TPA and EDA had their most polarizing effects on I_H, where TPA always inhibits current, while EDA has different properties depending on pH. EDA accentuated I_H in acidic conditions (pH 6.0), had no effect at physiological pH (7.6), and blocked guanidinium induced passive inward current (I_{Gua}) at basic pH (8.6) (16,17). Since EDA has two separate protonation states at pH 7.56 and pH 10.71 (18) it seemed plausible that when dually protonated EDA binds to the shared sites to dis-inhibit H^+ (similar to non-saturating Na^+ (1)). While singly protonated at pH 8.6, EDA may not bind at the shared sites, but rather acted like TPA and inhibited I_H. At pH 7.6 the mixture of both dually and singly protonated EDA would be present, creating a null effect of both accentuation and blockage of I_H.

It is the conclusion of this study that, 1) E2P is the primary conformational state through which I_H occurs. 2) While extracellular access blockage inhibits H^+ access, shared site binding may modulate I_H by accentuation. While not the initial focus of my study, I also further supported a previous hypothesis of EDA occlusion within the shared sites. The culmination of these studies will help future work identify mechanisms of action with regard to I_H, extracellular cation access and binding and provided a better understanding of a tool (EDA) for investigating the NKA.

REFERENCES

1. Mitchell, T. J., C. Zugarramurdi, J. F. Olivera, C. Gatto, and P. Artigas. 2014. Sodium and proton effects on inward proton transport through Na/K pumps. *Biophys. J.* 106:2555-2565.
2. Vedovato, N., and D. C. Gadsby. 2014. Route, mechanism, and implications of proton import during Na+/K+ exchange by native Na+/K+-ATPase pumps. *J. Gen. Physiol.* 143:449-464.
3. Rettinger, J. 1996. Characteristics of Na+/K(+)-ATPase mediated proton current in Na(+)- and K(+)-free extracellular solutions. Indications for kinetic similarities between H+/K(+)-ATPase and Na+/K(+)-ATPase. *Biochim Biophys Acta.* 1282:207-215.
4. Gatto, C., J. B. Helms, M. C. Prasse, K. L. Arnett, and M. A. Milanick. 2005. Kinetic characterization of tetrapropylammonium inhibition reveals how ATP and Pi alter access to the Na+-K+-ATPase transport site. *Am. J. Physiol. Cell. Physiol.* 289:C302-C311.
5. Kropp, D. L., and J. R. Sachs. 1977. Kinetics of the inhibition of the Na-K pump by tetrapropylammonium chloride. *Am. J. Physiol.* 264:471-487.
6. Forbush III, B. 1988. The interaction of amines with the occluded state of the Na,K-Pump. *J. Biol. Chem.* 263:7979-7988.
7. Stekhoven, F. M. A. H. S., Y. S. Zou, H. G. P. Swarts, J. Leunissen, and J. J. H. H. M. De Pont. 1989. Ethylenediamine as active site probe for Na+/K+-ATPase. *Biochim. Biophys. Acta.* 982:103-114.

8. Harry, T. W. M., V. D. Hijden, F.M.A.H.S. Stekohven and J. J. H. H. M. De Pont. 1989. Sidedness of the effect of amines on the steady-state phosphorylation level of reconstituted Na+/K+-ATPase. *Biochim. Biophys. Acta.* 987:75-82.

9. Stekhoven, F. M. A. H. S., H. G. P. Swarts, G. K. Lam, Y. S. Zou, and J. J. H. H. M. De Pont. 1988. Phosphorylation of (Na+ + K+)-ATPase; stimulation and inhibition by substituted and unsubstituted amines. *Biochim. Biophys. Acta.* 937:161-176.

10. Gatto, C., J. B. Helms, M. C. Prasse, S. Y. Huang, X. Zou, K. L. Arnett, and M. A. Milanick. 2006. Similarities and differences between organic cations inhibition of the Na,K-ATPase and PMCA. *Biochemistry* 45:13331-13345.

11. Stanley, K. S., D. J. Meyer, C. Gatto, and P. Artigas. 2016. Intracellular requirements for passive proton transport through the Na+,K+-ATPase. *Biophys. J.* 111:2430-2439.

12. Nakao, M., and D. C. Gadsby. 1986. Voltage dependence of Na translocation by the Na/K pump. *Nature.* 323:628-630.

13. Hilgemann, D.W. 1994. Channel-like function of the Na,K pump probed at microseconds resolution in giant membrane patches. *Science.* 263:1429-1432.

14. Holmgren, M., J. Wagg, F. Bezanilla, R. F. Rakowski, P. De Weer, and D. C. Gadsby. 2000. Three distinct and sequential steps in the release of sodium ions by the Na+/K+-ATPase. *Nature.* 403:898-901.

15. Holmgren, M., and R. F. Rakowski. 2006. Charge translocation by the Na+/K+ pump under Na+/Na+ exchange conditions: Intracellular Na+ dependence. *Biophys. J.* 90:1607-1616.

16. Ratheal, I. M., G. K. Virgin, H. Yu, B. Roux, C. Gatto, and P. Artigas. 2010. Selectivity of externally facing ion-binding sites in the Na/K pump to alkali metals and organic cations. *Proc. Natl. Acad. Sci*. 107:18718-18723.

17. Yaragatupalli, S., J. F. Olivera, C. Gatto, and P. Artigas. 2009. Altered Na+ transport after an intracellular α-subunit deletion reveals strict external sequential release of Na+ from the Na/K pump. *Proc. Natl. Acad. Sci.* 106:15507-15512.

18. Perrin, D. D. 1965. Dissociation constants for organic bases in aqueous solution. IUPAC Chem Data Ser.

APPENDIX

EFFECTS OF ION BINDING IN BEF3- BOUND NA,K-ATPASE

INTRODUCTION

The Na,K-ATPase (NKA) is a member of the P-type ATPase super family of protiens which are involved in ion translocation across the cell membrane. This group of proteins is solely named for the ability of a conserved aspartic acid residue to covelantly bind the γ-phosphate of ATP (1). While phopshorylated the NKA is held in two main conformations, 3 Na^+ occluded E1P(3Na) and externally open and unbound E2P. This phopshoenzyme intermediate is able to be mimicked using different metal-fluoride complexes such as AlF_x, MgF_x and BeF_x, of which BeF_x presents the highest apparent affinity for inhibtion with the most binding similarity to MgP_i (2) Previous work demonstrated that BeF_3^- has the highest affinity for binding of these three compounds.

The first demonstrated used of this compound in an electrophysiological system was done by Takeuchi et al. (3), by showing that while bound by BeF_3^- the NKA is unable to open to the cytoplasmic domain. Years later Vedovato and Gadsby (4) used BeF_3^- as a way to inhibit NKA cycling, while still facilitating both transient charge movement (Q_{Na}) and passive proton influx (I_H) at negative voltages. We followed up on this work by demonstrating that direct binding of BeF_3^- with intracellular Na^+ facilitated I_H and was unable to be washed off during our experiment (5). My work here shows that K^+ is able to interact with the NKA binding sites to inhbit both Q_{Na} and I_H in some capacity, while bound with BeF_3^-.

MATERIALS AND METHODS

Oocyte preparation and molecular biology

Oocytes were enzymatically isolated by 1–2 h of incubation (depending on the degree of desired defolliculation) in Ca^{2+}-free OR2 solution at pH 7.4 (in mM: 82.5 NaCl, 2 KCl, 1 $MgCl_2$, 5 HEPES) with 0.5 mg/mL collagenase type IA. Enzymatic treatment was followed by four 15-min rinses in Ca^{2+}-free OR2 and two rinses in OR2 with 1.8 mM Ca^{2+}. The ouabain-resistant Xenopus Q120R/N131D (RD)-α1, C113Y (CY)-α1 and the β3 subunit, in the pSD5 vector, were linearized with BglII and transcribed with an SP6 mMESSAGE mMACHINE (Thermo Fisher Scientific, Waltham, MA). Oocytes were injected with an equimolar mixture of cRNA for RDα1 or CYα1 with β3 cRNA, and then maintained in SOS solution (in mM: 100 NaCl, 2 KCl, 1.8 $CaCl_2$, 1 $MgCl_2$, and 5 HEPES) supplemented with horse serum and antimycotic-antibiotic solution (Gibco Anti-Anti; Thermo Fisher Scientific) at 16°C for 2–6 days until recordings were obtained. The RD (6) and CY (7) substitution are responsible for ouabain-resistant α1 subunit expression, allowing for selective inhibition of endogenous pumps with 1 μM ouabain and the acquisition of measurements exclusively from exogenous pumps.

Solutions

Oocytes were Na-loaded by 1-h incubation in a solution containing (in mM) 150 HEPES, 20 tetraethylammonium-Cl, and 0.2 EGTA (pH 7.2 with NaOH) until experimentation. Extracellular hydroxide solutions contained in mM: 133 methane sulfonic acid (MS), 5 $Ba(OH)_2$, 1 $Mg(OH)_2$, 0.5 $Ca(OH)_2$, titrated with 125 NMG^+ or 125 NaOH. External K^+ was added from a 3 M K-MS stock. Following demonstration of expression, 50 nL of 10 mM beryllium fluoride (BeF_x) was injected into the oocyte during

recording forming the NKA-$BeF3^-$ complex. BeF_x was made as stock solution in water with 10 mM $BeSO_4$ and 250 mM NaF (pH 7.4). Osmolarity of all recording solutions was 250-260 mosmol/kg.

Electrophysiology

An OC-725C amplifier (Warner Instruments, Hamden, CT), a Digidata 1550 A/D board, a Minidigi 1A, and pClamp 10 software (Molecular Devices) were used for two-electrode voltage-clamp recordings. Signals were filtered at 2 kHz and digitized at 10 kHz. Resistance of both microelectrodes (filled with 3M KCl) was 0.5–1 MΩ.

Data analysis

Apparent affinity ($K_{0.5}$) for K^+ was obtained by fitting the data to the Michaelis-Menten equation (Eq. 1): $I = I_{max}\ ([S]^{n_H}/(K_{0.5}^{n_H} + [S]^{n_H}))$ (Eq. 1). All half-maximal inhibitor affinities (IC_{50}) were obtained by fitting the date to a modified Michaelis-Menten (Hill1) equation (Eq. 2): $I = I_{min} + (I_{max} – I_{min})\ ([S]^{n_H}/(K_{0.5}^{n_H} + [S]^{n_H}))$ for inward current (Eq. 2), and $Q_{tot} = Q_{max}([S]^{nH}/(K_{0.5}^{nH} + [S]^{nH}))$ for transient charge movement. Transient charge (Q_{Na}) movement was obtained by integrating the area under the relaxation curve in the ON (as in ref. 5). Charge vs. voltage (Q-V) curves were fit with a Boltzmann distribution (Eq. 3): $Q = Q_{hyp} - Q_{tot}/(1 + e^{(V-V_{1/2})/k})$ (Eq. 3) where Q_{hyp} is the charge moved by hyperpolarizing voltage pulse, Q_{tot} is the total charge moved, $V_{1/2}$ is the center of the distribution and k is the slope factor.

RESULTS & DISCUSSION

Effects of K^+ on BeF_3^--bound RDα1β3 NKA

A representative continous recording of a BeF_3^- injection experiment on an RDα1β3 expressing oocyte. Maximal current with 10 mM K^+ was first demonstrated prior to injection, followed by injection and a rapid decline in outward current, representative of NKA cycling inhibition upon BeF_3^- binding. Once complete inhibiton of NKA cycling occurred K^+ was removed and then applied in a concentration depenedent manner. Although no outward current was present with K^+, there was a concentration dependent inhibition of I_H (Fig. 1B). Ouabain sensitive K-induced current (current in K^+ subtracted from current in NMG) demonstrates outward current at negative voltages, indicative of I_H blockage. Fig. 1C demonstrates that there is a measurable inhibition of I_H as [K^+] increases, indicated in the inset to be ~50-fold decrease in the apparent affinity for K^+.

Inhibition by K^+ is also seen in Q_{Na}, where it presents a reduction in total charge moved (Fig. 2A). Although difficult to explain, the rate constant of the RDα1β3 pump appear dramatically changed with BeF_3^--bound, where a fast component is directly followed by a slow component. Fig. 2B shows the total charge reduction in this representative trace is ~46% which is reduced from the nearly 95% reduction seen with 10 mM K^+ without BeF_3^--bound (Data not shown). The concentration-dependent reduced Q_{Na} in the presence of K^+ is similar to that of K^+ without BeF_3^--bound (Fig. 2C). However, there does not appear to be an apparent increase in Na^+ affinity (positive $V_{1/2}$ shift) without BeF_3^--bound (Chapter III, Fig. 6). The IC_{50} for K^+ in Q_{Na} is also increased, as it was in I_H, although to a lesser extent (Fig. 2D). These results as a whole indicate that although K^+

cannot induce NKA cycling, it is still capable of interacting with the shared sites, or access channel to inhibit ouabain-sensitive I_H and Q_{Na}.

Effects of K^+ on BeF_3^--bound CYα1β3 NKA

The CYα1β3 NKA is similar to RDα1β3, but appears to be closer enzymatically to WT Xenopus laevis NKA (8). Although K^+ was unable to produce outward current (as cycling is stopped with BeF_3^--bound), it did inhibit I_H (Fig. 3A). Maximal inhibiton of IH was slightly larger than that seen in the RDα1β3 NKA. Similarly, inhibition of Q_{Na} was also seen by K^+ in the BeF_3^--bound NKA (Fig. 3B), and as was the case with I_H, Q_{Na} inhibition by 10 mM K^+ was slightly stronger than in the RDα1β3 NKA (Fig. 3C). Unlike the BeF_3^--bound RDα1β3, the rate constants were not significantly different following BeF_x injection (Fig. 3B and 3D). However, because the rate constant is not significantly altered we were able to demonstrate a reduced rate in the presence of 10 mM K+ (Fig. 3D). These results are simliar qualitatively to those we see with RDα1β3, that K^+ is capable of interacting with the shared sites, or access channel to inhibit ouabain-sensitive I_H and Q_{Na} with BeF_3^--bound.

REFERENCES

1. Kaplan, J. H. 2002. Biochemistry of the Na,K-ATPase. *Annu. Rev. Biochem.* 71:511-535.
2. Cornelius, F., Y. A. Mahmmoud, and C. Toyoshima. 2011. Metal fluoride complexes of Na,K-ATPase: characterization of fluoride-stabilized phosphoenzyme analogues and their interaction with cardiotonic steroids. *J. Biol. Chem.* 286:29882-29892.
3. Takeuchi, A., N. Reyes, P. Artigas, and D. C. Gadsby. 2008. The ion pathway through the opened Na+,K+-ATPase pump. *Nature.* 456:413-416.
4. Vedovato, N., and D. C. Gadsby. 2014. Route, mechanism, and implications of proton import during Na+/K+ exchange by native Na^+/K^+-ATPase pumps. *J. Gen. Physiol.* 143:449–464.
5. Stanley, K. S., D. J. Meyer, C. Gatto, and P. Artigas. 2016. Intracellular requirementes for passive proton transport through the Na+,K+-ATPase. *Biophys. J.* 111:2430-2439.
6. Price, E. M., and J. B. Lingrel. 1988. Structure-function relationships in the Na,K-ATPase alpha subunit: site-directed mutagenesis of glutamine-111 to arginine and asparagine-122 to aspartic acid generates a ouabain-resistant enzyme. *Biochemistry.* 27:8400–8408.
7. Canessa, C. M., J. D. Horisberger, D. Louvard, and B.C. Rossier. 1992. Mutation of a cysteine in the first transmembrane segment of Na,K-ATPase alpha subunit confers ouabain resistance. *EMBO J.* 11:1681–1687.
8. Vedovato, N., and D. C. Gadsby. 2010. The two C-terminal tyrosines stabilize occluded Na/K pump conformations containing Na or K ions. *J. Gen. Physiol.* 136, 63-82.

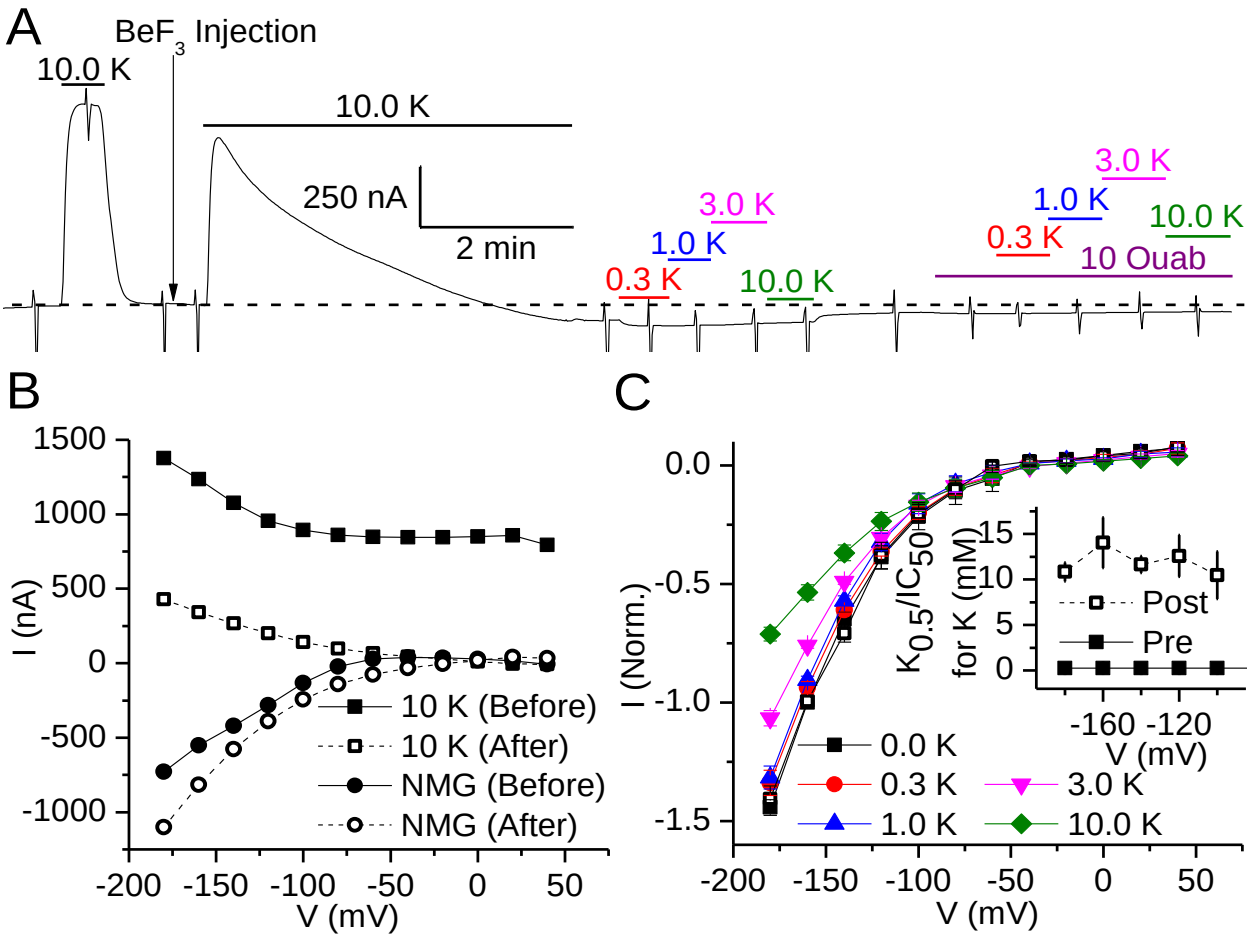

FIGURE 1. *I_H inhibition by K^+ in BeF_3^--bound RDα1β3 NKA.* (A) Continuous current recording from an RDα1β3 expressing oocyte 4-days after cRNA injection. (B) I-V plot of K-induced and NMG current at individual voltages pulses before and after BeF_x injection from A. (C) Normalized I-V plot of K^+ inhibition of I_H. Inset – $K_{0.5}$ for K^+ Pre-BeF_x; 0.25 ± 0.03 and 0.27 ± 0.01 mM at -180 and -100 mV, respectively. IC_{50} for K^+ Post-BeF_x; 10.84 ± 1.04 and 10.49 ± 2.60 mM at -180 and -100 mV, respectively. Maximal inhibition by 10 mM K^+ was 50.8 ± 1.5 % at -180 mV. Data points in C are average ± SEM from 4 oocytes normalized to current at -160 mV in NMG Pre-BeF_x.

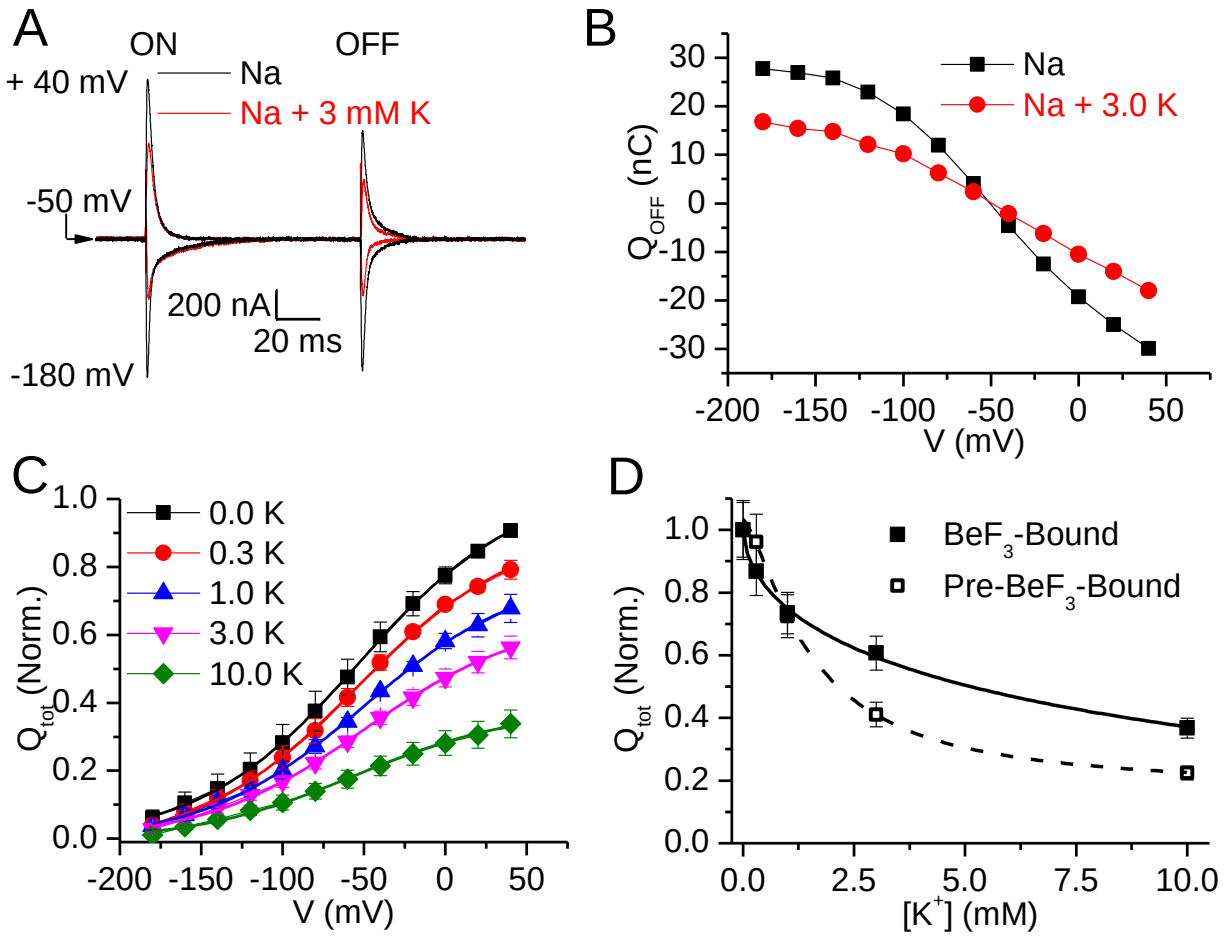

FIGURE 2. *Q_{Na} inhibition by K^+ in BeF_3^--bound RDα1β3 NKA.* (A) Transient charge movement trace following BeF_x injection without (black) and with (red) 3 mM K^+, elicited by voltages pulses from V_h = -50 mV to -180 mV and +40 mV. (B) Q-V plot of integrated values of Q_{OFF} fitted to a Boltzmann function (Eq. 2) in the absence (black) and presence (red) of 3 mM K^+, with a shared slope factor kT/ez_q = 39 mV, Q_{tot} = 20.1 nC, $V_{1/2}$= -42.7 mV in Na^+ alone, and Q_{tot} = 11.2 nC, $V_{1/2}$ = -39.8 mV in Na^+ + 3 mM K^+. (C) Average Q_{OFF}-V curves from four oocytes with increasing [K^+] applied, normalized to Q_{tot} in Na^+ alone. Lines represent fits of Eq. 3 to the average data; with a shared slope factor kT/ez_q = 49 mV the best fit $V_{1/2}$ values were -53.0 ± 1.3, -54.3 ± 1.4, -50.6 ± 1.7, -49.9 ± 2.1, and -

55.8 ± 3.4 mV for 0, 0.3, 1.0, 3.0, and 10 mM K^+, respectively. (D) Q_{tot} normalized to the total charge moved in Na^+ alone with increasing [K^+], lines represent fits to Eq. 2, the IC_{50} for K^+ in Pre-BeF_3^--bound NKA (open) and Post-BeF_3^--bound NKA (closed) were 1.87 ± 0.36 and 5.97 ± 1.96 mM, respectively. Data points in C and D are averages ± SEM from 4 oocytes normalized to Q_{tot} in Na^+ alone Post-BeF_x injection.

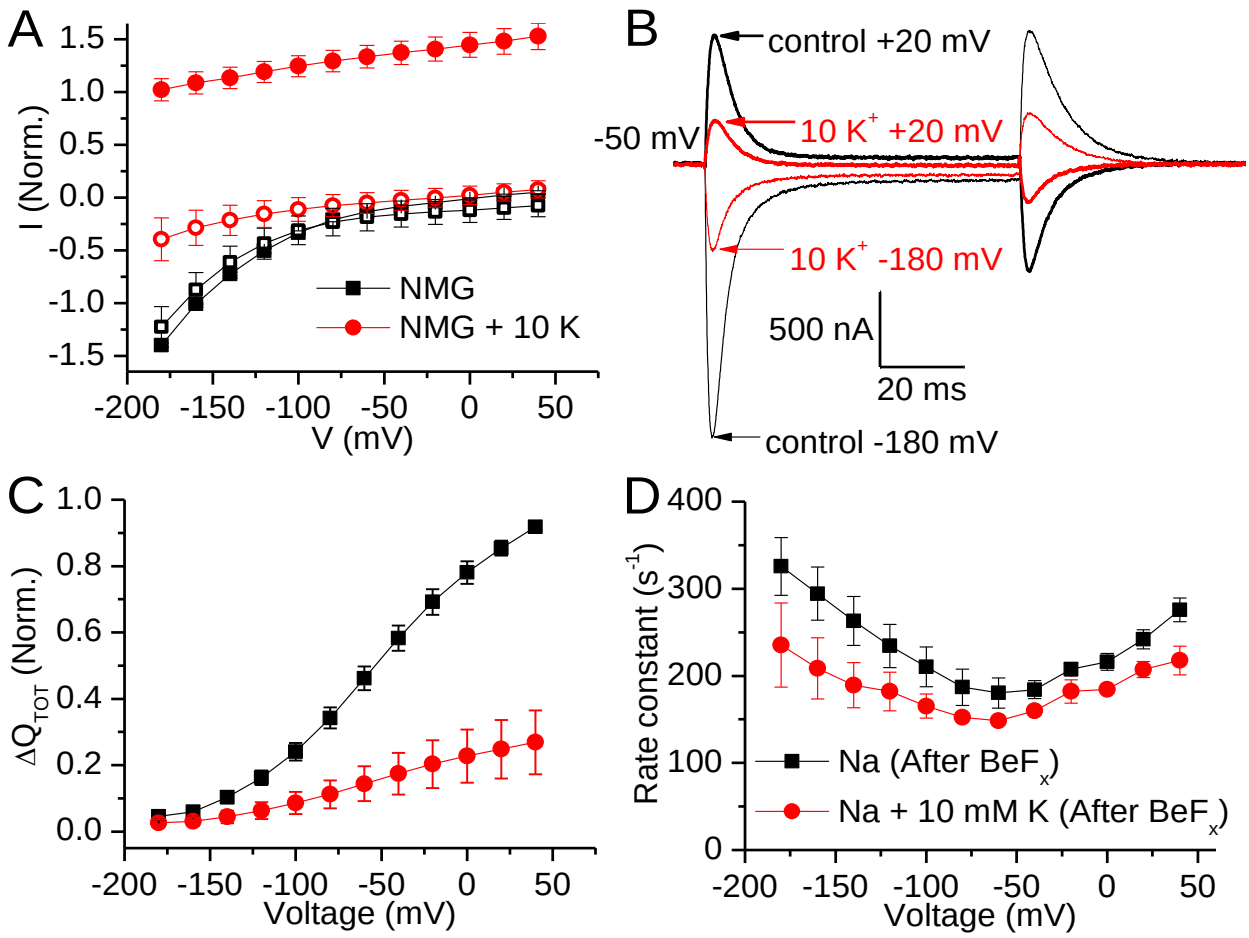

FIGURE 3. *Q_{Na} and I_H inhibition by K^+ in BeF_3^--bound CYα1β3 NKA.* (A) I-V plot of K-induced and NMG current at individual voltages pulses before and after BeF_x injection from A. Inhibition of I_H with 10 mM K+ was 61.9 ± 13.0% at -180 mV. (B) Transient charge movement trace following BeF_x injection without (black) and with (red) 10 mM K^+, elicited by voltages pulses from V_h = -50 mV to -180 mV and +40 mV. (C) Averaged Q-V plot from three oocytes with integrated values for Q_{OFF} fitted to a Boltzmann function (Eq. 3) in the absence (black) and presence (red) of 10 mM K^+, with a shared slope factor kT/ez_q = 42 mV. Lines represent fits of Eq. 3 to the average data; with a shared slope factor kT/ez_q = 49 mV the best fit $V_{1/2}$ values were -52.7 ± 0.9 and -54.6 ± 2.9 in Na^+ alone and Na^+ + 10

mM K^+, respectively. Q_{Tot} was reduced 67.8 ± 12.1% in the presence of 10 mM K^+. (D) Single exponential fits to the exponential time course decay of the transient currents stimulated by the ON voltage steps (Rate constant) of the slow time components of charge movement, with a reduction of rate constants in 10 mM K+ across all voltages. Data points in A are averages ± SEM from 4 oocytes normalized to I_H at -160 mV in NMG, Pre-BeF_x injection. Data points in C are averages ± SEM from 3 oocytes normalized to Q_{tot} in Na^+ alone Post-BeF_x injection, with data points in D simply being averages ± SEM from 3 oocytes Post-BeF_x injection.